Oceanography, Climate and Vegetation development of tropical Africa during the last glacial:

Palynology and geochemistry of marine sediments of ODP Site 1078 (off Angola)

Dissertation zur Erlangung des Doktorgrades der Naturwissenschaften

Dr. rer. nat.

am Fachbereich Geowissenschaften

der Universität Bremen

vorgelegt von

Ines Heßler

Bremen, Januar 2011

Tag des öffentlichen Promotionskolloquium:
14.04.2011

Mitglieder der Kommission:

Gutachter der Dissertation
Prof. Dr. Gerold Wefer
Prof. Dr. Hermann Behling

Prüfer
Prof. Dr. Katrin Huhn
Dr. Lydie Dupont

Weitere Mitglieder des Prüfungsausschusses
Prof. Dr. Gesine Mollenhauer
Annegret Krandick

Ines Heßler

Bremen, Januar 2011

MARUM-Zentrum für marine Umweltwissenschaften

Erklärung

Hiermit versichere ich, dass ich

1. die Arbeit ohne unerlaubte fremde Hilfe angefertigt habe,

2. keine anderen als die von mir angegebenen Quellen und Hilfsmittel benutzt habe und

3. die den benutzten Werken wörtlich oder inhaltlich entnommenen Stellen als solche kenntlich gemacht habe.

Bremen, den 13.01.2011

Ines Heßler

Contents

List of Figures

List of Tables

1 Abstract

In the last decades climate change research became more and more important due to the increasing impact of human activities on the Earth's climate system. The consideration of perspectives and results from paleoclimate observations has proven useful for climate change research, the verification of model outputs and thus future projections.

The late Quaternary, in particular the last glacial, is characterised by large and abrupt climatic shifts on millennial and centennial time scales, the so-called Dansgaard-Oeschger (D-O) cycles and Heinrich Stadials (HS). Both, the D-O cycle and HS are thought to originate in the North Atlantic and are transmitted through the atmosphere and ocean circulation which results in a near-global footprint. It has been suggested that the abrupt climatic shifts associated with HS are the effect of a reduction in the strength of the Atlantic Meridional Overturning Circulation (AMOC). According to the hypothesis of the bipolar seesaw, a reduction in the AMOC leads to a build-up of heat in the South Atlantic. Although the tropics have the potential to alter the global atmosphere-ocean dynamics through changes in the heat and freshwater balance, little is known and understood of their role in relation to abrupt climate perturbations.

This thesis contains on the one hand a compilation of high-resolution pollen records from South America and Africa covering the last glacial that documents the impact, timing and amplitude of abrupt climate change on the tropical vegetation. On the other hand this thesis focuses on the reconstruction of the vegetation, climate and oceanography of southern hemisphere Africa during the last glacial using marine sediments of Ocean Program Drilling Site 1078 (off Angola). The methods applied include palynology, stable oxygen isotopes and Mg/Ca of planktonic foraminifera.

The results of this thesis are summarised in three manuscripts with the first being already published in *Quaternary Science Reviews*, the seconds submitted to *Paleoceanography*, and the third planned to be submitted soon to *Climate of the Past*.

An overview of the vegetation development in the circum-Atlantic tropics during the last glacial (73.5-14.7 ka BP), focussing on D-O variability and HS, is given in Chapter 6.1. To reconstruct the response of vegetation to abrupt climate change, high-resolution pollen records from the South American and African tropics (between 23°N and 23°S) have been compiled from both terrestrial and marine sediment cores. Comparability among the records was achieved by grouping the pollen taxa into mega-biomes, which reflect the prevailing major vegetation types. The

tropical African pollen records appear to not register D-O variability, while vegetation changes during HS are recorded. A generally more pronounced signal of D-O and HS variability is found in the records from South America, which also show an opposite trend in the vegetation development north and south of the present-day position of the Intertropical Convergence Zone (ITCZ). The observed changes in the tropical vegetation are consistent with the hypothesis of a southward shift in the migration pattern of the ITCZ and a reduction in the AMOC. However, our observations are not consistent with the hypothesis that the circum-Atlantic tropics themselves played a key role in generating abrupt climate change.

Changes in the surface water hydrology of the tropical south-east Atlantic during the last glacial with special emphasis on abrupt climate change were reconstructed and are presented in Chapter 6.2. This study is based on high-resolution Mg/Ca and oxygen isotope measurements of planktonic foraminifera obtained from ODP Site 1078. According to the bipolar seesaw hypothesis, HS are thought to lead to a warming of the South Atlantic as a consequence of a slowdown of the AMOC. The results reveal insights into the behaviour of the Angola-Current (AC), the Angola-Benguela Front (ABF) and Benguela Current (BC) between 50 and 23.5 ka BP. In the AC the warming of surface waters associated with HS corroborates the hypothesis of bipolar seesaw. In contrast, in the BC the expected warming during HS is subdued by short periods of enhanced upwelling and cooling.

Finally, the vegetation development of tropical Angola and the southern Congo Basin during the last glacial and the deglaciation (50-10 ka BP), again focussing on HS, is presented in Chapter 6.3. Due to the linkage between ocean and atmosphere, it is thought that HS also influence the vegetation composition in the African tropics. To address the issue of the connection between the tropical African vegetation development and high-latitude climate change, a high-resolution marine pollen record originating from ODP Site 1078 is presented. Although several tropical pollen records register changes in the vegetation composition during HS (Chapter 6.1) the vegetation record of ODP Site 1078 shows no response. Model simulations conducted with two different Earth System Climate Models including a dynamical vegetation component support the assumption that the vegetation response during HS is masked by mechanisms that cancel out each other.

2 Kurzbeschreibung

Infolge des zunehmenden Einfluss des Menschen auf das globale Klima wurden wissenschaftliche Untersuchungen des Klimawandels in den vergangenen Jahrzehnten immer bedeutsamer. Die Berücksichtigung von Sichtweisen und Erkenntnissen aus Klimarekonstruktionen längst vergangener Zeiten hat sich als äußerst nützlich in Bezug auf die Klimaforschung und die Überprüfung von Modellversuchen und deren Zukunftsprojektionen erwiesen.

Das späte Quartär, im Besonderen die letzte Eiszeit, sind durch große und abrupte Klimaveränderungen gekennzeichnet. Diese sogenannten Dansgaard-Oeschger (D-O) Zyklen und Heinrich Stadiale (HS) haben ein hundert- bzw. tausendjähriges Muster. Es wird angenommen, dass sowohl die D-O Zyklen als auch die HS ihren Ursprung im Nord-Atlantik haben und infolge der Weiterleitung durch die atmosphärische als auch ozeanische Zirkulation beinahe global nachgewiesen werden können. Des Weiteren wird behauptet, dass die im Zusammenhang mit HS stehenden schnellen klimatischen Veränderungen auf eine Intensitätsabnahme der Atlantischen Umwälzzirkulation zurück zuführen sind. Gemäßder Hypothese des "bipolar seesaw" würde eine Reduzierung der Atlantischen Umwälzzirkulation zu einer Erwärmung des südlichen Atlantik führen. Obwohl die Tropen durch Veränderungen der Wärme und Frischwasser Balance das Potential besitzen die globale Atmosphären-Ozean Dynamik zu modifizieren ist wenig über deren Rolle hinsichtlich abrupter Klimaschwankungen bekannt.

Die vorliegende Dissertation enthält zum Einen eine Zusammenstellung von zeitlich hoch auflösenden Pollen-Datensätzen aus Südamerika und Afrika, welche den Einfluss, den zeitlichen Ablauf und die Amplitude von abrupten Klimaschwankungen auf die tropische Vegetation während der letzten Eiszeit dokumentieren. Ein weiterer Schwerpunkt dieser Doktorarbeit ist die Rekonstruktion der Vegetation, des Klimas und der Ozeanographie von Afrika südlich des Äquators während der letzten Kaltzeit und unter Verwendung von Meeresablagerungen von vor der Küste Angolas (Ocean Program Drilling Site 1078). Dies wurde realisiert durch die Anwendung von palynologischen Methoden, und dem Messen von stabilen Sauerstoffisotopen Verhältnissen und dem Verhältnis von Mg und Ca an planktonischen Foraminiferen.

Die Ergebnisse dieser Dissertation sind in drei Manuskripten zusammengefasst, wobei das Erste bereits in *Quaternary Science Reviews* veröffentlicht wurde. Das zweite Manuskript wurde bei der Zeitschrift *Paleoceangraphy* eingereicht und das Dritte wird in Kürze bei *Climate of the Past* eingereicht.

Ein Entwicklungsüberblick der Vegetation in den zirkumatlantischen Tropen während der letzten Kaltzeit (73.500-14.700 vor heute) mit dem Schwerpunkt auf den D-O Zyklen und HS ist in Kapitel 6.1 gegeben. Die Reaktion der Vegetation auf abrupte Klimaveränderungen wurde anhand einer Sammlung von zeitlich hochauflösenden terrestrischen als auch marinen Sedimentkernen aus Südamerika und Afrika (zwischen 23°N und 23°S) rekonstruiert. Eine Vergleichbarkeit der einzelnen Datensätze wurde durch die Zuordnung der einzelnen Taxa zu sogenannten mega-Biomen, welche die vorherrschenden Vegetationsarten darstellen, erreicht. Die Ergebnisse zeigen, dass die Afrikanischen Datensätze keine D-O Zyklen nachweisen, jedoch HS eindeutig von der Vegetation registriert werden. Generell ist das Signal von D-O Zyklen und HS in den Südamerikanischen Datensätzen stärker widergespiegelt. Zusätzlich zeigt dieses eine gegensätzliche Entwicklung nördlich und südlich der heutigen Position der Intertropischen Konvergenzzone. Die beobachteten Veränderungen in der tropischen Vegetation stimmen mit der Hypothese einer südwärts Verlagerung des jahreszeitlichen Verlaufsmusters der Intertropischen Konvergenzzone und einer Abschwächung der Atlantischen Umwälzungszirkulation überein. Allerdings untermauern unsere Ergebnisse nicht die Hypothese, dass den Tropen selber eine Schlüsselfunktion bei der Erzeugung von abrupten Klimaschwankungen zukommt.

In Kapitel 6.2 sind die Ergebnisse der Rekonstruktion von Veränderungen in der Oberflächenwasserhydrologie des südöstlichen Atlantik während der letzten Kaltzeit mit dem Schwerpunk auf abrupten Klimaschwankungen dargestellt. Diese Studie basiert auf zeitlich hochauflösenden Messungen von Mg/Ca und Sauerstoffisotopen an planktonischen Foraminiferen aus dem Sedimentkern ODP 1078. Entsprechend der Hypothese des "bipolar seesaw" wird angenommen, dass sich infolge einer Abschwächung der Atlantischen Umwälzzirkulation der südliche Atlantik erwärmt. Die Ergebnisse geben einen Einblick in das Verhalten des Angola Stroms, der Angola-Benguela Front und des Benguela Stroms zwischen 50.000 und 23.500 Jahren vor heute. Die Erwärmung der Oberflächengewässer im Angola Strom stehen im Zusammenhang mit HS und unterstützen entsprechend die Hypothese des "bipolar seesaw". Im Gegensatz dazu, wird die Erwärmung in der Region des Benguela Stroms durch kurze Perioden von verstärktem Auftrieb und Abkühlung abgeschwächt.

In Kapitel 6.3 ist die Entwicklung der Vegetation im tropischen Angola und dem südlichen Kongo Becken während der letzten Eiszeit und Abschmelzphase veranschaulicht, abermals mit dem Schwerpunkt auf HS. Basierend auf der Verbindung zwischen Ozean und Atmosphäre wird angenommen, dass die HS ebenfalls die Vegetation in den Afrikanischen Tropen beeinflussen. Um die Problematik des Zusammenhangs zwischen der Vegetation der Afrikanischen Tropen und den Klimaschwankungen aus den nördlichen Breiten anzugehen, wird ein zeitlich

hochauflösender mariner Pollen-Datensatz von dem Sedimentkern ODP 1078 präsentiert. Obwohl verschiedene Pollen-Datensätze aus den Tropen Veränderungen in der Vegetation im Zusammenhang mit HS aufzeigen (Kapitel 6.1), werden keine Abwandlungen der Vegetationszusammensetzung in dem Datensatz von ODP 1078 registriert. Anhand von Modellversuchen mit zwei verschiedenen Klimamodellen, welche eine dynamische Vegetationskomponente beinhalten, wird unsere Annahme unterstützt, dass Veränderungen in der Vegetation während HS durch sich überlagernde Mechanismen maskiert wurden.

3 Introduction

3.1 Motivation

The term "climate" refers to the average weather conditions of a given region over a longer period ranging from months to thousands or million of years. Climate fluctuates naturally driven by interactions between the atmosphere, oceans, land, and cryosphere. In recent decades significant changes in the global climate system have been detected and are projected to become more important during the next century. These findings focus increasing attention on climate science as it tries to improve the ability to assess future climate variations and their effect on the Earth's system.

According to the 4th Assessment report of the Intergovernmental Panel on Climate Change (IPCC, 2007), Africa is the most vulnerable continent to climate change. African climate is controlled by complex marine and terrestrial interactions that produce a variety of climates across the continent. Climate controls the ecosystems and hence biodiversity, the social and the economic development of Africa. Climate change scenarios (e.g. Hulme et al., 2001) predict drier and warmer conditions over Africa in the future, significantly impacting on the ecosystems, natural resources, economic and social structures.

Considering perspectives from paleoclimate observations, theories and modelling have been proven useful for climate change research. Examining the internal processes in the climate system during large climatic fluctuations in the past is important to assess how the same climate system might react during future changes. Based on paleoclimatic reconstructions, outputs from climate models can be verified and/or improved. Hence, paleoclimate data are the key to determine if climate models can realistically simulate (future) climate change. By incorporating past climate reconstructions of Africa into climate modelling, effects of a changing climate can be assessed on a regional level, an issue greatly important for the African society.

3.2 Late Quaternary Climate Variations

The climate of the late Quaternary was marked by a sequence of glacial-interglacial cycles that are recorded in marine sediments (Lisiecki and Raymo, 2005) and polar ice cores (e.g. Petit et al., 1999; EPICA members, 2004; NGRIP, 2004; Lambert et al., 2008) (Figure 1). The principal driver of these past climate changes are regular variations in eccentricity (~100 kyr cycle), obliquity (~41 kyr cycle) and precession (~23 kyr cycle) of the Earth's orbit, also

known as Milankovitch cycles (Milankovitch, 1920). Milankovitch (1920) hypothesised that ice ages occur when the Earth's solar orbit is configured so that insolation is low during northern hemisphere summers, allowing northern ice sheets to grow. Studies of deep-sea sediment cores have revealed that variations in the Earth's orbital geometry were fundamental in regulating the Quaternary ice ages (Hays et al., 1976; Imbrie et al., 1992; 1993). However, there are several discrepancies between Milankovitch's theory and observations casting doubt on the finer details of the hypothesis. For example the "100 kyr problem", where the dominance of the 100 kyr periodicity in climate records of the last 800,000 years is not understood (e.g. Winograd et al., 1992; Broecker, 1992; Emiliani, 1993; Raymo and Nisancioglu, 2003). This problem did not always exist as several long-term paleoclimatic reconstructions show ice volume proxies were almost exclusively dominated by the 41,000 year periodicity before ~800 kyr, and by 100,000 year eccentricity after ~800 kyr (e.g. Imbrie et al., 1993; Petit et al., 1999; EPICA members, 2004). Records dominated by the amount of summer insolation are, at almost every latitude, influenced by precession (23,000 year period) (e.g. Pokras and Mix, 1985; Prell and Kutzbach, 1987; McIntyre et al., 1989; Partridge et al., 2004; Stuut and Lamy, 2004; Daniau et al., 2007; Ziegler et al., 2010a; b).

The climate of the last glacial (MIS 2-4; 71-14.5 ka BP) was characterised by millennial scale variations of irregular periodicity (Figure 1). These climate oscillations are thought to have been global in nature and were transmitted through the atmosphere and oceans of both hemispheres (e.g. Alley et al., 1998; Hostetler et al., 1999; Broecker, 1996). Two different types of rapid climate fluctuation have been described. 1) Dansgaard-Oeschger oscillations (D-O), found in Greenland ice cores, are expressed in initial and abrupt warming episodes (interstadials) followed by gradual cooling (stadials) on timescales of about 1500 years (Dansgaard et al., 1984; Bond et al., 1993; NGRIP, 2004). D-O cycles are thought to be related to a weakening of deep-water formation in the North Atlantic due to dilution and freshening of surface waters by ice melting or other processes. Only when salt builds up in the ocean and freshwater supply is reduced, does deep-water formation resume (e.g. Alley, 1998). At the end of some D-O cycles, cold intervals associated with North Atlantic Heinrich events occur abruptly (Heinrich Stadials, HS). 2) Heinrich events are defined by the occurrence of ice-rafted debris (IRD) in the North Atlantic region (Heinrich, 1988; Bond et al., 1993; Broecker et al., 1994). Several studies have suggested that these cold intervals were triggered by iceberg discharge in the North Atlantic resulting in a considerable reduction of AMOC (e.g. Broecker et al., 1992). Based on interhemispheric coupling, the reduction of the AMOC and the related cooling of the northern hemisphere is associated to a heat build-up in the South Atlantic (Broecker, 1998; EPICA members, 2006). The concept of bipolar seesaw is supported by the work of the EPICA

members (2006) revealing a strong coupling between Dansgaard-Oeschger cycles and Antarctic warm events. Furthermore, Heinrich events can be correlated to the strongest Antarctic Isotope Maxima (AIM 1, 2, 4, 8, and 12) (EPICA members, 2006) (Figure 1).

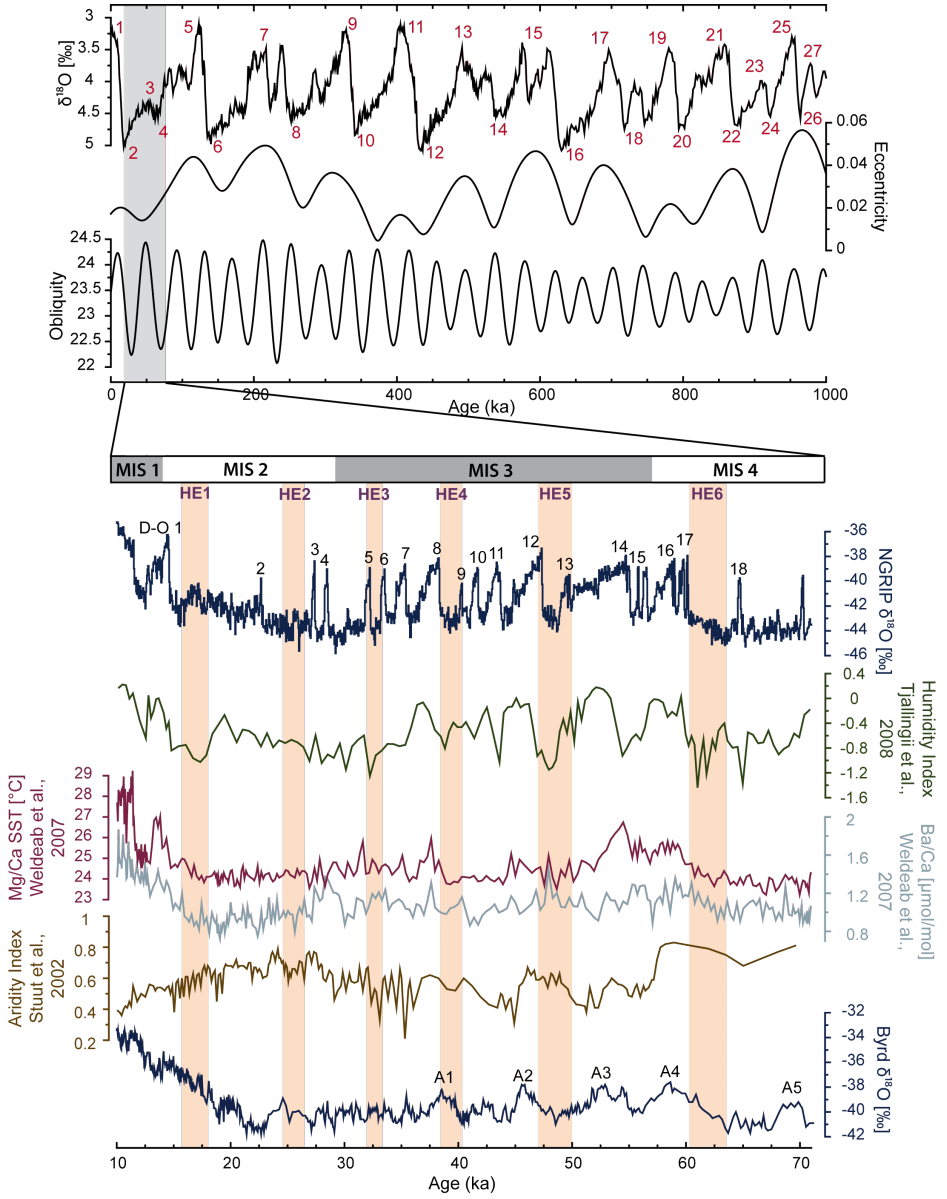

Figure 1: Late Quaternary climate records. Black δ^{18}O record on top of the figure (Lisiecki and Raymo, 2005 stack) indicates glacial-interglacial cycles with numbers reflecting Marine Isotope Stages (MIS). Heinrich Stadials (HE) are defined after the Greenland Ice Core Chronology 2005. Antarctic warming events (A1-5) are according to Blunier and Brooke (2001). Numbers on the NGRIP δ^{18}O records reflect D-O cycles

Although it appears that both D-O cycles and HS are registered globally, their manifestation varies geographically and the underlying mechanisms are still poorly understood. However, a paradigm has developed that the strength of the AMOC plays an important role (e.g. Sarnthein et al., 1994; McManus et al., 2004; Clark et al., 2007).

For a long time the Earth's tropics have been regarded as a key region for Quaternary climate variations, however, concerning abrupt climate change contrasting hypothesis exist. Some hypotheses suggest the tropics could be a trigger for abrupt climate changes. Since the tropical Atlantic SST has a strong control on the global atmospheric heat transport pattern, shifts in it would lead to changes in the transport of water-vapour from the tropics. The net freshwater balance in the Atlantic affects the density of the ocean surface waters and the northward penetration of latent heat (e. g. Cane and Clement, 1999; Ivanochko et al., 2005; Rahmsdorf, 2002). Others suggest the triggers for abrupt climate change, involving changes, mode switches and/or internal oscillations of the AMOC, are located at the North Atlantic high latitudes (e. g. Broecker et al., 1990; Rahmsdorf, 2002; Broecker 2003).

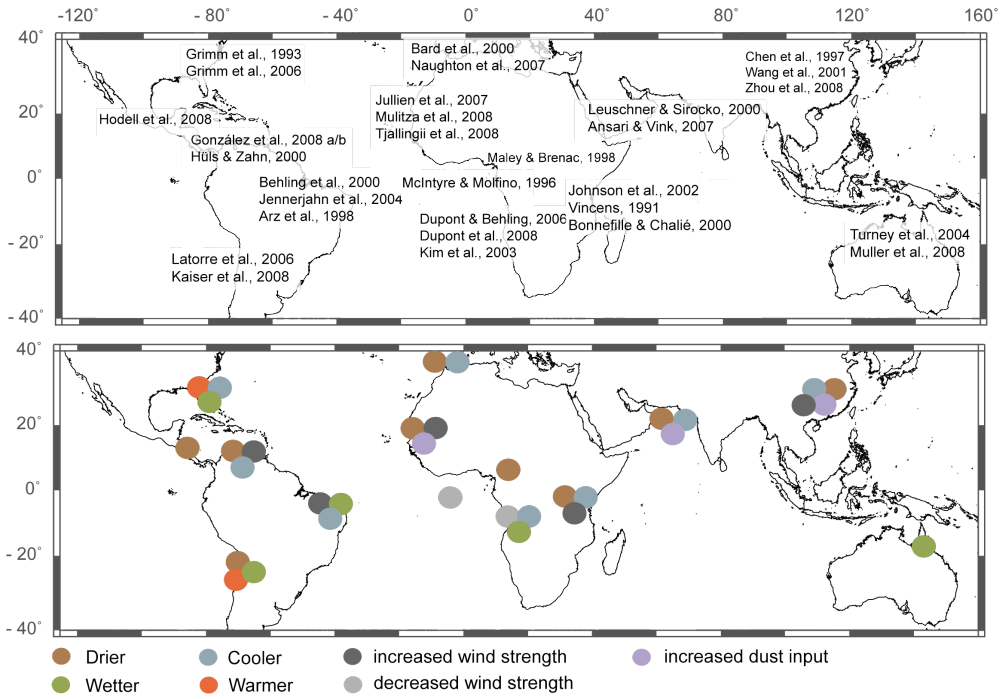

Figure 2: Impact of North Atlantic Heinrich Stadials in the Earth's tropics and subtropics

During the last years paleoclimate reconstructions and modelling experiments have been used to evaluate the impact of northern high-latitude millennial scale climate variability in the tropics and to identify potential forcing and feedback mechanisms (e.g. Leuschner and Sirocko, 2000;

Johnson et al., 2002; Turney et al., 2004; Tjallingii et al., 2008; Mulitza et al., 2008; González et al., 2008; 2009; Dupont et al., 2009). However, there is no consistent pattern in the magnitude and manifestation of rapid climate variations in paleoclimate records of the last glacial (Figure 2). During abrupt climate change wetter conditions and stronger trade winds are reconstructed for South America south of the equator (Behling et al., 2000; Latorre et al., 2006). North of the equator, however, opposite conditions prevailed (Hüls and Zahn, 2000; González et al., 2008 a, b) supporting the theory of a southward shift of the ITCZ during abrupt climate fluctuations (e.g. Chiang and Koutavas, 2004; Dahl et al., 2005). More arid conditions together with enhanced NW trade winds characterise Africa north of the equator (Mulitza et al., 2008; Tjallingii et al., 2008). In the southern hemisphere of Africa records from the eastern Rift system record drier conditions combined with an increased wind strength (Johnson et al., 2002; Stager et al., 2002) whereas the opposite is indicated by south-western African datasets (Kim et al., 2003; Dupont and Behling, 2006). On the Arabian Peninsula exceptional dry conditions are reported in association with abrupt climate events (Leuschner and Sirocko, 2000; Ansari and Vink, 2007), while wetter conditions have been reconstructed for northern Australia (Turney et al., 2004; Muller et al., 2008).

3.3 Scientific objectives

The climate, vegetation and oceanography of today's African tropics are controlled by the coupled atmosphere-ocean system. The large-scale hydrological cycle driven by the warm tropical oceans provides an important portion of the energy utilized for the general circulation of the atmosphere (Graham and Barnett, 1987). On a regional scale climate and vegetation composition are strongly affected by the position of the ITCZ and the intensity of the African Monsoon. The strong link between atmospheric and oceanographic conditions cause the position of the ITCZ to follow a seasonal cycle controlling the rainfall distribution in equatorial and tropical regions. During glacial times, however, it has been suggested the African monsoon was less active due to the presence of large polar ice sheets (e.g. Braconnot et al., 2000; Weldeab et al., 2007). A cooling of the North Atlantic surface waters during the last glacial is assumed to have shifted the ITCZ towards a more southerly position (Braconnot et al., 2000). The southward displacement of the ITCZ could have been accompanied by a reduction of convection at the low latitudes, resulting in a net decrease of atmospheric water vapour and a northward penetration of latent heat (Ivanochko et al., 2005). Paleoclimatic records appear to show that abrupt climate variations result in a further weakening of the African monsoon and a southward shift of the ITCZ (Stager et al., 2002; Peck et al., 2004; Jullien et al., 2007; Mulitza et al., 2008). The global distribution of vegetation is primarily controlled by climate. Paleovegetation studies are an important tool to reconstruct and understand climate changes, their interactions and

feedback. Modelling experiments suggest the glacial vegetation pattern of southern hemisphere Africa was significantly different from today (Prentice et al., 2000). However, the relationship between shifts in vegetation and climate change, their interactions and feedbacks are still poorly understood. In order to improve our understanding of the glacial vegetation development and its interaction with prevailing climate and oceanographic conditions high quality and high resolution records from southern hemisphere Africa are needed.

The main scientific objective of this thesis is the high temporal resolution reconstruction of vegetation, climate and oceanography of southern hemisphere Africa during Marine Isotope Stage 3 (50 - ~25 ka BP) with special emphasis on millennial scale climate variability using marine sediments from coastal Angola (Ocean Program Drilling Site 1078 C). The data sets have been generated to address the following scientific questions:

1. What are the driving forces and feedback mechanisms of possible shifts in the vegetation pattern in southern hemisphere Africa during the last glacial?

2. What are the interactions between the position of the ITCZ, strength of monsoon and trade wind system, precipitation, the prevailing vegetation composition and oceanic conditions?

3. What is the impact of (millennial-scale) climate variations on the vegetation, regional sea surface temperature, and other oceanographic features off the coast of Angola?

In order to answer the scientific questions several proxies have been investigated:

1. The pollen and spores content of marine sediments reflect the vegetation across large areas on the adjacent continent. Information about the prevalent vegetation types can be used to identify the dominant climatic and environmental conditions.

2. The ratio of magnesium to calcium (Mg/Ca) of planktonic foraminifera shells reflects the temperature of the surrounding seawater in which the shell calcified. The Mg/Ca ratio is therefore frequently used in paleoceanographic studies to estimate the past sea water temperature.

3. Stable oxygen isotopes (δ^{18}O) of the calcite of planktonic foraminifera in combination with Mg/Ca based temperatures have been used to calculate the δ^{18}O of seawater and to estimate changes in the seawater salinity (δ^{18}O water net salinity) during the last glacial.

Investigating these issues will contribute to the general understanding of past (abrupt) climate variations, their impact, timing and amplitude in southern tropical Africa and their global consequences.

3.4 Outline

Firstly Ocean Program Drilling Site 1078 and the environmental setting will be introduced before the proxies and methods are described in detail. The main part of this thesis is divided into three manuscripts.

Chapter 6.1 refers to the manuscript published in *Quaternary Science Reviews* in 2010, entitled, *Millennial-scale changes in vegetation records from tropical Africa and South America during the last glacial*. This review aims at documenting vegetation changes of the circum-Atlantic tropics in response to abrupt climate fluctuations of the last glacial. Comparability between different pollen records was gained by summarising the vegetation records in terms of major vegetation types (mega-biomes). Records from both South America and Africa show a response to North Atlantic HS, while the pattern of D-O variability is merely reflected in South American records. The hypothesis of a southward displacement of the ITCZ during periods associated with Heinrich events was supported by the fact that records from the northern hemisphere of South America show opposite responses than the one from the southern hemisphere.

In the second manuscript (Chapter 6.2), *Impact of abrupt climate change in the tropical south-east Atlantic during Marine Isotope Stage (MIS) 3* are the results of the analysis of planktonic foraminifera summarised. The reconstruction based on a paired analysis of the Mg/Ca temperature and the δ^{18}O values of planktonic foraminifera from ODP Site 1078 (off Angola) during the last glaciation (50-23.5 ka BP) with special emphasis on abrupt climate variability such as Heinrich Stadials (HS). The possibility to allocate the studied foraminiferal species (*Globigerina bulloides*, *Globigerinoides ruber*) to one of the dominant oceanographic features off the coast of southwest Africa (Angola-Current, Angola-Benguela Front, Benguela Current) enables us to reconstruct their thermal development and possible spatial variability. In the warm Angola Current HS are clearly recorded in the paleotemperature record, while in the Benguela upwelling system the impact seem to be masked by other processes.

The third manuscript (Chapter 6.3), *Masked millennial-scale climate variations in southwest African during the last glaciation*, addresses the vegetation development of Africa south of the equator between 50 and 10 ka BP using sediments of ODP Site 1078. It has been suggested by several studies that abrupt climatic shifts characteristic for the last glacial (e.g. HS) lead to a build-up of heat in the South Atlantic due to a reduction in the AMOC. Through the linkage between atmosphere and ocean these abrupt climate perturbation are thought to influence the vegetation composition also on the southern hemisphere African continent. Surprisingly, the dominant vegetation composition in south-west Africa reflects no changes during HS although

off the coast of south-west Africa increasing sea-surface temperature are clearly recorded as shown in the second manuscript. Indeed, model simulations indicate that the vegetation response during HS is disguised by mechanisms that cancel out each other.

In addition to the results presented in the three manuscripts data of dinoflagellate cyst assemblages have been obtained and are presented in the Chapter "Prospect for future research". The according publication is planned to follow in the coming few months. A data-model comparison between the here presented vegetation data and modelling experiments obtained during the PhD project of Dian Handiani is introduced in Chapter 8.2 and will also be conducted subsequently.

4 Ocean Drilling Program Site 1078 and its environmental setting

4.1 Ocean Drilling Program Site 1078

Ocean Drilling Program Site 1078 is located near the Bight of Angola (11°55'S, 13°24'E) in 427 m water depth (Figure 3). At Site 1078 four Holes (A-D) were cored reaching a maximum depth of 165.2 m below seafloor (mbsf) and covering the last 360 ka. The core location is situated between the high-productivity regions off the Congo River and the Angola-Namibia upwelling cell. Lithologically, the sediments are predominately composed of moderately bioturbated olive-grey and dark olive-grey silty clay with varying amounts of nannofossils and foraminifers (Wefer et al., 1998). Sediments from depths between 10 and 16 mbsf, covering the interval 50-23 ka BP, were investigated in this study.

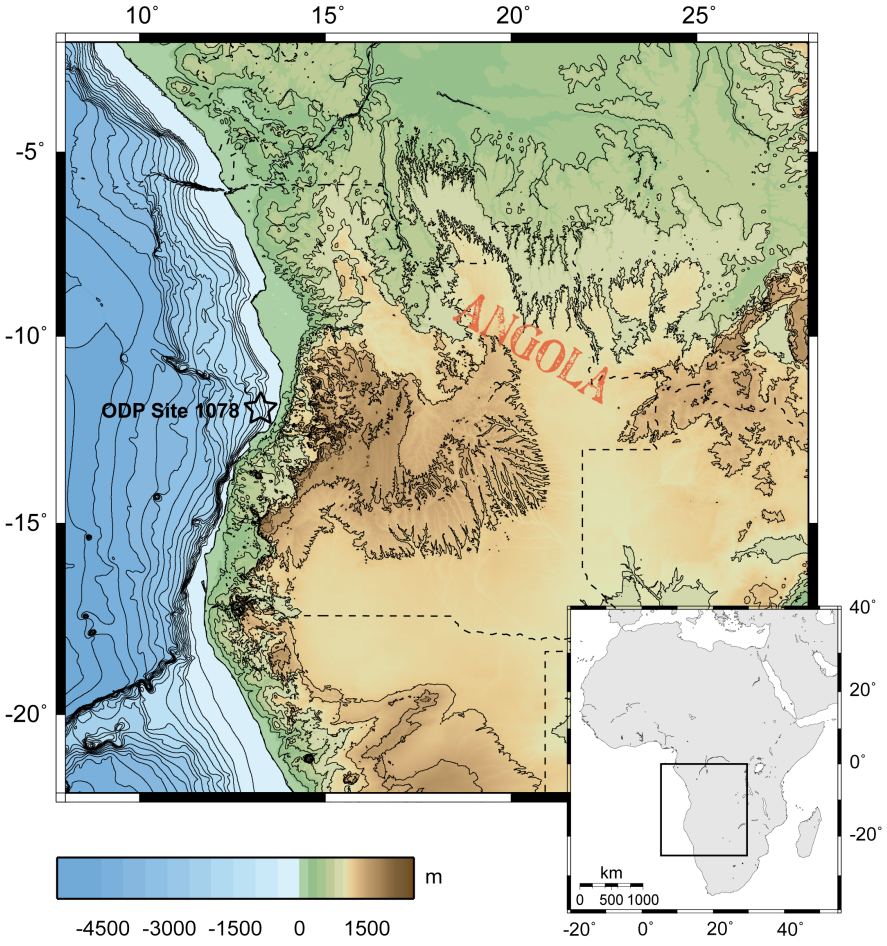

Figure 3: Bathymetric and oceanographic situation of the research area. Core location of ODP Site 1078 is marked by a star.

4.2 Chronostratigraphy of ODP Site 1078

The age-depth model of ODP Site 1078 hole C is based on accelerator mass spectrometry (AMS) radiocarbon dating of foraminifer tests and mollusc fragments at the Leibniz-Laboratory, Christian-Albrechts Universität Kiel, Germany. Using 15 AMS measurements Kim et al. (2003) and Rühlemann et al. (2004) established the age model for the last 22,000 years. To convert the uncorrected ^{14}C ages into calendar ages the CALIB 4.3 program and the marine calibration curve was used (Stuiver et al., 1998; Hughen et al., 2004). Eight additional AMS ^{14}C ages extended the age model to the period > 45-22 ka (Dupont et al., 2008). Since these radiocarbon dates are outside the range of the marine calibration curve of Stuiver et al. (1998) they were calibrated using Fairbanks et al. (2005). The AMS ^{14}C dates were corrected with a reservoir age of 400 years reflecting the present day global average (Hughen et al., 2004). Temporal variations in reservoir ages were not taken into consideration since they are difficult to reconstruct (e.g. Bard et al., 1994) and, for pre-Holocene records are smaller than the uncertainties in the radiocarbon dating (Fairbanks et al., 2005). Model simulations also show that temporal fluctuations in the marine reservoir age are of minor importance in the tropical Atlantic (Hughen et al., 2004; Franke et al., 2008). The oldest ^{14}C AMS date exceeds the actual limit of radiocarbon dating. As a result of large uncertainties in the calibration curve the age model for the period spanning 50-40 ka needs to be considered with caution.

4.3 Previous work at ODP Site 1078

Sea surface temperature variations during the past 22 kyr have been investigated using the alkenone method (Kim et al., 2002). In that study the authors focus on the teleconnection between the northern and southern hemispheres by comparing alkenone-derived SST records from both hemispheres. Kim et al. (2003) published a slightly extended data set of alkenone-derived temperature estimates covering the last 25 kyr. The emphasis of the second study was the reconstruction of SE trade wind intensity variations over the South Atlantic on millennial time scales. Kim et al. (2005) presented lipid biomarker and Rhizophora (mangrove) pollen counts in order to evaluate if high concentrations of mangrove pollen in marine sediments are related to relative sea level changes during the last deglaciation. The authors concludes that abrupt sea level rise and the consequent shelf flooding are the most important factors for the enhanced transport of mangrove material into the marine environment. Intermediate-depth temperatures for the time frame 24-8 cal kyr BP have been reconstructed at ODP Site 1078 using oxygen isotope ratios of endobenthic foraminifera (Rühlemann et al., 2003). The aim of that study was to test if changes in tropical mid-depth Atlantic temperature are suitable to track the strength of the meriodional overturning circulation (AMOC) that plays a crucial

role in global climate change. The extended benthic oxygen isotope record, now covering the last 22-0 cal kyr BP, suggests that a reduction in the strength of the AMOC during the periods of HS1 and the Younger Dryas was accompanied by abrupt and intense warming of the intermediate depth tropical Atlantic (Rühlemann et al., 2004). High-resolution palynological studies, covering the time span 30-0 ka BP were published by Dupont and Behling (2006), Dupont et al. (2007), and Dupont et al. (2008). The interpretation of the pollen records allows the detailed study of the vegetation development and related climatic conditions of southwest Africa during the last glacial, deglaciation and Holocene. In general, environmental conditions have been reconstructed to be cool and dry during the LGM and cool but wet during HS1. During the Younger Dryas period (YD) a gradual temperature increase is indicated which, however, started already well before the onset of the YD.

4.4 Oceanography

At present-day the South Atlantic plays a major role in the exchange of water masses between important deep-water sources in the North Atlantic (NADW) and the world's oceans. The South Atlantic receives water with different densities and characteristics (salinity, temperature, nutrients, oxygen) from different sources in the north and south. Mid-depth waters originate in the North Atlantic while waters from the south are provided from the Weddell Sea and the Circumpolar Current flowing through the Drake Passage (Reid, 1989, 1996). Warm and salty waters in the South Atlantic are from the Indian Ocean via the Agulhas Leakage (Gordon, 1986). High-saline and oxygen-rich NADW originating in the northern North Atlantic are transported south to merge with the Antarctic Circumpolar Current (ACC) in the South Atlantic. This is driven by strong westerly winds flowing eastwards into the southern sectors of Indian and Pacific Ocean. The southward outflow of NADW into the global oceans needs to be balanced by an equivalent amount of water flowing back northward into the Atlantic. These northward flowing waters are transported in upper or intermediate layers carrying heat across the equator as part of the warm water route of the thermohaline circulation (Hastenrath, 1982; Reid, 1989; Schlitzer, 1996).

Three major subsurface waters can be separated in the upper tropical and subtropical South Atlantic. The warm and salty South Atlantic Central Waters (SACW) characterise the upper tropical and subtropical ocean. Below the SACW, between ~ 600 and 1000 m, is the colder and less salty Antarctic Intermediate Water (AAIW). Between 1000 and 1200 m depth in tropics the Upper Circumpolar Deep Water (UCDW) is found. Below the UCDW, between about 1200 m and 3900 m (in the tropics), the NADW flows southward (Stramma and England, 1999).

The major near-surface, wind driven circulation of the South Atlantic is dominated by a system of gyres and by the equatorial and circumpolar currents (Figure 4) (Peterson and Stramma, 1991). Along the south-eastern continental shelf of Africa the Agulhas Current Retroflection plays an important role in the inter-ocean exchange of water masses from the South Atlantic and Indian Ocean.

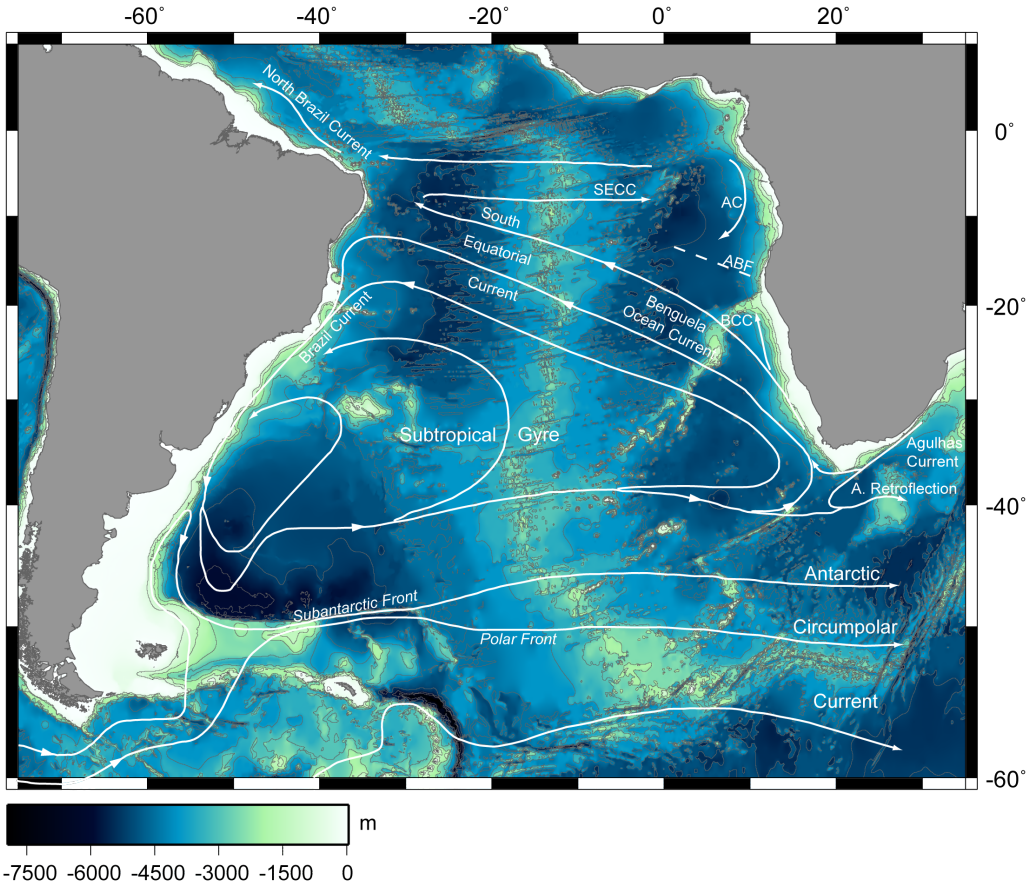

Figure 4: Schematic representation of the large-scale, upper-level geostrophic currents and fronts in the South Atlantic after Peterson and Stramma (1991). SECC = South Equatorial Counter Current, AC = Angola Current, ABF = Angola-Benguela Front, BCC = Benguela Coastal Current.

The warm Agulhas waters penetrate westward into the South Atlantic, whereas during progradation events occurring several times per year the warm waters reach even further into the southern Atlantic Ocean. Between 16° and 20°E the Agulhas Current retroflects back towards the Indian Ocean as the parallel flowing Agulhas Return Current (Lutjeharms and Van Ballegooyen, 1988). In the eastern South Atlantic, one of the World's four major eastern boundary currents, the Benguela Current (BC) controls the regional surface-water circulation. The BC is dominated by a coastal upwelling system, the Benguela upwelling system (Nelson and Hutchings, 1983; Shannon, 1985; Stramma and Peterson, 1989; Peterson and Stramma, 1991). Nelson and Hutch-

ings (1983) defined the effective northernmost boundary of the upwelling to be about 18°S, whereas Moroshkin et al. (1970) found evidence that seasonal components of the Benguela system extend as far north as 12°-13°S. At about 35°S a combination of the regional meteorology, oceanography and seafloor topography determines the southernmost boundary of the upwelling system (Shannon, 1985). Starting at about 35°S the Benguela Current flows north northwest along the coast of south-west Africa; separating at about 25°S into the coastal oriented Benguela Coastal Current (BCC) and the north-westward flowing Benguela Ocean Current (BOC) (Figure 4). The BOC feeds into the broad South Equatorial Current (SEC) which flows westward towards South America. Off the coast of Brazil the SEC is divided by the eastward flowing South Atlantic Counter Current (SECC) into two branches the Brazil Current and the northward directed North Brazil Current (Peterson and Stramma, 1991). Close to the African coast, between 8°-9° E the SECC turns south, dividing into two branches. One of the branches maintains its southward flow providing a source for the Angola Current (AC) (Moroshkin et al., 1970). At approximately 17°S the warm, saline waters of the AC meet the upwelling waters of the BC resulting in the development of a sharp thermal front, the Angola-Benguela Front (ABF) (Shannon et al., 1987) (Figure 4). This shallow front is nearly E-W oriented and extends to a distance of about 150 km offshore. Although the ABF is most distinct in the near-surface layer (upper 50-75 m water depth) there is evidence that the front may extend to a depth of several hundred meters. Despite the permanent nature of the front, seasonal differences in its characteristics are apparent. For instance, between July and September the front seems to be less well defined, and there is also evidence for a seasonal meridional migration of the ABF being farthest north during this time (Shannon et al., 1987).

4.5 Regional Climate

The general atmospheric circulation of the southern hemisphere is commonly simplified to the strength and location of the easterly wind belt at tropical latitudes, the westerly wind belt at middle latitudes and the polar easterlies at polar latitudes. The subject of this chapter is the meso-scale nature of the climate system of south-west Africa and Angola.

Year around the surface pressure field is characterised by a large, semi-permanent high-pressure cell over the subtropical Atlantic called the South Atlantic Anticyclone (Figure 5). The position of the South Atlantic Anticyclone shifts seasonally from about 30°S and 5°E during austral summer to about 26°S and 10°E during austral winter. The intensity of this high pressure system also varies throughout the year (Nelson and Hutchings, 1983; Tyson and Preston-Whyte, 2000). Over the African subcontinent the pressure field changes from a well developed low during austral summer to a weak high in winter (Nelson and Hutchings, 1983). The seasonal changes

in the prevailing pressure system are related to the position of the ITCZ, a zone of northern and southern hemisphere Trade wind convergence. During austral winter the ITCZ is located at its northernmost position between 15°-18°N. Associated with the development of a strong tropical trough over central Africa the ITCZ lies between 5° and 6°N in the west and between 15° and 20°S in the east during austral summer (Leroux, 2001) (Figure 5). The low pressure convergence zone is more clearly delineated over the ocean than over the continent. The surface expression of the ITCZ over the continent is seldom associated with precipitation; maximum convergence, cloudiness and rainfall often occur equatorward of the major flow discontinuity (Tyson and Preston-Whyte, 2000). Over southern Botswana and southern Angola another main convergence zone, the Congolian Air Boundary (CAB) (Figure 5), separates the airflows of the Atlantic and Indian Oceans (Tyson and Preston-Whyte, 2000; Nicholson, 2000). The CAB marks a region where low pressure systems tend to preferentially form (Tyson and Preston-Whyte, 2000), and the annual cycle of the CAB causes the rainfall in Angola to be concentrated during March-April (Hirst and Hastenrath, 1983).

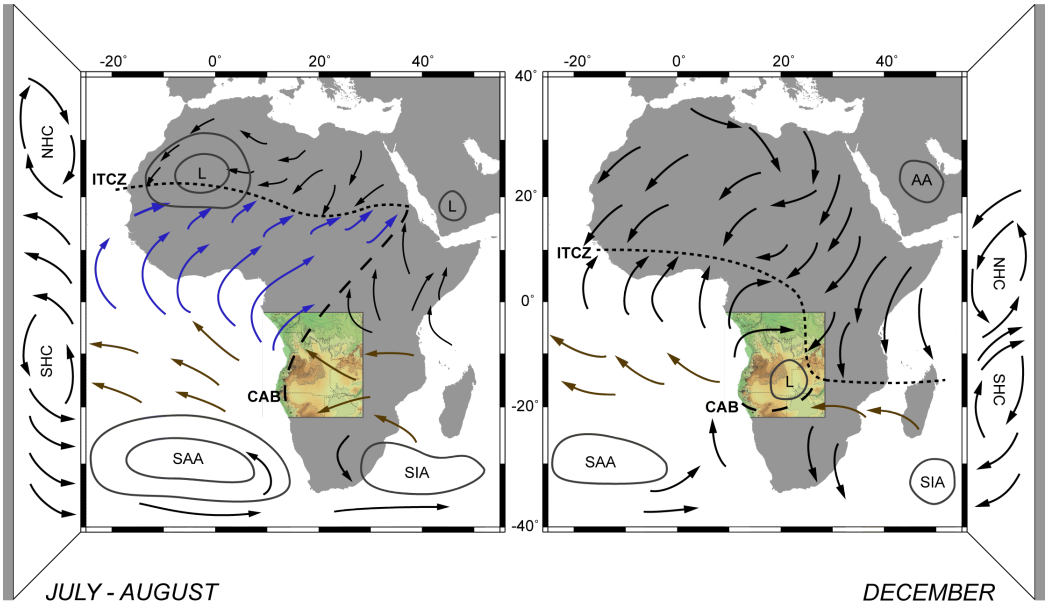

Figure 5: Schematic representation of general pattern of wind, pressure and convergence over Africa during austral summer and austral winter after Nicholson (2000). Dashed lines indicte position of Intertropical Convergence Zone (ITCZ) and Congolian Air Boundary (CAB). Arrows in the left panel indicate 3-dimensional atmospheric circulation. Arrows on screen indicate surface winds; black arrows = low level wind pattern, blue arrows = West African Monsoon, brown arrows = Trade winds. NHC = northern Hadley cell, SHC = southern Hadley cell, SAA = South Atlantic Anticyclone, SIA = South Indian Anticyclone, AA = Arabian Anticyclone.

Rainfall in southwest Africa is mainly influenced by the mid-latitude westerlies, the ITCZ and sea surface temperature (SST) off the continent (Nicholson and Entekhabi, 1987; Nicholson, 2000). According to Nicholson and Entekhabi (1987) it appears that the relationship between SST and rainfall is strongest at latitudes between 15° and 5°S. The highest precipitation along the coast of southwest Africa is coincident with the period of highest SST from March to April. The opposite situation prevails between June and August when both SST and precipitation are lowest (Hirst and Hastenrath, 1983). The West African Monsoon delivers moisture from the equatorial and southern tropical Atlantic Ocean towards tropical Africa is the West African Monsoon (Tyson and Preston-Whyte, 2000; Gasse et al., 2008, Giresse 2008). Although the monsoon plays a minor role in Angola, it is an important climatic feature in tropical Africa. The West African Monsoon winds originates from the South Atlantic Anticyclone and penetrates into northwest Africa during austral winter (Figure 5). Due to its direction (SSW, SW, or WSW) and speed the monsoon can not be clearly distinguished from the general westerly circulation prevailing year round in the equatorial region (Gasse et al., 2008; Giresse, 2008).

The meridional components of the atmosphere play a significant role in the transportation of water vapour and heat. There are three primary circulation cells, the Hadley cell, the Ferrell cell and the Polar cell, whereas the northern and southern Hadley cells dominate the tropical atmosphere. During austral summer the northern Hadley cell is located in the southern hemisphere (Figure 5). The southern Hadley cell is compressed and at 10°-15°S a region of maximum surface convergence develops between the two cells. Surface winds that emerge from near-surface air flows within the Hadley cell are known as Trade winds. The dominant winds of southern hemisphere Africa are the southeast Trade winds which are present throughout the year. Based on the annual migration of the Hadley cells the southeast Trade winds are most intense during austral winter and weakest during austral summer. Off the coast of southwest Africa the Benguela upwelling is driven by the southeast Trade winds which results in dry winds near the coast (Tyson and Preston-Whyte, 2000). A further important meteorological feature of southwest Africa, particularly of Angola, are Berg winds coming from the mountains lasting for hours up to several days. These Berg winds mainly occur during austral autumn and winter and are hot and dry westward blowing winds, generally vigorous, gusty and laden with dust and sand (Nelson and Hutchings, 1983; Shannon, 1985; Giresse, 2008).

4.6 Vegetation on the adjacent continent

One of the most complex and widely used descriptions of Africa's vegetation is the classification and map of White (1983). Based primarily on physiognomic parameters and grouped according to their floristic regions (phytochoria), White (1983) defined 17 main phytogeographical regions

for the African continent (Figure 6). Publications focusing particularly on the vegetation composition of Angola are rare, as a result of a civil war lasting decades. Shaw (1947) compiled a detailed description of the vegetation of Angola before the war began. Accordingly, the following discussion is based only on information given by White (1983) and Shaw (1947) and will focus on the vegetation of Angola and the southern Congo Basin.

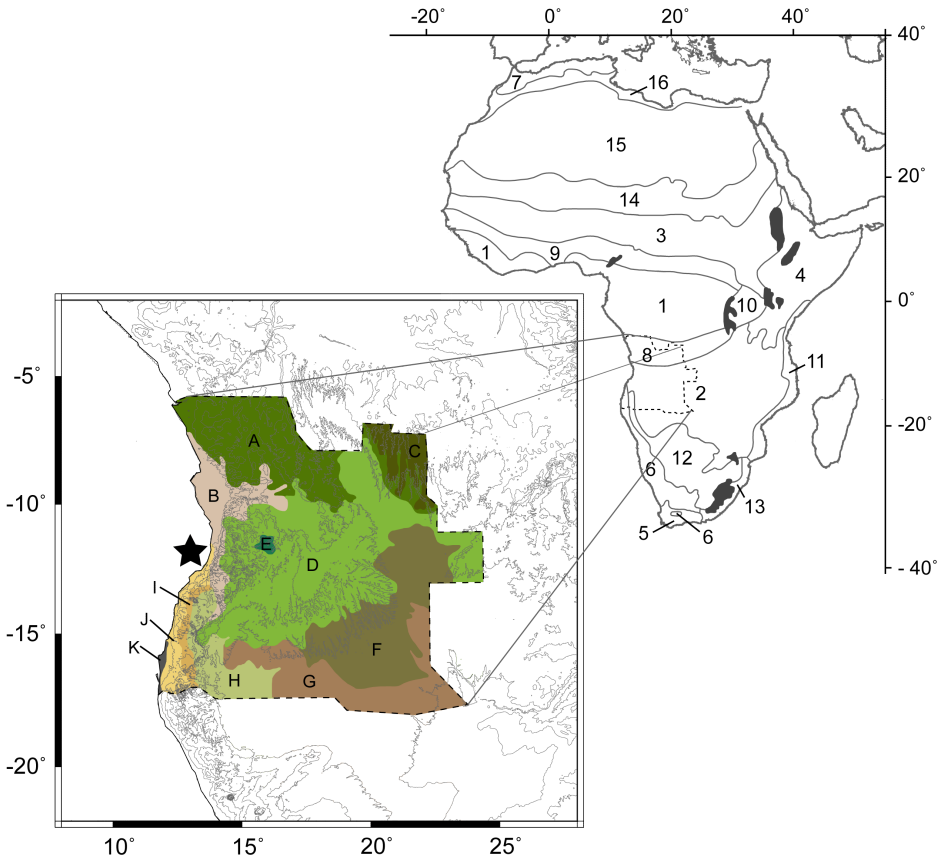

Figure 6: Africa's phytogeographical Regions and simplified vegetation types of the pollen source area of ODP Site 1078 (marked with a black star) after White (1983). Phytogeographical region: 1 = Guineo-Congolian center of endemism, 2 = Zambezian, 3 = Sudanian, 4 = Somalia-Masai, 5 = Cape region, 6 = Karoo-Namib, 7 = Mediterraenan, 8 = Guinea-Congolia/Zambezian transition zone, 9 = Guinea-Congolia/Sudania transition zone, 10 = Lake Victoria regional mosaic, 11 = Zansibar-Inhambane regional mosaic, 12 = Kalahari-Highveld transition zone, 13 = Tongoland-Pondoland regional mosaic, 14 = Sahel transition zone, 15 = Sahara transition zone, 16 = Mediterraenan/Sahara transition zone; Vegetation types: A = Mosaic lowland tropical forest and secondary grassland, B = undifferentiated Zambezian woodland, C = Guineo-Congolian tropical forest, D = Zambezian Miombo woodland, E = undifferentiated Zambezian woodland, F = Mosaic of thicket, edaphic- and secondary grassland, G = dry deciduous forest and secondary grassland, H = *Colophospermum mopane* woodland and scrub woodland; I = transition of woodland to Karoo-Namib scrubland; J = bushy Karoo-Namib scrubland, K = Desert

In general the vegetation of Angola is comparably uniform, with tropical grasslands (savanna) being the dominant biome. Tropical forest of the Congo reaches into Angola only in the extreme north. True desert and semi-desert occurs only within a narrow coastal area in the south-west of Angola. However, Angola's topography, soils and climatic conditions make vegetation composition highly diverse and complex when considered in detail (Figure 6).

The north of Angola and the southern Congo Basin belong to the complex Guinea-Congolia/Zambezian transition zone. Large parts of this zone, only 500 km wide, are covered by a mosaic of lowland semi-evergreen tropical forest, secondary grassland and wooded grassland. Restricted areas in the north of the transition zone are traversed by drier types of tropical seasonal forest. Towards the south a mosaic of Zambezian dry evergreen forest, Miombo woodland, edaphic and secondary grasslands occur. The main part of Angola is represented by the Zambezian phytochoria with woodland being the most characteristic type of vegetation. Climatically, the Zambezian region is situated within Walter's tropical summer-rainfall zone with a single rainy season. Precipitation varies between 500 and 1400 mm, generally decreasing from north to south, however, large regional variations occur. Average temperatures are related more to altitude than latitude and vary between 18° and 24°C. Highlands such as the Huambe Mountains, the Benguela Plateau and the Bié Plateau constitute large areas of Angola, and support the Afromontane and Afroalpine vegetation communities. On these mountainous areas and the flanking escarpment Miombo woodland prevails. Miombo woodland is floristically and physiognomically very different from other types of woodland and is nearly always dominated by *Brachystegia*, with or without *Julbernardia* and *Isoberlinia*. An important representative of Afromontane forests, *Podocarpus*, grows in more humid localities. Starting on the eastern slopes of the Bié Plateau a mosaic of *Brachystegia bakerana* thicket, edaphic and secondary grassland prevail. A mosaic of dry deciduous forest and secondary grassland dominates the south and southeast of Angola. A small region in the southwest of Angola is covered by *Colophospermum mopane* woodland and scrub woodland. Communities dominated by *Colophospermum mopane* are widespread in drier parts of the Zambezian phytogeographical region. Mopane grows under a wide variety of climate conditions, however, its actual distribution is limited by fire and competition with other species. Towards the west the Kalahari-Highveld transition zone follows as a narrow band. In Angola this phytochoria is merely represented by a transition zone of *Colophospermum mopane* scrub woodland and Karoo-Namib scrubland. The northernmost extension of the Karoo-Namib region is a narrow zone along the southern coast of Angola where bushy Karoo-Namib scrubland and Namib-desert elements are the prevailing vegetation types.

5 Methodology

5.1 The palynological method

Terrestrial ecosystems including vegetation are an integral component of the Earth's climate system. The global vegetation distribution is mainly influenced by the prevailing climate through precipitation, temperature, light and atmospheric CO_2 (e.g. Liu et al., 2006). Therefore, changes in climate, whether driven by natural or anthropogenic forcings, lead to changes in the vegetation. Changes in the vegetation cover, however, also influences the climate substantially by altering the energy budget, surface albedo, exchange of heat and water, and atmospheric CO_2 (Foley et al., 1998; Liu et al., 2006; Bonan et al., 2008). Processes and mechanisms coupling climate and vegetation play an important role in climate change, especially since interacting feedbacks are likely to modify the magnitude of climate change (e.g. Wramneby et al., 2010).

The late Quaternary has been characterised by a regime of alternating glacial and interglacial conditions that are also reflected in the vegetation composition (e.g. Fletcher et al., 2010; Jiménez-Moreno et al., 2010; Takahara et al., 2010; and references therein). Paleovegetation studies utilize the knowledge of the global vegetation system and its feedback mechanisms to interpret the reconstructed vegetation as climate conditions (e.g. González et al., 2008; 2009; Dupont et al., 2006; 2007; 2008). The reconstruction of vegetation is based on palynological methods. Palynology is the study of palynomorphs, organic particles sized between 5 to 500 ţm found in sedimentary records. Palynomorphs include pollen, spores, fungi, dinoflagellates, chitinozoans, achritarchs amongst other. Marine palynology developed initially as a stratigraphic tool in the petroleum industry (e.g. Muller, 1959). Meanwhile, marine palynology has proved to be a useful tool to reconstruct past vegetation and environmental conditions on the adjacent continent using pollen and spores (e.g. Behling et al., 2002; Hooghiemstra et al., 2006; Dupont et al., 2008), while prevailing paleoceanographic conditions can be reproduced using dinoflagellate cysts (e.g. González et al., 2008; Marret et al., 2008).

The research field of marine palynology has several advantages over the records obtained from terrestrial sites such as lakes, bogs and dung. One of the most important advantages is that information can be obtained for regions where terrestrial records are not continuous and/or not available (e.g. northern African tropics). A discontinuity in the terrestrial records may occur when sedimentation was interrupted by unfavourable environmental conditions. The scarcity of terrestrial pollen records may further be attributed to the lack of suitable deposition sites or to unfavourable climate conditions that prevented organic accumulation. In such cases when good terrestrial records are not availably, vegetation records from offshore marine cores can

be used to gain a unique insight about the vegetation development on the adjacent continent. Using marine sediments for the reconstruction of terrestrial vegetation requires the consideration of several factors. It is important to evaluate if the pollen source area can be reconstructed and if the transport mechanisms (wind, rivers, ocean currents) can be recognised and assessed. Furthermore, the temporal resolution of the marine core might not be always be as high as a terrestrial pollen record, possibly requiring the adjustment of the scientific questions. Marine vegetation records can be difficult to interpret since the pollen originate from a large source area, and therefore may include several types of vegetation (Dupont and Wyputta, 2003). Nevertheless, the results of various studies demonstrate that palynological methods have been successfully applied to marine sediments (e.g. Lézine and Vergnaud-Grazzini, 1993; Haberle and Maslin, 1999; Behling et al., 2000; 2002; Ansari and Vink, 2007; Behling et al., 2000; 2002; Hooghiemstra et al., 2006; Dupont et al., 2006; 2007; 2008; 2009; Marret et al., 2008; González 2008; 2009).

5.1.1 Origin and transport of organic terrigenous material

The distribution of pollen and spores in marine sediments depends not only on the composition of the vegetation in the source area but also on the distance from the continent to the ocean floor and the transport processes delivering the terrigenous material (Groot, 1971; Groot and Groot, 1971; Heusser, 1988). Fluvial and aeolian transport deliver pollen and spores from their origin to the marine sediments. Raynor et al. (1974) pointed out that the transport of large quantities of pollen from their source region is governed by the diurnal cycle and meteorological conditions. These authors also suggested that pollen grains carried from heated land masses over cooler water bodies tend to form large, discrete clouds with maximum concentrations at some distance above surface. The three main stages that need to be considered in the fluvial transport of pollen and spores are 1) the transfer of pollen and spores from vegetation to the river channel, 2) transport within the river channel, and 3) the pattern of deposition in the receiving basin (Chmura et al., 1999). In general, fluvial transported pollen and spore assemblages provide a more inclusive vegetation record than primarily wind transported assemblages. In contrast, pollen deposits in coastal waters distant to river mouths are biased towards those taxa which are effectively transported by wind; particularly wind pollinated arboreal species (Chmura et al., 1999).

The relative importance of transport processes, however, varies regionally as shown by several studies from different regions (Muller, 1959; Hooghiemstra and Agwu, 1986; Heusser, 1988; Traverse, 1990; Dupont, 1999; van der Kaars, 2001; Dupont and Wyputta, 2003). Transport by rivers is especially high and important in humid tropical areas (Dupont, 1999), whereas

aeolian transport of pollen and spores dominates in arid areas where river discharge is limited (Hooghiemstra, 1986). The sedimentation of pollen and spores delivered by rivers and wind is thought to be comparable to the sedimentation of fine silt and clay sized particles (Heusser, 1988). Wefer and Fischer (1993) suggest that pollen and spores are caught in larger aggregates leading to an increased sinking velocity of about 100 m per day in the marine realm. The lateral transport of pollen and spores by oceanic surface and/or bottom currents needs to be evaluated for every location. However, several studies have shown that the distribution of pollen and spores in marine sediments reflect the position of climatic zones and the related vegetation on the adjacent continent, thus providing a tool to reconstruct changes in both during the past (Hooghiemstra, 1986; Heusser, 1988; Dupont and Agwu, 1991).

The distribution pattern of pollen and spores in marine sediments is furthermore related to the quantity of grains produced by each species which differs considerably (Groot and Groot, 1971; Duffin and Bunting, 2008). Therefore, knowledge and estimations of pollen production need to be considered to interpret the reconstructed past vegetation composition as accurately as possible. Arboreal plants are, compared to grasses or sedges, poor pollen producers resulting in a relative under-representation of arboreal taxa in marine sediments (Duffin and Bunting, 2008). However, there are a number of other factors that complicate the study of pollen sequences in marine sediments. For example, many plants have a wide ecological and geographical distribution, making it difficult to narrow down the pollen source area. Moreover, the level of identification of pollen and spores is often limited to the genus or even family level, increasing the number of possible source areas (van der Kaars, 2001).

Dupont and Wyputta (2003) used a trajectory model combined with cluster analysis to reconstruct the potential pathways of pollen and spores from the African continent into the tropical eastern Atlantic. According to this work, Angola and the southern Congo Basin can be assigned as the main source area for pollen and spores identified in the sediments of ODP Site 1078. Their results also indicate a predominantly aeolian transport towards the Angolan Basin. During spring and summer transport of terrigenous particles towards the ocean is low since most clustered trajectories do not pass over land. Easterly winds prevail during fall and winter carrying pollen, spores and other terrestrial particles far from the interior of the African continent towards the Atlantic. Trajectories and clusters were modeled for two time-slices, the present-day and the LGM, and indicate a stable pollen source area throughout the last glacial-interglacial cycle at least (Dupont and Wyputta, 2003). These authors also suggested that the dispersal of pollen and spores by ocean currents is minor in this area. Besides the transport of pollen and spores through the air, river transport plays an important role at ODP Site 1078. Large parts of the

pollen and spores found in the sediments may originate from the Balombo river that drains a small high-altitude region in the Huambe Mountains of Angola (Dupont et al., 2007).

5.1.2 Palynological preparation

The preparation of palynological samples followed a standard procedure in accordance with Faegri and Iversen (1989). In order to avoid damage of organic-walled dinoflagellate cysts the oxidative acetolysis step was omitted.

Firstly, the sediment sample volume was measured (mostly ~3 cm^3) by water displacement, the sample transferred to a container, and macerated using spoon a the minimum amount of purified water required. Samples were then treated with 10% hydrochloric acid (HCl) in order to remove calcareous components. During the decalcification process two tablets of exotic *Lycopodium clavatum* spores (2 tablet = 21358 spores) were added to determine pollen or dinoflagellate cyst concentrations (specimens/cm^3) and pollen or dinoflagellate cyst influx (specimens/cm^2/yr) (Stockmarr, 1971). The removal of silicates was carried out using 40% hydrofluoric acid (HF) with samples remaining in the HF solution for a minimum of 48 hours. After neutralisation with 40% potassium hydroxide (KOH), samples were briefly ultrasonically sieved over an eight micron (8 μm) mesh to extract particles smaller than 10 μm. The residue was concentrated by centrifugation and decanted into micro-tubes for storage.

For identification of pollen grains, spores, palynomorphs and dinoflagellate cysts slides were prepared by mounting 10 μl of residue in glycerine, evaporating the distilled water and covering the remaining material with a cover slip. The advantage of these non-fixed mobable sample slides is the ability to turn and unfold unrecognisable specimens to improve identification. Sample slides were microscopically examined at 400 times magnification, whereas 1000 times magnification was used when the subtlest details were required for a clear assignment. For pollen samples including spores and other palynomorphs, about 300 specimens were counted for each sample. Likewise, for each sample about 300 dinoflagellate cysts were counted. For a few samples with low specimen concentrations in the sediments, only 100-250 specimens were counted. Identification of pollen grains and spores was achieved using the references collection of the University of Göttingen, Department of Palynology and Climate Dynamics, the African Pollen Database (http://medias.obs-mip.fr/pollen/), and several publications (Bonnefille and Riollet, 1980; Maley, 1970; Sowunmi, 1973; 1995; Ybert, 1979). Pollen percentages were calculated on the basis of the pollen sum including terrestrial pollen taxa, aquatic pollen taxa (mainly Cyperaceae and *Typha*) and fern spores.

5.2 The Mg/Ca method

The calcite shells of planktonic foraminifera are one of the most important archives used for paleoceanographic reconstructions. Both their trace element and isotopic composition carry information about variations in surface water conditions. During the precipitation of foraminiferal shell calcite the incorporation of magnesium is influenced by the temperature of the surrounding seawater so that Mg/Ca of the foraminiferal calcite increases with increasing temperature (Elderfield and Ganssen, 2000; Barker et al., 2005). Therefore, the Mg/Ca ratio of planktonic foraminifera is widely used to reconstruct past seawater temperature (Elderfield and Ganssen, 2000; Lea et al., 2000; Stott et al., 2002; Steinke et al., 2005; Mohtadi et al., 2010). The sensitivity of the Mg/Ca thermometer (~9% per °C) makes it a very useful tool, especially for tropical regions where changes In SST are thought to have been small (Dekens et al., 2002). Mg/Ca thermometry has the advantage over other paleotemperature proxies in that it is measured on the same calcite as the oxygen isotopes, offering the possibility to reconstruct changes in the oxygen isotope composition of seawater (Elderfield and Ganssen, 2000). To obtain accurate Mg/Ca paleotemperatures a species-specific calibration is essential (Mashiotta et al., 1999; Lea et al., 2000; Dekens et al., 2002; Rosenthal and Lohmann, 2002; Anand et al., 2003). This method can also be applied to investigate changes in the thermal structure of the water column using multiple species from different depth and/or seasonal habitats (e.g. Barker et al., 2005). Variations of the Mg/Ca of seawater is not expected on glacial-interglacial timescales (Rosenthal et al., 2000; Barker et al., 2005) and the Mg/Ca of seawater is constant throughout the ocean as the residence time for both elements is more than a million years (Goldberg and Arrhenius, 1958). However, post-depositional dissolution on foraminifera shells can influence shell composition and thus temperature reconstruction (Brown and Elderfield, 1996; Rosenthal et al., 2000; Dekens et al., 2002, Regenberg et al., 2006; Mekik et al., 2007).

5.2.1 Foraminifera

Measurements of Mg/Ca and stable oxygen isotope ratios (Chapter 5.3) were accomplished using two different species of planktonic foraminifers. Changes in near-surface water conditions are reflected by the pink variety of the surface-dweller *Globigerinoides ruber* (d'Orbiny). The pink form of *G. ruber* became extinct in the Indian and Pacific Ocean during the late Pleistocene, but continued living in the warm waters of the Atlantic Ocean and Mediterranean Sea (Thompson et al., 1979). These authors also suggested that in the Atlantic the white variety of *G. ruber* predominate in the colder period of the year while the pink pigmented variation occurs during the warmer periods of the year. *G. ruber* is found under oligotrophic and mesotrophic conditions and has dinoflagellate symbionts which make it light-depend (Hemleben et al., 1989;

Zaric et al., 2005). Sediment trap studies suggest *G. ruber* (pink) occurs within a temperature range between 16.4° and 29.6°C, with optimum temperatures around 26°C (Zaric et al., 2005).

The second species used for this study is the non-spinose and symbiont barren *Globigerina bulloides* (d'Orbigny) which is typical for upwelling environments (Bé and Tolderlund, 1971, Hemleben et al., 1989). *G. bulloides* occurs in a water depths above 400 m, but is mainly found in and above the thermocline (Hemleben et al., 1971). In the South Atlantic, the highest concentrations of *G. bulloides* are usually observed between October and March in water temperatures ranging from 0° to 27°C (Bé and Tolderlund, 1971). Sediment trap studies could not establish a clear signal of SST influence but a dependency on nutrients and hence on the intensity of upwelling (e.g. Zaric et al., 2005).

5.2.2 Preparation and measurement

For Mg/Ca and oxygen isotopes analyses of *G. ruber* (pink) and *G. bulloides*, 155 samples of 10 cm^3 volume were taken from ODP Site 1078 hole C. The average sample resolution of 2 cm results in an average temporal resolution of 200 years. The sediment samples were washed over a 63 μm sieve, dried and further divided by dry sieving. About 40 specimens of *G. bulloides* were hand picked from the 250-315 μm size fraction and were gently crushed. Since *G. ruber* (pink) was not abundant in the sediment, specimens from both the 250-315 μm and 315-400 μm size fractions were combined. Between 15 and 40 specimens of *G. ruber* (pink) were taken from the 250-400 μm fraction, gently crushed between two clean glass plates and transferred to micro-centrifuge tubes for cleaning.

Sample cleaning followed the cleaning protocol described by Barker et al. (2003) based on that of Boyle (1981) and Boyle and Keigwin (1985). The first step, clay removal, composed of five water washes where each time 500 μl water (Seralpur > 18MΩ water used throughout) was added to each tube, the samples were ultrasonicated briefly and the water siphoned off after 30 seconds. After the water washes, two washes with 250 μm methanol were used to further remove clays before a final rinse with water. Following the clay removal the oxidation step was applied to remove organic matter. For this purpose 250 μl alkali buffered 1 % H_2O_2 solution was added to each sample and then heated for 10 minutes in a boiling water bath. Every 2.5 minutes, the vials were rapped on the bench top to release any gaseous build-up. After 5 minutes, the samples were placed in an ultrasonic bath for a few seconds to maintain the contact between reagent and sample. This step was repeated to ensure the removal of organic matter. Following oxidation each sample was transferred into fresh acid cleaned micro-tubes. Re-absorbed ions on test fragments were removed with a weak acid leach in 250 μl of 0.001 M HNO_3. During

leaching the samples were ultrasonicated for 30 seconds before the acid was removed and the samples rinsed with water to avoid dissolution. After repeating the weak acid leach step the samples were dissolved using 500 μl of 0.075 M HNO_3. Once dissolved, any remaining solids were removed by centrifuging for 10 minutes and transferring the supernatant into clean sample tubes.

Samples were measured with an ICP-OES (Perkin Elmer Optima 3300 RL with an ultrasonic nebulizer U-5000 AT Cetac Technologies Inc. at the Department of Geosciences, University of Bremen. Instrumental precision of the ICP-OES was assessed by analysis of an in-house standard solution every fifth sample. It is important that the used standard solution (Mg/Ca ratio of 2.9 mmol/mol) has an Mg/Ca similar to the analysed foraminifer samples. Since the Mg/Ca ratio of both *G. ruber* (pink) and *G. bulloides* only differ slightly the same in-house standard solution was used for measurements.

Rosenthal et al. (2004) conducted an interlaboratory comparison study of Mg/Ca and found offsets among participating laboratories. Therefore, direct comparison between data sets originating from different laboratories are difficult to implement. In order to allow our data to be directly compared with that from other laboratories the international limestone references material (ECRM752-1), with a Mg/Ca ratio of 3.75 mmol/mol (Greaves et al., 2008), was routinely analysed twice with each batch of 50 samples. Additionally, Al/Ca, Fe/Ca and Mn/Ca were measured to monitor the efficiency of the cleaning (e.g. Barker et al., 2005).

5.2.3 Temperature calibration

Obtaining paleotemperatures from Mg/Ca data requires the application of an empirical temperature calibration. Generally good agreement has been found between calibrations based on laboratory culturing, plankton tow, sediment trap, and core top studies, however, the different techniques have their advantages and disadvantages. The advantage of calibrations from culture experiments (e.g. Nürnberg et al., 1996; Lea et al., 1999, Mashiotta et al., 1999) is clearly that foraminifera calcify under prescribed and exactly known temperatures. However, it needs to be considered that these controlled environments do not reflect growth and calcification under natural conditions. Established temperature calibrations based on core top (Elderfield and Ganssen, 2000; Lea et al., 2000; Dekens et al., 2002) or sediment trap studies (Anand et al., 2003; McConnell and Thunell, 2005) reflect the material that eventually will form the paleoceanographic record. However, a disadvantage compared to culture experiments is clearly that the temperature is not known precisely, but rather must be estimated by, for example, the calcification temperature estimated from foraminiferal δ^{18}O (Elderfield and Ganssen, 2000;

Anand et al., 2003). Further complications can arise from possible post-depositional alteration including dissolution.

In this study, the calculation of paleotemperatures based on the Mg/Ca ratio of *G. bulloides* was accomplished using the temperature calibration of Mashiotta et al. (1999). In their calibration, culture experiments with living foraminifera provided the basis of the Mg/Ca-temperature relationship for *G. bulloides*. Two core-top points were added to the culture data, increasing the exponential fit and resulting in the following equation.

(1) Mg/Ca (mmol/mol) = 0.474 exp.[0.107 x SST (°C)] $R^2 = 0.98$

The standard error of equation 1 is ± 0.09, units of ln(Mg/Ca), which is equivalent to ± 0.8°C. The 95% confidence interval varies from ± 0.3°C at 16°C to ± 0.6°C at both 10° and 25°C. In order to directly calculate the temperature from the Mg/Ca ratio equation 1 is rearranged.

(2) SST (°C) = [ln(Mg/Ca)-ln(0.474)]/0.107

Paleotemperatures for *G. ruber* (pink) were calculated using the temperature calibration of Anand et al. (2003) based on core-top samples.

(3) Mg/Ca (mmol/mol) = 0.30 exp. [0.089 x SST (°C)]

The standard error of this expression is ± 0.6°C. In order to estimate the sea surface temperature equation 3 must also be rearranged.

(4) SST (°C) = [ln(Mg/Ca)-ln(0.30)]/0.089

5.2.4 Potential Dissolution effect

One possible source of error for the Mg/Ca-paleothermometer is the partial dissolution of foraminiferal calcite within the water-column, at the water-sediment interface, and within the sediments (Berger, 1970). Rosenthal et al. (2000) indicate that dissolution alters the bulk shell chemistry rather than selectively removing more soluble individuals. Since different parts of the shell were formed at different water depths and temperatures, and by different biomineralisation mechanisms, different types of shell calcite display different dissolution susceptibilities (Rosenthal et al., 2000; Hathorne et al., 2009).

Several studies from different geographical regions indicate a decrease in the Mg/Ca ratio in foraminiferal tests as a result of dissolution (Rosenthal and Boyle, 1991; Brown and Elderfield, 1996; Dekens et al., 2002; Regenberg et al., 2006). The degree of alteration of the Mg/Ca ratio, and therefore the bias of the reconstructed SST towards colder estimates, increases with water depth. Although dissolution alters the Mg/Ca ratio of the shells, the initial relationship with temperature seems robust (Rosenthal et al., 2000), meaning simple dissolution corrections can be applied. However, different species have variable resistance to dissolution (Berger, 1970; Dekens et al., 2002; Regenberg et al., 2006; Mekik et al., 2007; Yu et al., 2008). The Mg/Ca ratio of both surface dwelling species used in this study (*G. ruber*, *G. bulloides*) seems to be sensitive to temperature but is not systematically affected by dissolution (Dekens et al., 2002; Mekik et al., 2007). Therefore, surface dwellers such as *G. ruber* and *G. bulloides* do not require a correction for calcite dissolution to evaluate surface temperatures (Mekik et al., 2007). However, these findings are contrary to the results of Regenberg et al. (2006) who found an influence of dissolution on the Mg/Ca ratio of *G. ruber*. Even so, the very shallow depth of ODP Site 1078 (426 m water depth) is well above the lysocline so a dissolution effect on the foraminiferal Mg/Ca its not expected. Therefore no dissolution correction was applied to the Mg/Ca data in this study.

5.3 The Oxygen Isotope ratio δ^{18}O

The stable oxygen isotope composition is often regarded as the primary tool with which reconstruct past oceanographic and climatic conditions. The potential to be recorded in various (palaeo)-environmental archives (e.g. ice cores, marine and terrestrial carbonates, water) makes a unique proxy. The most abundant stable oxygen isotope within the Earth's system is ^{16}O (99.76%), followed by ^{18}O (0.2%) and ^{17}O (0.04%). Whenever a phase transition occurs within the Earth system the isotopes are fractionated, either kinetically or through equilibrium fractionation.

Temperature-dependet kinetic fractionation is associated with unidirectional processes such as evaporation and precipitation. During this type of fractionation, water evaporating from the sea surface is depleted in heavy ^{18}O relative to the ocean, while rain precipitating from a cloud is enriched relative to the cloud moisture. Since the World's tropical oceans are the major source of atmospheric water vapour the amount of ^{18}O is highest there. Towards the poles, as a result of gradual rainout, the remaining moisture and hence precipitation becomes depleted in ^{18}O. As a result the isotopic composition of precipitation varies strongly with latitude and altitude. On glacial-interglacial timescales the waxing and waning of continental ice, characterised by low oxygen isotope values, has a very strong effect on the isotopic composition of seawater. During

glacial intervals, the large continental ice sheets have preferentially stored the lighter isotope (^{16}O) resulting in an accumulation of the heavy isotopes (^{18}O) in the ocean. Hence, variations in the size of ice sheets are reflected in a variable isotopic composition of water (Shackleton, 1967). However, the average composition of glacial ice sheets must have varied with their size and latitudinal position, so the isotopic composition of the ocean is not a linear function of ice volume (Mix and Ruddiman, 1984).

First proposed by Urey (1947), the oxygen isotope ratio of carbonate minerals can be used to reconstruct temperature due to the thermodynamic or equilibrium fractionation between ^{18}O and ^{16}O occurring during mineral precipitation. Therefore, the shells of planktonic foraminifera record both, the oxygen isotope composition and temperature of the seawater from which they grew. Variations in the composition of ambient seawater are rather small compared to those of the atmosphere. Both the salinity and oxygen isotope composition of seawater are controlled by the precipitation-evaporation balance. The relationship between δ^{18}O and salinity varies considerably throughout the ocean because of the varying isotopic composition of the freshwater. Accordingly, high salinities and high δ^{18}O seawater occur at low latitudes, and low salinities and δ^{18}O values are found at high latitudes. Throughout the Quaternary, δ^{18}O values of seawater have also been subject to large variations due to fluctuations in the continental ice volume. This so called global "ice volume effect" was estimated to be about 1.3‰ for the last deglaciation (Fairbanks, 1989), and these changes need to be considered when absolute SST is reconstructed from the δ^{18}O of planktonic foraminifera.

When the δ^{18}O of foraminiferal calcite and the temperature of calcification (e.g. via Mg/Ca thermometry) are known, the stable oxygen isotope composition of seawater, depending on global ice volume and local temperature and salinity, can be established based on a paleotemperature equation. There are a number of temperature calibrations in use for oxygen isotopes in planktonic foraminifera. These are derived from culturing experiments (Bemis et al., 1998), core-top calibrations (Shackleton, 1974), inorganic calcite precipitation (Kim and O'Neil, 1997), or have been established using a field based temperature-oxygen isotope relationship (Mulitza et al., 2003).

Besides the temperature and the δ^{18}O of the ambient seawater, the stable isotopic composition of planktonic foraminifera is influenced by several complicating factors. Physiological (vital) effects such as the photosynthesis of symbionts (e.g. Spero and Lea, 1993; 1996; Bemis et al., 1998), calcification rate (e.g. Spero and Lea, 1993; 1996), addition of gametogenic calcite at depth (e.g. Duplessy et al., 1981) as well as the pH of the seawater in which the calcification

occurs (Spero et al., 1997; Zeebe, 1999), influence the degree to which foraminiferal calcite is produced in oxygen isotopic equilibrium with the ambient seawater. Further factors that might bias the δ^{18}O signal are the seasonality of different species and their vertical migration through the water column (Sautter and Thunell, 1991). Post depositional artefacts, such as bioturbation and calcite dissolution may alter the isotopic signal of the mean foraminifer population in the sediment.

Nevertheless, the stable oxygen isotope composition of marine carbonates, especially foraminifera, is the main proxy used in paleoceanography. It is commonly used to reconstruct the structure of the upper water column (e.g. Mulitza et al., 1997), the variability of the ocean circulation (e.g. Vidal et al., 1997), seawater density (e.g. Lynch-Stieglitz et al., 1999), sea surface salinity (e.g. Lea et al., 2000), continental ice volume (e.g. Waelbroeck et al., 2002), freshwater input into the ocean (e.g. Duplessy et al., 1991), and the stratification of surface waters (e.g. Niebler et al., 1999).

5.3.1 Preparation and measurement

Measurements of the stable oxygen isotope ratio ($\delta^{18}O_{calcite}$) of *G. bulloides* were conducted for the intervals used for Mg/Ca analysis. Depending on the availability of material, between 6 and 12 specimens were picked from the size fraction 315-250 μm size. The analysis of $^{18}O/^{16}O$ ratio of calcite was performed using a Finnigan MAT 251 mass spectrometer with an automated carbonate preparation device at the Department of Geosciences, University of Bremen. The external standard error of the stable oxygen isotope analyses is < 0.06‰. Oxygen isotope values of carbonates are reported relative to the Vienna Pee Dee Belemnite (VPDB), here calibrated using the National Bureau of Standards (NBS) 18, 19, and 20 standards. The oxygen isotope composition of foraminifera (δ^{18}O), is usually expressed as the difference between the $^{18}O/^{16}O$ ratio of the sample and that of the standard (see next subchapter) as parts per thousand (per mil [‰]).

$$\delta^{18}\text{O } [‰] = \frac{(^{18}O/^{16}O)sample - (^{18}O/^{16}O)standard}{(^{18}O/^{16}O)standard} \text{ x } 1000$$

Due to the lack of availability of *G. ruber* (pink) no $^{18}O/^{16}O$ measurements could be accomplished on shells for that species. In the present study the empirical temperature calibration of Shackleton (1974) is used:

$$T\ [°C] = 16.9 - 4.38 \text{ x } (\delta^{18}\text{Ocalcite} - \delta^{18}\text{Osw}) + 0.1 \text{ x } (\delta^{18}\text{Ocalcite} - \delta^{18}\text{Osw})^2$$

where T represents the *in-situ* temperature during calcite precipitation (°C), δ^{18}Ocalcite stands for the oxygen isotope composition of the calcite (‰, VPDB), and δ^{18}Osw stands for the oxygen isotopic composition (‰, VSMOW) of the seawater from which the calcite precipitated.

6 Results

6.1 Millennial-scale changes in vegetation records from tropical Africa and South America during the last glacial

Ines Hessler[a*], *Lydie Dupont*[a], *Raymonde Bonnefille*[b], *Hermann Behling*[c], *Catalina González*[d], *Karin F. Helmens*[e], *Henry Hooghiemstra*[f], *Judicael Lebamba*[h], *Marie-Pierre Ledru*[i], *Anne-Marie Lézine*[g], *Jean Maley*[h], *Fabienne Marret*[j], *Annie Vincens*[b]

[a] MARUM - Center for Marine Environmental Sciences, University of Bremen, 28359 Bremen, Germany

[b] CEREGE, CNRS/Université Aix-Marseille/IRD/CdF, BP 80, 13545 Aix-en-Provence cedex 04, France

[c] Department of Palynology and Climate Dynamics, Albrecht-von-Haller-Institute for Plant Sciences, University of Göttingen, Göttingen, Germany

[d] Faculty of Geosciences, University of Bremen, Bremen, Germany

[e] Departement of Physical Geography and Quaternary Geology, Stockholm University, SE-106 91 Stockholm, Sweden

[f] Department of Paleoecology and Landscape Ecology, Institute for Biodiversity and Ecosystem Dynamics, University of Amsterdam, Science Park 904, 1098 XH Amsterdam, Netherlands

[g] Laboratoire des Sciences du Climat et de l' Environement, UMR 1572 CNRS-CEA, F-91198 Gif-sur-Yvette cedex, France

[h] Dept. Paléoenvironments, ISEM, Université Montpellier 2-CNRS, Montpellier, France

[i] IRD-UMR 203, Institute of Evolution Sciences, University of Montpellier,2, Montpellier, France

[j] Department of Geography, University of Liverpool, Liverpool, UK

[*] Corresponding Author: Tel.: +49 (0) 421 - 218 65682, Email: ihessler@marum.de

Published in Quaternary Science Reviews 29 (2010), 2882-2899

6.1.1 Abstract

To reconstruct the response of vegetation to abrupt climate changes during the last glacial we have compiled pollen records from the circum-Atlantic tropics between 23°N and 23°S from both marine and terrestrial sediment cores. Pollen data were grouped into megabiomes to facilitate the comparison between the different records. Most tropical African records do not appear to register Dansgaard-Oeschger (D-O) variability, although there are vegetation changes during Heinrich Stadials (HS). There is a stronger signal of D-O and HS variability in the South American records. Records close to the modern northern and southern limits of the Intertropical Convergence Zone (ITCZ) show opposite trends in vegetation development during HS and D-O cycles. The pollen data from tropical South America corroborate the hypothesis of a southward shift in the migration pattern of the ITCZ and a reduction in the Atlantic Meridional Overturning Circulation (AMOC) during HS.

6.1.2 Introduction

The last glacial (73.5 to 14.7 ka, following the definition of Sanchez Goñi and Harrison, this volume) was marked by large and abrupt climate variability in the form of D-O cycles and Heinrich events (e.g. Bond et al., 1997; Sarnthein et al., 2001). Periods associated with North Atlantic Heinrich events and the Younger Dryas (YD) climatic perturbation have been shown to occur at a global scale (Voelker et al., 2002). The EPICA members (2006) corroborated the seesaw hypothesis (e.g. Crowley, 1992, Rühlemann et al., 1999) showing a strict coupling of all Antarctic warm and Greenland cold events. The response to these events varies geographically and the mechanisms behind them are still poorly understood although it is generally accepted that the strength of the AMOC plays an important role (e.g. Sarnthein et al., 1994; McManus et al., 2004; Clark et al., 2007).

D-O cycles that are prominent in Greenland ice cores are characterised by rapid warming followed by progressive cooling. The 1,500 years D-O cycles are thought to be related to a weakening of deep water formation in the North Atlantic by dilution of the surface waters through ice melt or other processes. Deep water formation resumes as a response to the build-up of salty waters (e.g. Alley, 1998).

Heinrich (1988) documented layers (Heinrich layers) with high lithic fragment content that are associated with the abrupt occurrence of cold intervals (HS) at the end of D-O cycles in the North Atlantic. It is thought that these cold intervals are triggered by iceberg discharges in the North Atlantic resulting in a reduction or possible shutdown of the AMOC (e.g. Broecker et al., 1992; see also Sanchez Goñi and Harrison, this volume). However, recent studies (e.g. Hall et al., 2006) indicate that

the collapse of the AMOC preceded the deposition of Heinrich layers and argue that Heinrich events are a response rather than the cause of AMOC collapse (Shaffer et al., 2004; Flückiger et al., 2006; Clark et al., 2007). Since there are several chronological limits for D-O cycles and HS in the literature in this review we followed the timings and durations given in Wolff et al. (this volume).

There are two contrasting hypotheses concerning the role of the tropics in relation to abrupt climate change. The first invokes changes in the tropical atmosphere-ocean dynamics as a cause of abrupt changes, and specifically argues the decrease in water-vapour transport out of the tropical Atlantic during stadials would lead to an increased net freshwater balance in the Atlantic affecting the density of ocean surface waters and the northward penetration of latent heat (e.g. Cane and Clement, 1999; Ivanochko et al., 2005; Schmittner et al., 2000). The second hypothesis attributes changes in the tropics to a slow-down of the AMOC, which might have been triggered by large iceberg discharges in the North Atlantic (e.g. Broecker, 2003; Rahmstorf, 2002). Our examination of vegetation records from the tropical regions of Africa and South America aims to shed light on the plausibility of these two hypotheses.

The aim of this paper is to document vegetation changes in tropical Africa and South America, specifically focussing on intervals coincident with D-O cycles as registered in Greenland and HS as identified in the North Atlantic. By reviewing the existing low and high resolution pollen data of tropical Africa and South America covering Marine Isotope Stage (MIS) 2, 3 and 4 (Table 1), we aim to document the impact (if any), timing and amplitude of rapid climate changes on the regional vegetation. Our synthesis provides the opportunity for a direct comparison of (1) sites situated north and south of the equator on the same continent, (2) responses of the tropical African and South American vegetation, and (3) pollen data with results of other terrestrial indicators. This synthesis also allows us to test the hypothesis that abrupt climate change in the tropics is the result of shifts in the migration pattern of the ITCZ during the last glacial coupled with changes in the AMOC (e.g. Peterson et al., 2000; Mulitza et al., 2008).

The climate of the circum-Atlantic tropics today is strongly coupled to the latitudinal position of the ITCZ, a low pressure belt of warm, moist air surrounding the Earth near the equator (Ruddiman, 2001). Due to the strong linkage between variations in atmospheric and oceanic conditions the position of the ITCZ follows a seasonal cycle, with an abrupt shift from its northernmost position during boreal summer to its southernmost position during austral summer. These variations in the position of the ITCZ affect the rainfall distribution in equatorial and tropical regions, resulting in alternating wet and dry seasons (Figure 7). Far from the equator the dry season (winter) is severe and the rainy season (summer) short; near the equator two short dry seasons occur (Ruddiman, 2001).

The annual migration of the ITCZ is influenced by the distribution of land and ocean. Over the

ocean the ITCZ is well defined by the combination of convergence of trade winds and subsequent convection and heavy rainfall. As a result moist air masses from the tropical Atlantic penetrate eastwards into the interior of the African continent during austral summer. In East Africa the penetration of the easterly flow is limited by the highlands. Over land, the meridional oscillation of the ITCZ across the equator responds to the seasonal insolation cycle and the near-surface convergence and convection become widely separated during the season of maximum excursion (northern- or southernmost ITCZ position). Thus, the latitude of surface convergence between trades and monsoon over north-western Africa in August is around 18-20°N, whereas the latitude of the rainbelt (associated with convection) is about 10°N (Leroux, 1983; Nicholson, 2000). In South America during austral summer, when the ITCZ is located at its southernmost position, trade winds transport moisture from the equatorial Atlantic towards the Amazon basin causing the South American Summer Monsoon (Gan et al., 2004). These trade winds are channelled to the southeast to 20-23°S by the Andean Cordillera. During the winter season the ITCZ moves to its northernmost position at ~ 10°N.

The vegetation distribution within the tropical regions is strongly affected by the length and the intensity of the dry season. However, it is not only the total amount of annual precipitation that is important, but also the seasonal distribution of rainfall. The presence or absence of a consistent cloud cover also influences the plant growth by limiting the solar radiation and the effective evapotranspiration. Additionally, the temperature has an effect on the evapotranspiration and therefore influences the moisture availability. In the tropics temperature alone rarely limits vegetation growth except in high mountain areas.

The present day African vegetation around the equator consist of tropical forests including evergreen rainforest in the Congo basin and in the moist part of western Africa, to semi-evergreen and deciduous forest in northern Cameroon or southern Congo. North and south of the forest fringes there is a narrow belt of natural grass savannah. North of the xerophytic shrubland of the Sahel zone and along the coast of Namibia and southwest Angola desert vegetation occurs (White, 1983; BIOME4, Kaplan et al., 2003). The modern South American vegetation is dominated in the north by savannah, evergreen and semi-evergreen broadleaf forest. In the east and southeast deciduous forest and woodland, savannah, xerophytic shrubland and warm-temperate mixed forest prevail (BIOME4, Kaplan et al. 2003).

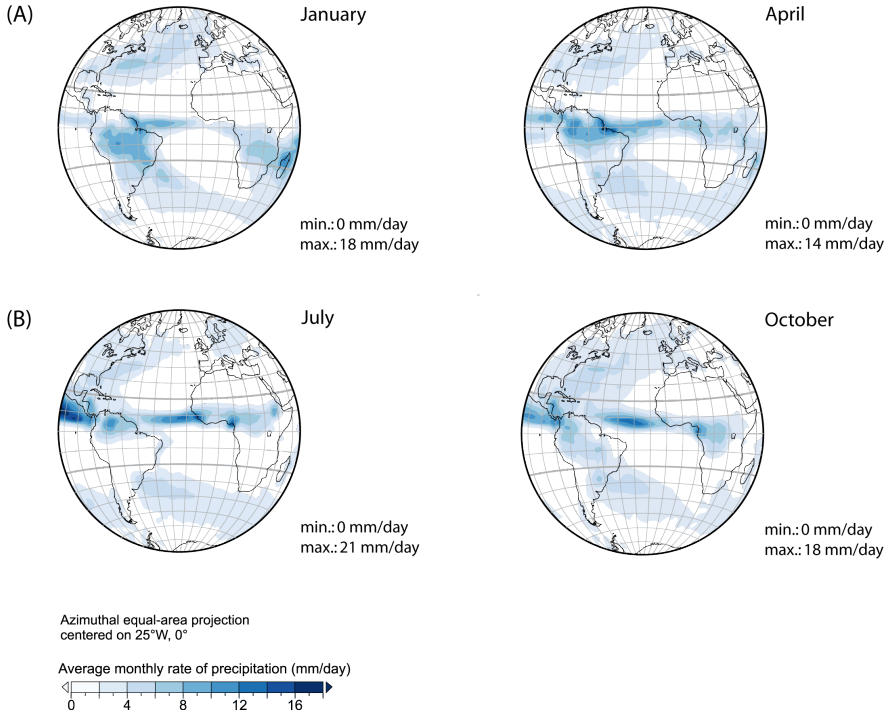

Figure 7: Rate of precipitation over tropical Africa and South America, (A) austral summer (January, April) and (B) austral winter (July, October)

6.1.3 Chronology

The age models of most of the sediment records reviewed here were determined based on conventional, accelerator mass spectrometry (AMS) radiocarbon dating or peak-to-peak correlation with other well-dated marine sediment cores (Table 2). The chronology of some marine sequences off western and north-western Africa (Table 2) where radiocarbon dating is not feasible is based on peak-to-peak correlation of isotopic records (e.g. Lézine et al. 2005; Lézine and Denèfle, 1997). The age models of the Cariaco Basin sequence and the marine record off northeast Brazil (GeoB3104-1) are based on a combination of radiocarbon dating and correlation with ice-core records. The original Cariaco records are aligned with the 230Th dated Hulu Cave speleothems (Wang et al., 2001; Hughen et al. 2006). In this review, however, we adapted the time scale to the Greenland Ice Core Chronology 2005 (GICC05) (Skinner, 2008; Wolff et al., this volume), aligning the steep drops in the reflectance curve of the Cariaco sediments with the start of Greenland Interstadials (GI). The time scale for the marine core GeoB3104-1 (Jennerjahn et al., 2004) has also been adapted to the new GICC05 ages. The age model of the Colônia record is a combination of radiocarbon dates and tuning of the arboreal pollen record to precessional insolation fluctuations (Ledru

et al., 2009). The age models of the Fúquene-2 and Fúquene-7C records are a combination of radiocarbon dates, frequency analysis in the depth domain, and tuning of the arboreal pollen record to the LR04 benthic oxygen isotope record (Lisiecky and Raymo, 2005; Mommersteeg and Hooghiemstra, in review; Bogotá-Angel et al., in review).

In order to make all records comparable we merely interfered in the original age models by converting dates into calendar ages if they were published as ^{14}C-dates. However, different calibration curves were used for different records which add uncertainties in the comparison between sites. Additionally, the age models of marine sequences dated by the radiocarbon method include a marine reservoir age generally of 400 years which reflects the present-day global average (Hughen et al., 2004). In general, temporal and/or regional variations in reservoir ages are not taken into consideration in dating marine cores because they are difficult to reconstruct (e.g. Bard et al., 1994) and, for pre-Holocene records are exceeded by the uncertainties in the radiocarbon dating (Fairbanks et al., 2005). Model simulations also show that temporal fluctuations in the marine reservoir age are less significant in the tropical Atlantic compared to the northern high-latitudes (Franke et al., 2008, Hughen et al., 2004).

6.1.4 Registration of abrupt climate variability in pollen records

We have reviewed pollen records from tropical Africa and South America that potentially show abrupt climate variability during the last glacial (Table 1, Figure 8). The criteria we established to select appropriate pollen records mainly based on the covered timeframe (at least part of MIS 2 and/or 3 and/or 4), a sufficient age control, and a temporal resolution better than 1000 years for at least a substantial part of the record. Additionally, the availability of original data sets by personal communication and/or databases was important. Eventually, only eight South American and eight African records withstood our criteria (Table 1 and 2). However, the acceptance of two pollen records requires further explanation. The Lake Malawi record of DeBusk (1998) has for the most part of the record a temporal resolution of 1000 years/sample, though the period including HS 4 provides a significantly higher resolution. Thus, this record has the highest temporal resolution for the period associated with HS 4 of all African pollen records (Figure 9). The eligibility of the South American marine record GeoB 3104 (Behling et al., 2000) based on the shorter but high-resolution neighbouring core GeoB 3910 (Dupont et al., 2009) and by providing significant insights in the vegetation development of NE Brazil during the subsequent time period (Figure 10). We excluded core KW 31, located south of the Niger Delta (Lézine and Cazet, 2005) despite a sufficient time resolution due to substantial gaps in the pollen record (Table 1).

The temporal definition for the last glacial, MIS 2, 3 and 4, and HS was adapted from Sanchez Goñi and Harrison (this volume). In order to achieve comparability across the records, however, being aware of the simplification of the original pollen diagrams and loss of information, we grouped all pollen taxa into mega-biomes (Table 3). We have described the main changes in the biomes for each record (Figure 9, 10, 11, and 12) considering the original interpretation to emphasise the coherence between the original and biomizised data.

We assigned the pollen taxa to Plant Functional Types (PFTs) following Jolly et al. (1998) and Peyron et al. (2006) modified by Vincens et al. (2006) and Lebamba et al. (2009) for the African records, and after Marchant et al. (2009) for the South American ones. The PFTs are then grouped into major vegetation types (mega-biomes: Table 3) to allow direct comparison of the records (Figures 9, 10, 11, and 12). In some cases, the response to millennial-scale climate variability is obscured by this rather coarse classification of the vegetation, particularly when this variability is expressed as within-biome fluctuations in species composition rather than between-biome transitions. Therefore, for each site, we have also selected a taxon that best illustrates the vegetation response to millennial-scale variability.

In Figure 11 we present the original grouping for the Cariaco Basin pollen record (González et al., 2008). Since the grouping is based on the regional ecological preferences of every taxon it is better suitable for the Venezuelan flora. For similar reasons the original grouping of pollen taxa is given for the Fúquene record in Figure 12, which is based on the altitudinal zonation of the Eastern Cordillera of Colombia (Van Geel and Van der Hammen, 1973; Mommersteeg, 1998; Mommersteeg and Hooghiemstra, in review).

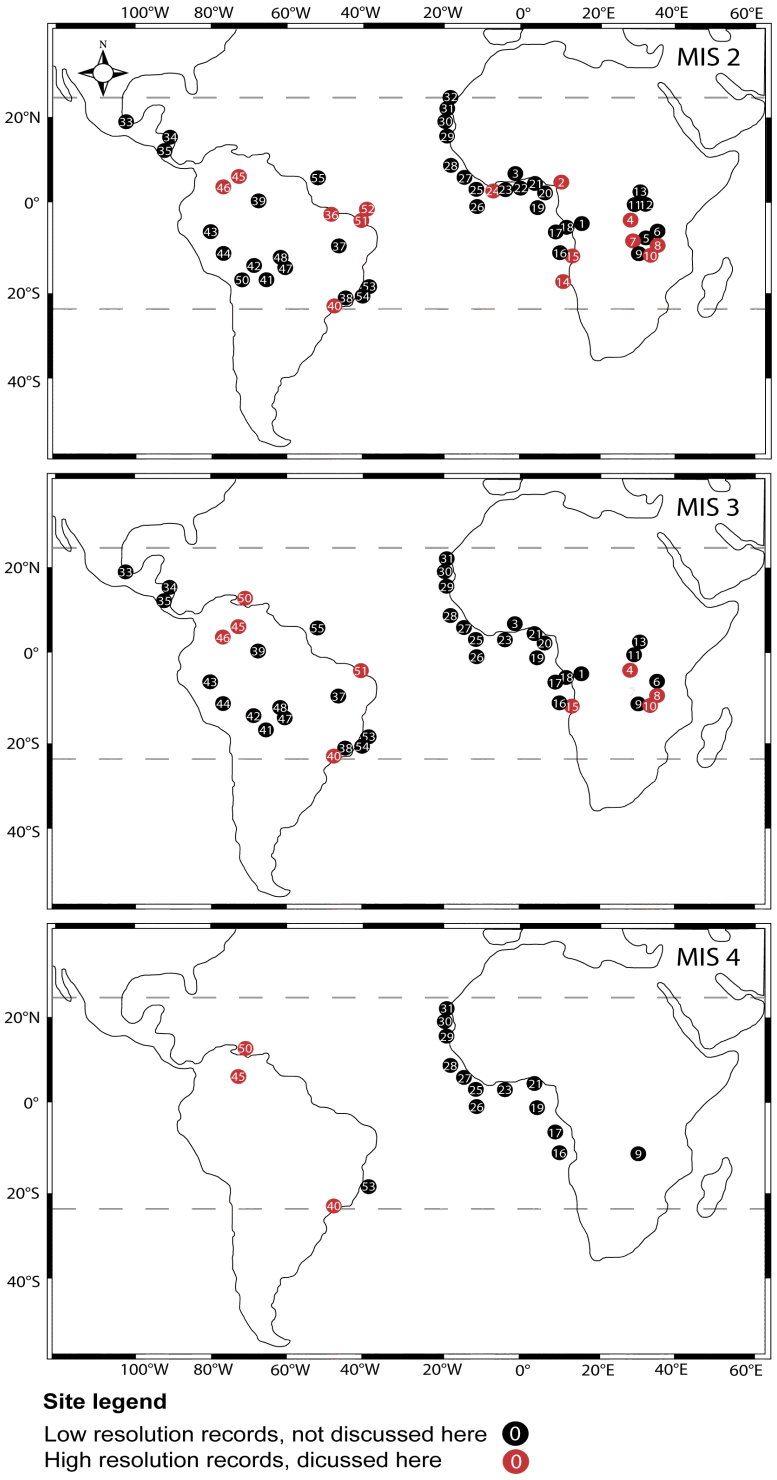

Figure 8: Locations of high and low resolution pollen records during MIS 2, 3 and 4.

Tropical Africa

The pollen record from Kashiru Swamp in east equatorial Africa (Bonnefille and Riollet, 1988; Bonnefille et al., 1992) provides a vegetation record over the past ca. 50 ka (Table 1 and 2). Between 50 ka and 40 ka the pollen record of the Kashiru site is characterised by high percentages of arboreal taxa (mainly warm-temperate mixed forest, tropical forest, Figure 9), indicating a relatively wet climate. From 40 ka to the end of the deglaciation, the vegetation is more open with widespread grassland, mainly C_4 grasses, as well as savannah and xerophytic scrubland vegetation. An increase in temperate plants during this period suggests a lowering of the upper forest line as a consequence of cooler climate (Bonnefille and Riollet, 1988; Bonnefille and Chalié, 2000), although decreased atmospheric CO_2 during glacial times may have limited tree growth and favoured grass development (Jolly and Haxeltine, 1997; Harrison and Prentice, 2003). A short-term humid phase, characterised by lacustrine conditions and an expansion of *Podocarpus* forests (temperate-montane forest, Table 3, Figure 9), occurred at about 24 ka and is followed immediately by forest development (Bonnefille and Riollet, 1988). Although of sufficient duration and time resolution, the Kashiru pollen sequence does not display D-O variability, but vegetation response to HS appears to have been recorded.

The pollen record from the Mpulungu sub-basin of southern Lake Tanganyika, east equatorial Africa (Figure 9, Table 1 and 2) (Vincens, 1991; Vincens et al., 1993) provides a record of vegetation changes during MIS 2. The pre- and post-Last Glacial Maximum (LGM) vegetation is dominated by grassland/dry shrubland and savannah/xerophytic scrubland vegetation (Figure 9) with isolated patches of woodland and large swamp areas around the lake. During the LGM, tropical forest elements increased slightly whereas swamp taxa (see original diagram Vincens et al., 1993) are at their lowest abundance. The frequency of tropical forest taxa like *Brachystegia* and *Uapaca*-type *kirkiana* increased at the glacial-interglacial transition. A simultaneous decrease in Ericaceae (grassland and dry shrubland, Table 3, Figure 9) and an increase in drought-tolerant mountainous *Olea* and *Myrica* (temperate forest, Table 3) are interpreted as indicating an expansion of open dry forest or dry montane woodland on the uplands surrounding the basin (Vincens et al., 1993). The Mpulungu record is too short to show D-O cycles of MIS 3 and 4.

A high-resolution pollen record covering the period between 45-4.4 ka was obtained from Lake Masoko, southern Tanzania, east equatorial Africa (Figure 9, Table 1 and 2) documenting particularly changes in the seasonal vegetation of the southern Miombo (Vincens et al., 2007). Miombo woodlands are a widespread and characteristic vegetation of the tropical forests of southern Africa dominated by species of *Brachystegia* (tropical forest and warm temperate forest, Table 3, Figure 9) (White, 1983). Between 42 and 23 ka the regional vegetation was dominated by savannah and xerophytic shrubland as well as grassland and dry shrubland (Figure 3). In the

original pollen diagram the main vegetation composition is basically expressed by high values of Poaceae (savannah and xerophytic shrubland, grassland and dry shrubland, Table 3) and low values of local miombo woodland taxa (Vincens et al., 2007). Regrowth of forest occurred during the LGM with expansion of warm temperate mixed forest although grassy vegetation remained abundant. From the onset of the Bölling/Alleröd period (B/A) to the end of the YD there was a further increase in warm temperate mixed forest taxa. Although the authors did not interpret the vegetation changes in terms of millennial-scale climate change, some vegetation changes might be a response to HS. The mountainous species *Olea* (warm temperate mixed forest, temperate-montane forest, Table 3) is well represented between 45 and 40.2 ka and appears to show a response to at least two HS (Figure 9). *Olea* increased following periods of HS 4 and HS 1, however, changes in *Olea* representation are not observed for HS 2 and HS 3. Vincens et al. (2007) interpreted the general expansion of *Olea* between 45 ka and 33 ka and between 16 ka and 14.1 ka as reduced moisture availability compared to today, which might be a result of North Atlantic HS.

The Lake Malawi record (core M86-18P) of DeBusk (1998) gives further insight in the east African vegetation history during the last glacial. Since the temporal resolution for the timeframe between 10.5 ka to 38 ka is about 1000 years/sample, millennial-scale climate variability can not be detected in this particular period. In contrast, the sequence between 38 ka and 43 ka has a resolution of 200 years, and is therefore the most detailed HS 4 record available for eastern Africa (Figure 9, Table 1 and 2). Prior to HS 4 the vegetation in the catchment of Lake Malawi is dominated by an open vegetation type composed of elements belonging to the biomes grassland/dry shrubland and savannah/xerophyic scrubland (Figure 9). At the same time pollen percentages of *Olea capensis* (temperate-montane forest, Table 3) are at their minimum representing dry conditions on the surrounding highlands. Subsequently, the percentages of temperate-montane forests and warm-temperate mixed forests start to increase with their maximum occurring in the beginning of HS 4. According to DeBusk (1998) montane forests expanded during this period whereas woodland was reduced in the area but still present. Another expansion of temperate-montane forests, with its main component being *Olea capensis*, appears to correlate with the LGM, but is less strong than that during HS 4 (Figure 9). This forest expansion was interpreted by DeBusk (1998) as resulting from the substantial cooling of the climate and the increase in effective moisture by decreasing evaporation.

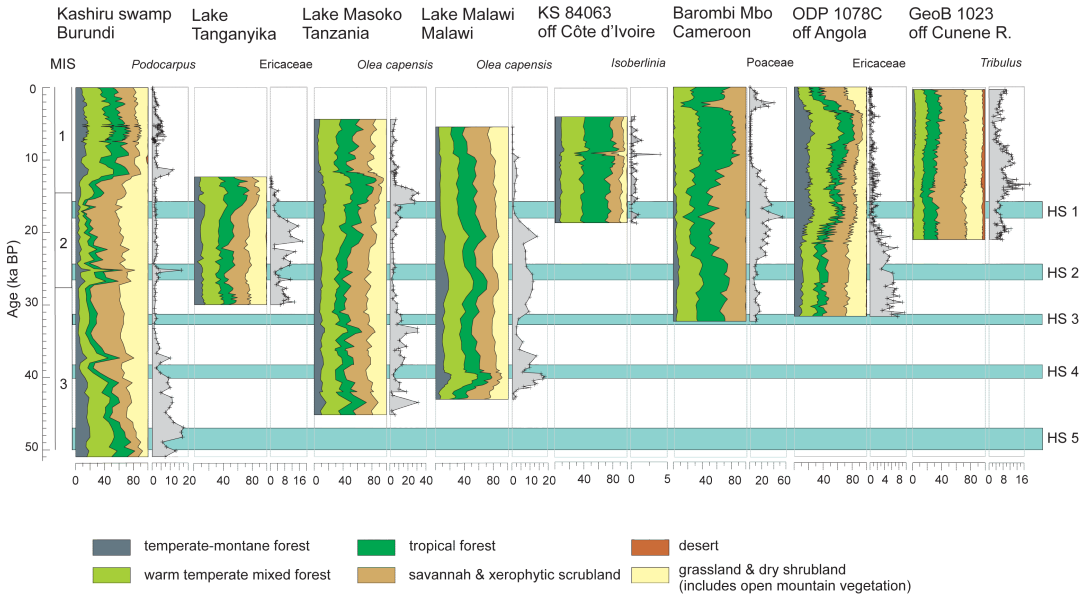

Figure 9: Summary diagrams showing vegetation changes, using the biomisation scheme given in Table 3,for high resolution sites from tropical Africa. An additional indicator pollen taxon is shown for each site. Fractions are expressed as percentages (X-axes).

The pollen record of Lake Barombi Mbo, a large crater lake of 110 m maximum depth, provides a vegetation and climate record of western equatorial Africa north of the equator covering the last 32 ka (Maley and Brenac, 1998). During the pre-LGM glacial period, the forest cover was rather similar to that of today with high values of tree pollen percentages, belonging to tropical forest and warm temperate mixed forest (Figure 9). The mountainous taxon *Olea capensis* (mainly warm temperate mixed forest, Table 3) reached maximum abundance during HS 2. Moreover the high frequency of this tree was interpreted to result from its extension on the crater walls close to the lake indicating relatively cool climate conditions (Maley and Brenac, 1998). The interval spanning the LGM and HS 1 is marked by an abrupt increase in savannah and xerophytic scrubland vegetation (Figure 9). This increase is mostly based on high values of Poaceae (savannah and xerophytic shrubland, Table 3) that we also chose as the indicator taxon for this record. However, if we take the original diagram of Maley and Brenac (1998) into account it is obvious that maximum values of Poaceae occur mostly during HS 1. In contrast, the LGM coincides with peaks of Cyperaceae which is considered to represent lowering of the lake level (Maley and Brenac, 1998). Cyperaceae percentages are excluded in the calculation of tropical biomes since it is regarded as an aquatic taxon (e.g. Jolly et al., 1998). After a long transgressive phase between ca. 18.5 to 14.7 ka a last lowering in the amount of forest taxa appeared during YD. The Barombi Mbo record (Figure 9, Table 1 and 2) does not show millennial-scale climate variability despite a mean temporal resolution of 600 years in the late Pleistocene. However,

marked vegetation changes occur during periods that may be associated with HS 1 and HS 2.

The marine core from ODP Site 1078 C (Dupont and Behling, 2006; Dupont et al. 2008) provides a record of vegetation changes in tropical southwest Africa from 31.7 ka onwards (Figure 9, Table 1 and 2). During glacial times the prevailing mega-biomes in the source area of ODP 1078 (Angola and the southern Congo basin) were savannah and xerophytic scrubland as well as grassland and dry shrubland including open mountainous vegetation. Ericaceae as a typical Afroalpine vegetation element and an important constituent within the grassland/dry shrubland megabiome (Table 3) has been chosen to represent the vegetation development of the sensitive high mountain areas during the last glacial (Figure 9). The interval between 31.7 and 22 ka was generally characterised by open vegetation in the mountains and an expansion of desert and semi-desert vegetation in the lowlands. Between 22 and 19 ka temperate-montane forest became more abundant mainly resulting from increased percentages of Afromontane *Podocarpus*. Dupont et al. (2008) suggests that the increase in *Podocarpus* reflects an expansion of forest at intermediate altitude. In the lowlands a simultaneous increase in tropical forests representatives like *Mallotus* indicates that rain forests became more widespread. The last deglaciation is dominated by *Podocarpus* pollen with a maximum occurrence during the enclosed HS 1. In Figure 9 this is reflected by increasing percentages of the temperate-montane forest biome. However, *Podocarpus* is a prolific pollen producer and this pollen is readily transported by wind, and may be overrepresented in the pollen diagram. Nevertheless, its abundance in HS 1 suggests that *Podocarpus* forests were present locally. Simultaneously, grassland and dry shrubland retreated as indicated by low pollen percentages of Ericaceae and grasses. After HS 1, the percentages of lowland forest pollen (tropical forest and warm temperate mixed forest) increased. The expansion of rainforest and warm temperate mixed forest is accompanied by a southward displacement of deserts and steppes (xerophytic shrubland, Table 3). Although the record has been analyzed in high-resolution and the time interval represented is sufficient enough there are no indications of D-O variability. Only HS 1 clearly had an impact on the vegetation.

A marine sediment record (GeoB1023-5) located in front of the Cunene River mouth off the coast of Namibia, tropical southwest Africa has been used to reconstruct vegetation changes on the adjacent continent for the past 21 ka (Table 1 and 2, Figure 9) (Shi et al., 1998). The vegetation of the pollen source area of GeoB1023-5 (13-21°S, west of 24°E) is throughout the whole record dominated by savannah and xerophytic shrubland as well as grassland and dry shrubland with only minor changes in the vegetation composition (Figure 9). However, within-biome vegetation changes occur and are mostly indicated by variations in the pollen percentages of specific taxa. Since the taxon *Tribulus* (savannah and xerophytic

shrubland, Table 3) indicates by high pollen percentages arid conditions and vice versa, it is considered to best illustrate climate change in GeoB1023-5. Although there are only minor changes within the mega-biome diagram high *Tribulus* percentages indicate for instance increased aridity during the LGM and subsequent to HS 1 (Figure 9). Additionally, the original pollen data suggests a lower-than-present temperature during the LGM indicated by high abundances of temperate taxa. The diagram published by Shi et al. (1998) shows also an increase of grass pollen in association with low percentages of desert/semidesert taxa and increasing values of dry forest/woodland taxa after the LGM, indicating increased temperatures and humidity. The timeframe covered by this record is too short to display D-O cycles. Moreover, the indications of vegetation changes associated with HS 1 are ambiguous, despite the high temporal resolution (185 years).

The pollen sequence from the deep-sea marine core KS84063 off Ivory Coast, north-western equatorial Africa (Lézine et al., 1994; Lézine and Denèfle 1997) only covers the timeframe from ~ 5 ka to 19 ka (Figure 9, Table 1 and 2) and consequently does not display D-O cycles. Although there are only small vegetation changes apparent in the biome diagram (Figure 9), HS 1 and the YD are marked in Lézine et al. (1994) and Lézine and Denèfle (1997) by maximum pollen concentrations, Saharan dust input and the presence of Saharan desert taxa. In order to illustrate the increased aridity particularly during HS 1 we also plotted *Isoberlinia* as an important component of the regional tropical forests (Figure 9, Table 3). Moreover, Lézine et al. (1994) and Lézine and Denèfle (1997) show the sporadic occurrence of the Afromontane taxon *Podocarpus* (temperate-montane forest, Table 3) which is usually restricted to the highlands further east. The authors suggested that during these dry events lower temperatures were responsible for the extension of *Podocarpus* forest towards middle and low altitudes. In contrast, the occurrence of Saharan taxa originates from intensified meridional air-mass exchange. At the end of the deglaciation (~ 12 ka), *Podocarpus* forest retreated to its present day altitudinal distribution.

Tropical-subtropical South America

The high resolution pollen record of MD 03-2622 from the Cariaco Basin, off Venezuela, enables insight into the sensitivity of vegetation to changing environmental conditions during the period from 28 to 68 ka (Figure 10 and 11, Table 1 and 2) (González et al., 2008). Although sea-level changes have had an impact on the record (González and Dupont, 2009), the pollen diagram clearly shows the cold intervals associated with D-O stadials and with HS (González et al., 2008). By applying the biomisation procedure as in the other records the Venezuelan vegetation seems rather unaffected by millennial-scale climate variability (Figure 10). However, using the grouping method after González et al. (2008) GIs are obviously characterised by the expansion of tropical evergreen and semi-deciduous forests (Figure 11) suggesting increased precipitation and river

discharge. In contrast, Greenland Stadials (GS) show the opposite trend with the dominance of open vegetation (mainly savannah vegetation) and salt marsh taxa (e.g. Chenopodiaceae, Figure 10, Table 3) indicating drier climatic conditions in the lowlands. Furthermore, during GS the enhanced orographic precipitation promoted the expansion of montane forests (González et al., 2008). The reflection of HS in the Cariaco Basin is a more extreme case of GS vegetation change, combined with the effects of increased sea-level that promotes the expansion of salt marshes and the succession of coastal vegetation (González and Dupont, 2009).

The GeoB 3104-1 core from the upper continental slope northeast off Fortaleza (Figure 10, Table 1 and 2) provides a vegetation record from north-eastern Brazil reaching back over 50 ka (Behling et al., 2000). The in the following paragraph described marine neighbouring core GeoB 3910-2 (Fischer et al., 1996; Dupont et al., 2009) provides a high resolution vegetation record covering HS 1, hence representing a detailed complement to GeoB 3104-1. During the last glacial merely small changes appear in the biome diagram (Figure 10) resulting in a vegetation composition similar to present-day with a dominance of semi-arid caatinga (savannah and xerophytic shrubland, grassland and dry shrubland, Table 3) vegetation. However, considering the original diagram (Behling et al., 2000; Jennerjahn et al., 2004) the forest vegetation became more abundant during HS 1, HS 3, HS 4, and possibly HS 5 (although the dating of the lower part of the sequence is rather uncertain). An increase in forest also occurred during HS 2, but was less pronounced. These potentially wetter conditions are also expressed in the increased pollen influx rates, shown in Figure 10.

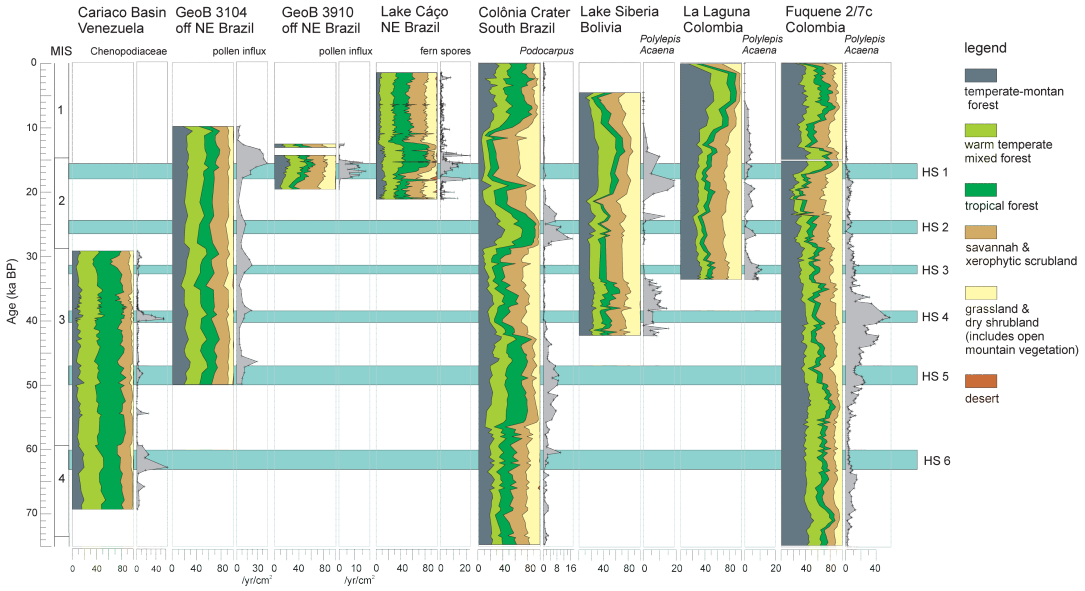

Figure 10: Summary diagrams showing vegetation changes for South America using the biomisation scheme given in Table 3. The overlapping parts of the two Fúquene records are essentially the same. Here we have plotted the upper 15 ka of Fúquene-2 and the part 15-75 ka of Fúquene-7C. An additional indicator pollen taxon is shown for each site. Unless otherwise stated, fractions are expressed as percentages (X-axes).

Sediment core GeoB 3910-2 (Dupont et al., 2009), located offshore Northeast Brazil, supports the results of the neighbouring and above described GeoB 3104-1 (Behling et al., 2000) by providing a highly detailed vegetation history during the period including HS 1 (Figure 10, Table 1 and 2). At the beginning of HS 1 an increased pollen influx (Figure 10) suggests increased precipitation in the catchment area of GeoB 3910-2. However, Dupont et al. (2009) assume that the vegetation was still open, dominated by savannah and grassland vegetation, and the increased water supply results firstly in increased erosion. During the second part of HS 1 (16.6-14.9 ka) higher percentages of forest taxa (Figure 10) imply a denser vegetation cover. Considering the original pollen diagram it becomes also obvious that diversity of trees increased significantly (Dupont et al., 2009). Subsequent to HS 1 the vegetation retreats gradual into a composition dominated by savannah and grassland which is comparable with that before 18 ka.

The pollen record from Lagoa do Caçó (Figure 10, Table 1 and 2) in north-eastern Brazil covering the past 20 ka (Ledru et al., 2001; Ledru et al., 2006) provides a detailed record of vegetation change during HS 1. Open grassland and savannah vegetation prevailed during the LGM, though at 17.5 ka an increase in forest attendants indicated by fern spores marked the initial establishment of forests (Figure 10). Dense moist forest was well established by 17 ka. Two brief intervals of forest decline occurred during the late glacial at 15 and 13.5 ka. The forest was destroyed at 12.8 ka probably

by fire, and the region was characterised by savannah and xerophytic scrubland vegetation during the Holocene (Ledru et al., 2006).

A long core from a peat bog in the impact crater Colônia near São Paulo, south-eastern Brazil (Figure 10, Table 1 and 2) provides a vegetation record that covers a complete interglacial-glacial-interglacial cycle with sub-millennial temporal resolution for most of the sequence (Ledru et al., 2009). In this review we show the last 75 ka of the Colônia pollen record, which is in agreement with the adapted timeframe for the last glacial from Sanchez Goñi and Harrison (this volume). There are possible indications of D-O variability, particularly between 80 and 40 ka, indicated by higher arboreal pollen percentages. However, the age-model relies on the assumption that forest growth is coupled to precession.

The beginning of the glacial was characterised by a slight decrease in tree pollen frequencies but an increase in the frequency of *Podocarpus* (temperate-montane forest, Table 3). The taxon *Podocarpus* was chosen as representative for the record (Figure 10) since it is a typical tree for humid temperate regions in mid-altitudes. Between 55.8 to 40.9 ka an expansion of tropical forests occurred in the pollen source area of the Colônia crater. The floristic composition was very similar to that observed during the interglacial. Another expansion of tropical forests occurred from 30 to 23 ka and was characterised by an assemblage of plant taxa that might characterise a cold tropical forest. During the periods from ca. 40 to 30 ka and from 23 to 12 ka tropical forest was replaced by open vegetation dominated by grasses. The Atlantic forest (Table 3), as a regional variety of tropical forests, hardly survived these dry episodes, though small patches remaining in protected areas around the crater (Ledru et al., 2009). In general, the variabilities of forest taxa seem to be correlated to precession and moisture availability. The floristic composition of the forest varied in each precession cycle attesting to varying climatic conditions and interference of high latitude climate change in this tropical region (Ledru et al., 2009).

The pollen record from the La Laguna depression (Helmens et al., 1996), located on the outer slopes of the Eastern Cordillera of Colombia west of the high plain of Bogotá, shows vegetation changes since 30 ka (Figure 10, Table 1 and 2). Palynological data suggest a warming event, the La Laguna Interstadial that might be associated with the period between HS 1 and HS 2 (Figure 10). Expansion of temperate-montane dwarf forest determining the upper forest limit are represented by increasing percentages of *Polylepis-Acaena* (Table 3) pollen during the La Laguna Interstadial, which might indicate an upward shift of the upper forest limit resulting from higher temperatures (Figure 10). The pre-LGM period (before 25 ka) is characterised by relatively high proportions of grassland pollen and relatively low abundances of arboreal taxa, indicating the site was located in the belt with grasspáramo (grassland and dry shrubland) vegetation. Helmens et al. (1996) recognized the occurrence of an interstadial period in the middle of the LGM (La Laguna Interstadial)

from 23 to 20.5 ka. At this time glaciers retreated, extensive soil formation took place, and the upper Andean forest limit and mean annual temperature rose considerably. During the La Laguna Interstadial, grass pollen dominates the original diagram but pollen of *Polylepis-Acacena* are also well represented. In general, the LGM shows open grasspáramo conditions implying a lowering of the upper forest limit by 1100 m (early part of LGM) to 900 m (late LGM) and a drop in mean annual temperature (Helmens et al., 1996). Interstadial conditions are again registered during the Lateglacial, i.e. during the Guantiva Interstadial (Van Geel and Van der Hammen, 1973; Van der Hammen and Hooghiemstra, 1995; Van Śt Veer et al., 2000) at around 14 ka, when declining grass pollen percentages and increased pollen values of trees suggest slightly warmer temperatures than during the La Laguna Interstadial.

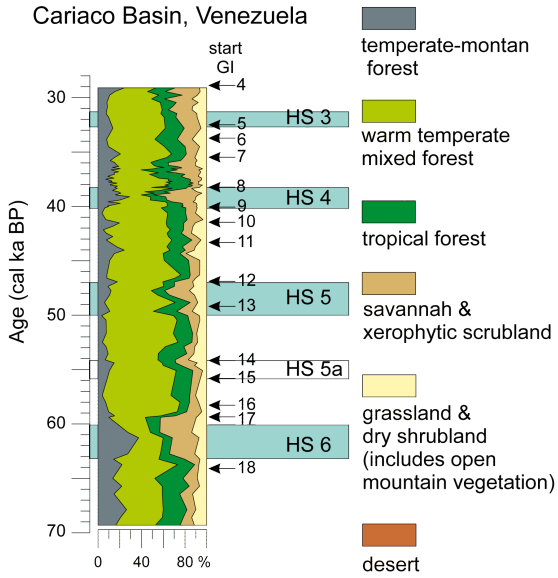

Figure 11: An additional summary grouping is given for the record of the Cariaco Basin with montane forest elements, semi-deciduous trees of the tropical seasonal forest, evergreen trees of the tropical rain forest, savannah elements, and xerophytic shrubland after Gonzalez et al. (2008). The Cariaco record hints at the existence of Dansgaard-Oeschger cycles. The start of each Greenland interstadial (GI, see also Wolff et al., this issue) is indicated by an arrow.

The pollen records of Fúquene-2 (Van Geel and Van der Hammen, 1973) and Fúquene-7C (Mommersteeg, 1998; Mommersteeg and Hooghiemstra, in review) come from Lake Fúquene, located at 2580 m elevation in the Eastern Cordillera of Colombia, ~ 600 m below the present-day upper Andean forest limit. Pollen record Fúquene-7C shows a gap in the Lateglacial period and therefore we used the pollen record Fúquene-2 for the last ~ 15 ka

(Figure 10 and 12, Table 1 and 2). The combined Fúquene records reflect the last 85 ka but since we concentrate on the last glacial, chronological defined by Sanchez Goñi and Harrison (this volume), only the last 75 ka are shown (Figure 10 and 12). The upper Andean forest limit reflects the transition between montane forests and tropical alpine grasslands (páramo). This ecozone, characterised by the ~ 13.5°C annual isotherm, shifted between ~ 2100 m during the LGM and 3300 m during the warmest part of the Holocene. We inferred temperatures from ~ 8°C cooler to ~1°C warmer than at present-day, respectively. The record of changing biome contribution (Figure 10) shows a suite of interstadials; in the original pollen record (Figure 12) interstadials are even more clearly expressed. The trees *Quercus*, *Polylepis-Acaena*, and *Podocarpus*, all elements within the temperate-montane forest biome (Table 3), show the most significant response to millennium scale climate variability. These taxa, *Quercus* in particular, occur in a broad range of climatological moisture allowing the conclusion that the arboreal pollen record reflects mainly temperature change.

A 40 ka pollen record (Figure 10, Table 1 and 2) has been obtained from a small, closed lake basin at 2920 m altitude in the eastern Cordillera of Bolivia, western South America (Siberia: Mourguiart and Ledru, 2003). Abrupt climate variations are not obvious in spite of a mean time resolution of about 750 years. From ca. 40 to 29 ka the vegetation was dominated by an open forest with cloud forest elements (temperate-montane forest). According to Mourguiart and Ledru (2003) the low arboreal pollen percentages during the LGM suggest an open landscape, dry and cold climatic conditions, indicating a drastic lowering of moisture availability from the Amazonian region. Increasing percentages of *Polylepis-Acaena* (temperate-montane forest, Figure 10) and the algae *Botryococcus* correspond to a short and abrupt increase in moisture around 23 ka. Between 20 ka and 13 ka, a moist tropical forest developed. An initial increase in *Polylepis-Acaena* at 20 ka is attributed to an increase in moisture, immediately followed by the development of the moist forest which can be attributed to an upslope shift of the upper forest line and to more adiabatic moisture from the Amazonian Basin due to an increase in temperatures.

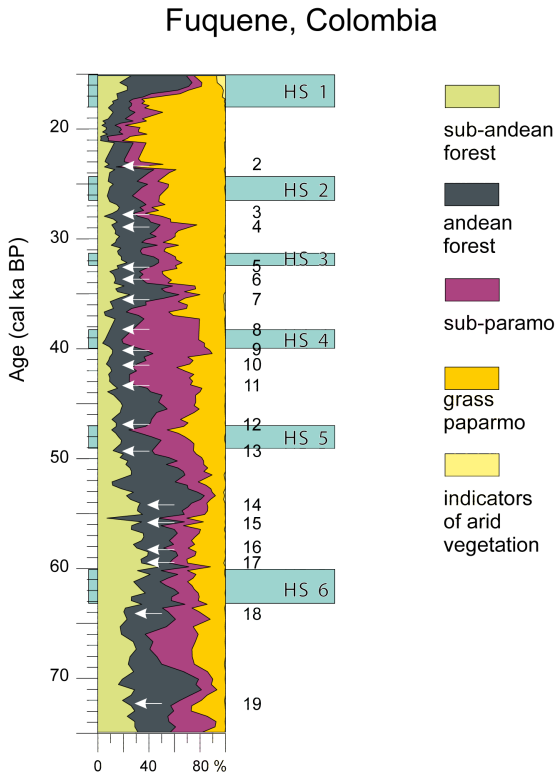

Figure 12: An additional summary grouping is given for the Fúquene-7C record, in which the grouping is according the altitudinal vegetation zones in the Eastern Cordillera of the Andes. Increments of sub-Andean forest elements (green) are found in association with the Greenland Interstadials (numbers). Start of each interstadial (Wolff et al., this issue) is indicated by an arrow.

6.1.5 Discussion

Tropical Africa

There are eight records from tropical Africa, but only six of these include MIS 3. The longest record, from Kashiru swamp in Burundi, extends back to 50 ka. Most of these records show changes in vegetation in response to periods associated with Heinrich events (Table 4, Table 5). In nearly all African records HS 1 is recorded with a sufficient temporal resolution, however, with an inconsistent pattern of vegetation response. The period including HS 2 is only existent in five of these records while the Lake Malawi record has a marginal time resolution during this period. Pollen records that cover the time periods including earlier Heinrich Stadials (HS 3 and 4) are available from just two East African records (Lake Masoko and Lake Malawi). Only the Kashiru swamp pollen record (Burundi) reach back to 50 ka, hence containing the period associated with HS 5.

However, despite several of the records having sufficient temporal resolution during the end of MIS 3 and the first part of MIS 2, there is no indication of vegetation changes corresponding to D-O cycles. The absence of D-O variability

is also shown by other palaeoenvironmental records from the region. Multiza et al. (2008), for example, found no traces of D-O variability (although they do see prominent HS variability) in grain size records from a marine core off the mouth of the Senegal River. On the other hand, elemental Zr/Ti- and Si/Ti records from Lake Malawi show changes related to both D-O cycles and HS, which are interpreted as a shift to predominantly northerly winds and relative arid conditions in the Malawi Basin (Brown et al. 2007). We suggest that the absence of D-O variability is a real phenomenon in northwestern Africa, and that only the most marked climate changes corresponding to the Heinrich event were registered in the vegetation of tropical Africa.

The absence of vegetation changes corresponding to HS 1 in the marine record off Ivory Coast is surprising because other palaeoclimatic indicators do show marked changes during this interval. The nearby marine record off the Senegal River mouth, for example, shows decreased river flow and increased aeolian dust during HS 1 through 5 (Mulitza et al. 2008). The magnetic grain size record of Lake Bosumtwi in Ghana also shows strong increases during HS 1, HS 2 and the YD (Peck et al. 2004). Peck et al. (2004) interpreted this as a result of increased aeolian dust input and increased erosion due to reduction in vegetation cover. Where multiple Heinrich events are registered, the vegetation changes are not identical (Figure 9 and 10). In general, in all the tropical African sites, the vegetation changes during Heinrich events are much less pronounced than those registered in extra-tropical regions of the northern hemisphere (see e.g. Europe: Fletcher et al., this volume). This is consistent to the idea of an attenuation of the North Atlantic climate signal into the tropical regions (e.g. Broecker, 2003; Rahmstorf, 2002).

There is clearly a need for more records from tropical Africa, particularly from the northern equatorial tropics since there is no high resolution pollen record existing at all. Additionally, our interpretation of the existing records is limited by the rather low sample resolution of most cores and the grouping of the pollen taxa into global mega-biomes. Despite that the existing records hint that the response to rapid climate changes in Africa is not as strong as in other regions. However, they are consistent with the hypothesis that tropical climate changes are associated with a shift in the migration pattern of the ITCZ during HS due to reduction in the strength of the AMOC. In general the mean response of the tropical African vegetation to those HS that are available in a sufficient time resolution can be summarized as an increase in arboreal taxa perhaps due to an increase in moisture availability. Nevertheless, the annual pattern of the ITCZ and the related Congolian Air Boundary is highly complicated over the African continent that we can not assume a consistent behaviour of this system during different HS. Additionally, the effects of elevation, atmospheric CO_2, evaporation and possible interfering mechanisms are still poorly investigated and understood (e.g. Gasse et al., 2008).

The results which are provided by this review

are not consistent with the hypothesis that the circum Atlantic tropics themselves play a key role in generating rapid climate changes.

Tropical South America

There are eight sites from South America with sufficiently high resolution to record millennial-scale variability (Table 4, Table 5). The records from the northern (Cariaco Basin) and southern (Lagoa de Caçó, GeoB3910) present-day limits of the ITCZ show that vegetation responds to both HS and to D-O variability. In the northern sites, lowland forests characterise GI while the vegetation becomes more open during GS. The opposite signal is found at the southern limit: vegetation cover increases during GS and becomes more open during GI. The records from Lake Caçó and GeoB3910 even mimic the two phase internal structure of HS 1 (Ledru et al., 2001; Jennerjahn et al., 2004; Dupont et al., 2009). The opposition of vegetation changes at the northern and southern limits of the ITCZ support the hypothesis of a southward shift in the migration pattern of the ITCZ during HS (Martin et al., 1997; Peterson et al, 2000).

Records for southeast Brazil and western South America (Colônia, Lake Siberia, La Laguna) do not seem to register rapid climate changes associated with D-O variability in a consistent way. Changes in forest cover at Colônia are related to precessional variation rather than rapid climate change.

The vegetation of the three high altitude sites (Lake Fúquene, La Laguna, and Lake Siberia) is less limited by moisture deficiency and respond more to changes in temperature. At Lake Siberia, there are reductions in forest cover during HS, and traces of D-O variability in the abundance of trees from moist open forests between HS 4 and HS 3. D-O variability is reflected in the Lake Fúquene record by altitudinal shifts in the lower montane forest belt, which extends upslope during GIs. Similarly, the La Laguna record indicates an upward shift in the Andean forest limit resulting from increased temperatures following HS 2 and HS 1 which might also reflect traces of D-O variability.

6.1.6 Perspective

This paper attempts to review and synthesise vegetation records from tropical Africa and South America covering the last glacial and to explore the response of the tropical vegetation to climate changes during a period characterised by millennial-scale climate variability and rapid warming events. Records from both continents show vegetation response to HS; the response to D-O variability is more muted in tropical South America and absent from records from Africa. The records from northern South America show opposite responses in the northern and southern hemispheres, which support the hypothesis of a southward shift in the position of the ITCZ during HS. However, there are insufficient vegetation records from northern Africa to determine whether this pattern is mirrored on that continent.

There is a clear need for more, and higher-resolution, records from both regions. There is also an urgent need for improved dating of key records. The creation of age models indepen-

dent of orbital-tuning techniques is required in order to be able to study leads and lags in the climate system. We have not included some key records from the Colombian Andes (e.g. Funza-1, Funza-2 and Fúquene-9C) because the existing age models are currently being reviewed.

It may not be possible to obtain high-quality records from terrestrial sites for some regions, either because of the lack of suitable basins or because recent climate conditions have prevented organic accumulation. An obvious example of this is the northern African tropics. An alternative is to make more use of pollen records from offshore marine cores. Not all such cores will provide a sufficiently high-resolution record to document rapid climate changes during the last glacial, but there are regions where this has proved possible and we have shown that such records can provide useful insights into the nature of the vegetation response to rapid climate changes. Marine records can be difficult to interpret because they record pollen coming from a very large source area, which may therefore include several different biomes (Dupont and Wyputta, 2003). Nevertheless, and again as we have shown here, it is possible to use such records to document latitudinal shifts in key biomes.

For comparison purposes, we have expressed extent high-resolution pollen records from the African and South American tropics in terms of changes in major vegetation types (or mega-biomes) drawing on pre-existing schemes for converting pollen taxa to PFTs and PFTs to mega-biomes. However, the pre-existing schemes for Africa and South America are not mutually compatible, and our classification is to a large extent subjective. The data set of high resolution pollen records produced through this synthesis exercise, in conjunction with the records from other regions (Fletcher et al., this volume; Takahara et al., this volume; Jiménez-Moreno et al., this volume; Kershaw et al., this volume), will allow standard biomisation methods (see Prentice et al., 2000) to be applied in a globally consistent way to reconstruct global vegetation changes through the last glacial.

Acknowledgement

The authors are thankful to Sandy Harrison for many valuable discussions and suggestions.

The African Pollen Database http://fpd.mediasfrance.org/bibli.do and the pollen database of the World Data Center for Paleoclimatology http://www.ncdc.noaa.gov/paleo/ have been most helpful in making the compilations. We are grateful to George H. DeBusk as well, who made available his Lake Malawi dataset via the African Database. We also would like to thank our reviewers for their constructive comments and helpfull suggestions that improved the manuscript.

This paper was conceived and developed at a series of workshops sponsored by the UK QUEST (Quantifying Uncertainty in the Earth System) programme of NERC in support of the QUEST project DESIRE (Dynamics of the Earth System and the Ice-core REcord) and are a contribution to the ongoing work of the QUEST Working Group on Abrupt Climate

Change. We are grateful to QUEST for their long-term support of the Working Group on Abrupt Climate Change. Financial support during the final production of this paper was given through DFG-Research Center / Cluster of Excellence "The Ocean in the Earth System" and DFG.

Table 1: Pollen records from Africa and South America covering at least part of MIS 4, 3 and 2.

Site name	Map Code	Record type	Lat.(°)	Long.(°)	Elevation (m)	Period covered (ka)	Interval (ka)	Sampling resolution (yr/sample)	Reference
Ngamakala Pond, Congo	1	terrestrial	-4.07	15.38	400	3-32	10-15	> 1000	Elenga et al., 1994
							15-24	470	
							24-29	> 1000	
							29-32	270	
Barombi Mbo, Cameroon	2	terrestrial	4.51	9.40	300	0-32	10-32	590	Maley and Brenac, 1998
Lake Bosumtwi, Ghana	3	terrestrial	6.50	-1.42	99	0-33	10-33	> 1000	Maley, 1991
Kashiru Bog, Burundi	4	terrestrial	-3.47	29.57	2240	0->40	10-29	410	Bonnefille and
							30-31	1000	Riollet, 1988
							31-40	640	
Lake Rukwa, Tanzania	5	terrestrial	-8.42	32.72	793	0.3-21	10-13	375	Vincens et al., 2005
							13-14	170	
							14-19	> 1000	
							19-21	330	
Irunga, Tanzania	6	terrestrial	-7.82	35.91	2100	0-40	poor age	control	Mumbi et al., 2008
Lake Tanganyika	7	terrestrial	-8.50	30.85	773	9-25	12-15	250	Vincens, 1991
							15-26	610	Vincens et al., 1993
							26-27	140	
							27-28	330	
							28-30	180	
Lake Masoko, Tanzania	8	terrestrial	-9.33	33.75	840	4.4-45	10-17	300	Vincens et al., 2007
							17-45	550	
Lake Malawi	9	terrestrial	-11.29	34.44	475	0-120	10-60	>1000	Cohen et al., 2007
Lake Malawi, M86-18P	10	terrestrial	-11.22	34.42	470	10.5-45	10.5-38	1000	DeBusk, 1998
							38-43	200	
Muchoya Swamp, Uganda	11	terrestrial	-1.17	29.48	2260	0-42	poor age	control	Taylor, 1990; Morrison, 1968
Ahakagyezi Swamp, Uganda	12	terrestrial	-1.7	29.54	1830	0-26		AH1 >1000 AH2 ~1000	Taylor, 1999
Mubwindi Swamp, Uganda	13	terrestrial	-1.2	29.45	2000	2.5-43		> 1000	Marchant et al., 1997
off Cunene River Mouth, GeoB 1023	14	marine	-17.15	11.02	-1978	MIS 1-2	13-22	185	Shi et al., 1998

continued on next page

Site name	Map Code	Record type	Lat.(°)	Long.(°)	Elevation (m)	Period covered (ka)	Interval (ka)	Sampling resolution (yr/sample)	Reference
off Angola, ODP 1078	15	marine	-11.92	13.40	-426	MIS 1-3	10-22 22-27 27-32	140 830 280	Dupont et al., 2008
off Angola, GeoB1016	16	marine	-11.77	11.68	-3411	MIS 1-8		>1000	Shi and Dupont, 1997
Congo deep-sea delta, GeoB 1008	17	marine	-6.59	10.32	-3124	MIS 1-6		>1000	Jahns, 1996
Congo deep-sea delta, T89-16	18	marine	-5.70	11.67	-824	MIS 1-3	irregular	sampling	Marret et al., 2001
Gulf of Guinea, GIK 16867	19	marine	-2.20	5.00	-3891	MIS 1-6		>1000	Dupont et al. 1998
South of Niger River delta, KW 31	20	marine	3.52	5.57	-1181	MIS 1-3	10-15 15-17 21-25 30-40	200 670 500 670	Lézine and Cazet, 2005
West of Niger River delta, GIK 16856	21	marine	4.81	3.40	-2861	MIS 1-6		>1000	Dupont and Weinelt, 1996
off Ghana, KS 12	22	marine	3.87	-1.94	-2955	MIS 1-2	10-15 15-22	500 >1000	Lézine and Vergnaud Grazinni,1993
off Ivory Coast, KS 84-067	23	marine	4.12	-4.12	-3500	MIS 1-11		>1000	Fredoux and Tastet, 1993
off Ivory Coast, KS 84-063	24	marine	4.40	-4.18	-3135	MIS 1-2	10-12 13-14 14-19	220 330 450	Lézine et al., 1994; Lézine and Denèfle, 1997
off Liberia, GIK 16776	25	marine	3.74	-11.40	-4242	MIS 1-12		>1000	Jahns et al., 1998
Gulf of Guinea, GIK 16772	26	marine	-1.21	-11.96	-3913	MIS 1-8		>1000	Marret, 1994
off Sierra Leone, M30 (KL184)	27	marine	7.70	-14.39	-2330	MIS 2-4?		>1000	Agwu and Beug, 1982
off Guinea, GIK 16415	28	marine	9.57	-19.11	-3851	MIS 1-20		>1000	Dupont and Agwu, 1992
off Mauretania, V22-196	29	marine	15.83	-18.95	-3728	MIS 1-6		>1000	Lézine, 1991
off Mauretania, GIK 12329	30	marine	19.37	-19.93	-3320	MIS 1-6		>1000	Agwu and Beug, 1982

continued on next page

Site name	Map Code	Record type	Lat.(°)	Long.(°)	Elevation (m)	Period covered (ka)	Interval (ka)	Sampling resolution (yr/sample)	Reference
off Mauretania, ODP 658	31	marine	20.75	-18.58	-2263	MIS 1-17		>1000	Dupont et al., 1989
off Mauretania, GIK 16017	32	marine	21.25	-17.80	-812	MIS 1-2		>1000	Hooghiemstra, 1988
Lake Patzcuaro, Mexico	33	terrestrial	19.58	-101.58	2044	6-44		> 1000	Watts and Bradbury, 1982
Lake Petén Itzá, Guatemala (pollen record)	34	terrestrial	16.92	-89.83			28-40	> 1000	Bush et al., in press
Lake Quexil, Guatemala	35	terrestrial	16.92	-89.82	110	8-43?	poor age	control	Leyden et al., 1994
Lake Caco, North Brazil	36	terrestrial	-2.97	-43.42	120	0-19	10-19	80	Ledru et al., 2001
Salitre, Lake Campestre, Brazil	37	terrestrial	-9.00	-46.77	970	0-50		> 1000	Ledru et al., 1996
Morro da Itapeva, Brazil	38	terrestrial	-22.78	-45.53	1850	0-35		> 1000	Behling, 1997
Lake Pata, Brazil	39	terrestrial	0.16	-66.41	190	0->40		> 1000	Colinvaux et al., 1996
Colônia, Brazil	40	terrestrial	-23.87	-46.71	900	0-130	11-12	330	Ledru et al., 2009
							14-19	710	
							21-31	420	
							31-130	580	
Siberia, Bolivia	41	terrestrial	-17.83	-64.72	2920	0-50	12-19	780	Mourguiart and
							23-50	750	Ledru, 2003
Consuelo, Peru	42	terrestrial	-13.95	-68.98	1360	0-48		> 1000	Bush et al., 2004
Laguna La Compuerta, Peru	43	terrestrial	-7.30	-78.36	3950	0-33		> 1000	Weng et al., 2006
Laguna Junín, Peru	44	terrestrial	-11	-76.17	4100	0->40	10-15	330	Hansen et al., 1984
							15-26	920	
							26-40	> 1000	
Fúquene, Colombia	45	terrestrial	5.45	-73.46	2540	Fq-2: 0-42	2-11	280	Van Geel and Van der Hammen, 1973; Mommersteg, 1998; Mommersteg and Hooghiemstra, in review
							11-13	250	
							13-45	520	
						Fq-7C: 0-85	2-3	250	
							4-6	>1000	
							6-10	140	

continued on next page

Site name	Map Code	Record type	Lat.(°)	Long.(°)	Elevation (m)	Period covered (ka)	Interval (ka)	Sampling resolution (yr/sample)	Reference
							12-16	1000	
							16-21	220	
							21-22	1000	
							23-37	300	
							38-39	1000	
							39-85	410	
La Laguna, Bogotá Colombia	46	terrestrial	4.92	-74.03	2900	0-35	9-15	500	Helmens et al., 1996
							15-23	670	
							23-24	140	
							24-30	1000	
							30-35	380	
Laguna Chaplin Bolivia	47	terrestrial	-14.28	-61.04	190	0-50		>1000	Burbridge et al., 2004 Mayle et al., 2000, 2007
Laguna Bella Vista, Bolivia	48	terrestrial	-13.37	-61.33	200	0-50		>1000	Burbridge et al., 2004 Mayle et al., 2000, 2007
Lake Titicaca	49	terrestrial	-17.0	-67.0	3810	0-22	13-22	~1000	Paduano et al., 2003
Cariaco Basin, Venezuela, MD 03-2622	50	marine	10.71	-65.17	-877	MIS 3-4		420	González et al., 2008 González and Dupont, 2009
off NE Brazil GeoB 3104	51	marine	-3.67	-37.72	- 767	MIS 1-3	10-18	670	Behling et al., 2000
							21-40	>1000	
							41-50	900	
off NE Brazil, GeoB 3910-2	52	marine	-4.15	-36.21	-2362	MIS 2		125	Dupont et al., 2009
off SE Brazil, GeoB 3229	53	marine	-19.63	-38.72	-780	MIS 1-5		>1000	Behling et al., 2002
off SE Brazil GeoB 3203	54	marine	-21.62	-39.99	-1090	MIS 1-3		>1000	Behling et al., 2002
off Amazon fan ODP 932	55	marine	5.13	-47.18	-3334	MIS 1-3	9-11	330	Haberle and Maslin, 1999
							11-20	>1000	
							20-40	>1000	
							40-49	>1000	

Table 2: Chronological information for sites providing high-resolution pollen records from Africa and South America

Site	Interval	Chronological control						
		AMS	^{14}C	U/Th	other radiometric	Tephra	Varved	Tuning
Africa								
Kashiru Bog, Burundi	0-40 ka	9	15	-	-	-	-	-
Lake Tanganyika	9-25 ka	6 (core MPU-12)	1 (core MPU-11)	-	-	correlate MPU-11 and MPU-12	-	Diatom correlation
Lake Masoko, Tanzania	4.4-45 ka	18	-	-	-	-	-	-
Lake Malawi, M86-18P	10.5-45 ka	3	3	-	-	-	-	-
off Ivory Coast, KS 84-063	4-19 ka	-	-	-	-	-	-	Correlation with SU8118
Barombi Mbo, Cameroon	0-32 ka	-	12	-	-	-	-	-
off Angola, OPD 1078	0-30 ka	-	24	-	-	-	-	-
off Cunene River Mouth, GeoB 1023	0-22 ka	7	2	-	-	-	-	-
South America								
Cariaco Basin, Venezuela MD 03-2622	26-68 ka	-	-	-	-	-	-	Reflectance curve correlation to ODP 1002
off NE Brazil, GeoB3104	12-50 ka	12	-	-	-	-	-	-
off NE Brazil, GeoB3910-2	11-23 ka	7	-	-	-	-	-	-
Lake Caco, North Brazil	0-19 ka	17	-	-	-	-	-	-
Colonia, Brazil	0-130 ka	-	6	-	-	-	-	Comparison to speleothem tuning to precession
Siberia, Bolivia	0-50 ka	11	-	-	-	-	-	-
La Laguna, Bogota, Colombia	0-35 ka	9	3	-	-	-	-	-
Fúquene-2, Colombia	0-42 ka	3	-	-	-	7	-	Orbital tuning
Fúquene-7C, Colombia	0-85 ka	7	-	-	-	-	-	Orbital tuning

Table 3: Definition of mega-biomes from Africa and South America in terms of major vegetation types, local vegetation names, and plant functional types (PFTs) and characteristic pollen taxa.

Mega biome	Component biomes	Equivalent local vegetation names	Component PFTs	Characteristic pollen taxa
Temperate-montane forest	Cool temperate rain forest, Cool mixed forest	Temperate rain forest, Upper montane forest, High Andean forest, Cloud forest, Afromontane forest, temperate-montane dwarf forest, temperate rainforest	Tree fern, Temperate (spring-frost avoiding) cold-deciduous broad-leaved tree, Temperate (spring-frost tolerant) cold-deciduous broad-leaved tree, Temperate evergreen sclerophyll broad leaved tree, Cool temperate evergreen needle-leaved tree, Temperate drought-intolerant forb, Herbs	*Podocarpus*, *Olea capensis*, *Myrica*, *Polylepis-Acaena*, *Quercus*
Warm-temperate/ mixed forest	Warm temperate rain forest, Warm-temperate evergreen broad-leaved forest Warm-temperate mixed forest	Lower montane forest, Sub-Andean forest, Upper Andean forest, Afromontane forest, temperate rainforest	Tree fern, Tropical wet evergreen broad-leaved tree, Tropical mesic drought-deciduous broad leaved tree, Tropical xeric drought-deciduous broad leaved tree, Warm-temperate evergreen needle-leaved tree, Warm-temperate evergreen broad-leaved tree, Temperate evergreen broad-leaved tree, Cool temperate evergreen needle-leaved tree, Cold evergreen needle-leaved tree Temperate drought-intolerant forb	*Olea capensis*

continued on next page

Mega biome	Component biomes	Equivalent local vegetation names	Component PFTs	Characteristic pollen taxa
Tropical forest	Tropical rain forest, Tropical seasonal forest, Tropical dry forest,	Amazonian forest, Atlantic forest, Guinean-Congolian rain Guinean-Congolian deciduous forest, Zambezian forest, Lake Victoria Mosaic. Cerrado, Restinga, Cactus forest, Andean xerophytic bush, Miombo woodland, tropical evergreen forest, tropical semi-deciduous forest, moist tropical forest	Tree fern, Tropical evergreen broad-leaved tree, Tropical wet evergreen broad-leaved tree, Tropical mesic evergreen broad-leaved tree, Tropical mesic drought-deciduous broad-leaved tree, Tropical xeric drought-deciduous broad-leaved tree, Tropical drought-intolerant forb, Wet/dry tropical lianas, Wet tropical herbs	*Brachystegia*, *Uapaca*-type *kirkiana*, *Isoberlinia*, *Mallotus*
Savannah and xerophytic shrubland	Tropical dry forest Steppe, Savannah	Pampa, Caatinga, Steppes, Sudanian savannah, Somalia-Masai region, Zambezian savannah	Tropical xeric drought-deciduous broad-leaved tree, Drought-tolerant small-leaved low or high shrub, Eurythermic drought-adapted forb, Tropical arid drought-deciduous broad-leaved tree, Eurythermic drought-tolerant forb, Dry tropical herb, Graminoid	Poaceae *Tribulus*, Chenopodiceae
Grassland and dry shrubland	Cool grass shrublands, Cool grassland, Temperate xero-phytic woods/shrub	Páramo, Grasspáramo, Subpáramo, Heather, Cushion Heather Afroalpine, tropical alpine grassland	Temperate sclerophyll broad-leaved tree, Rosette or cushion forb, Eurythermic drought-adapted forb, Dry tropical herbs, Herbs, Graminoid	Poaceae Ericaceae
Desert	Desert	Coastal desert, semi-desert	Desert shrubs, Eurythermic drought-adapted forb	

Table 4: Summary of vegetation changes through D-O cycles at individual high-resolution sites from Africa and South America. Vegetation description follows Figs. 4 and 5 except for the Cariaco Basin (Fig.5) and Fúquene (Fig.6).

D-O cycle		Kashiru swamp	Lake Masoko	Colonia	GeoB3104	Cariaco Basin	Fúquene
D-O 1	GS (YD)	temperate-montane forest	forest with *Olea capensis*	open grassland, dry shrubland	steppe, semidesert	no data	subpáramo
	GI	tropical forest		forest peaks at 12+19ka	forest,		Andean forest
	D-O warming						
D-O 2	GS (HS1)	grassland + dry shrubland savannah + xerophytic shrubland, little forest	warm-temperate mixed forest		steppe, semidesert		Andean forest, grasspáramo grasspáramo
	GI						
	D-O warming						
D-O 3	GS (HS2)	temperate-montane forest, tropical forest	grassland + dry shrubland, savannah + xerophytic shrubland little forest	temperate rainforest	forest?, steppe steppe, semidesert		
	GI						
	D-O warming						
D-O 4	GS	grassland + dry shrubland savannah + xerophytic shrubland					Andean forest, grasspáramo
	GI						
	D-O warming						
D-O 5	GS (HS3)			tropical forest	forest, steppe	semideciduous forest savannah, montane forest	
	GI	little forest		open grassland, dry shrubland	steppe semidesert	semideciduous forest, savannah	
	D-O warming						
D-O 6	GS						
	GI		grassland + dry shrubland, forest with *Olea capensis*				
	D-O warming						
D-O 7	GS						Andean forest
	GI					semideciduous forest	
	D-O warming						
D-O 8	GS			temperate rainforest		evergreen+gallery forest savannah, montane forest	grasspáramo
	GI	more forest		grassland + dry shrubland,		evergreen+gallery forest	subpáramo
	D-O warming						

continued on next page

D-O cycle		Kashiru swamp	Lake Masoko	Colonia	GeoB3104	Cariaco Basin	Fúquene
D-O 9	GS (HS4)	temperate-		declining forest	forest, steppe	montane forest	
	GI	montane forest,			steppe,	semideciduous forest,	
	D-O warming	less tropical			semidesert	evergreen+gallery forest	
D-O 10	GS	forest,					Andean forest, subpáramo
	GI	increasing					
	D-O warming	savannah					
D-O 11	GS	xerophytic		temperate			grasspáramo
	GI	shrubland	temperate-	rainforest		semideciduous forest	subpáramo
	D-O warming		montane forest				
D-O 12	GS				forest?, steppe	montane forest	Andean forest, subpáramo
	GI		no data		steppe,	semideciduous forest	
	D-O warming				semidesert		
D-O 13	GS (HS5)	temperate-			forest, steppe	semideciduous forest	grasspáramo
		montane forest				savannah	
	GI	tropical forest			steppe	semideciduous forest	
	D-O warming				semidesert		
D-O 14	GS	no data			no data	semideciduous forest	Andean forest, subpáramo
	GI					savannah	Andean forest
	D-O warming						
D-O 15	GS (HS5a)						sub-Andean forest
	GI					semideciduous forest	
	D-O warming						
D-O 16	GS			temperate-			
	GI			montane forest,			
	D-O warming			savannah+			
D-O 17	GS			xerophytic			
	GI			scrubland			
	D-O warming						
D-O 18	GS (HS6)					montane forest, savannah	
	GI					montane forest, evergreen	
	D-O warming					+gallery forest	
D-O 19	GS					no data	subpáramo
	GI						Andean forest
	D-O warming						

Table 5: Summary of inferred climate changes through D-O cycles at individual high-resolution sites from Africa and South America

D-O cycle		Kashiru swamp	Lake Masoko	Colonia	GeoB3104	Cariaco Basin	Fúquene
D-O 1	GS (YD)	cool,	moderately	dry, wetter at	moderately dry	no data	moderately cool
	GI	moderately wet	wet, short dry	19 and 12 ka	moderately wet		moderately cold, dry
	D-O warming		seasons				
D-O 2	GS (HS1)	cool and	moderately wet				cold, dry
	GI	moderately dry,			moderately dry		cold
	D-O warming	effect of low CO_2					
D-O 3	GS (HS2)	wet	cool and dry	wet	moderately wet?		
	GI				moderately dry		
	D-O warming						
D-O 4	GS	cool and					
	GI	moderately dry,					moderately cold
	D-O warming	effect of low CO_2					
D-O 5	GS (HS3)			dry	moderately wet	dry, cool	
	GI				moderately dry	very dry	
	D-O warming						
D-O 6	GS						
	GI		moderately dry				
	D-O warming		and cool				
D-O 7	GS						warm
	GI					wet	
	D-O warming						
D-O 8	GS			moderately wet		wet, cool	cold, dry
	GI	wet		dry		wet	cool, dry
	D-O warming						
D-O 9	GS (HS4)	cool and			moderately wet	dry, cool	
	GI	increasingly			moderately dry	very wet	
	D-O warming	drier, and/or					
D-O 10	GS	effects of low CO_2					moderately cold, dry
	GI						
	D-O warming						

continued on next page

D-O cycle		Kashiru swamp	Lake Masoko	Colonia	GeoB3104	Cariaco Basin	Fúquene
D-O 11	GS			wet			cold, dry
	GI		moderately wet			wet	cool, dry
	D-O warming						
D-O 12	GS				moderately wet?	cool	moderately cold, dry
	GI		no data		moderately dry	wet	
	D-O warming						
D-O 13	cool,			moderately wet	dry	cold, dry	
	GI	moderately wet			moderately dry	wet	
	D-O warming						
D-O 14	GS	no data			no data	moderately dry	moderately cool
	GI						warm, wet
	D-O warming						
D-O 15	GS (HS5a)						very warm, wet
	GI					wet	
	D-O warming						
D-O 16			moderately dry				
	GI						
	D-O warming						
D-O 17	GS						
	GI						
	D-O warming						
D-O 18	GS (HS6)					dry, cool	
	GI					wet	
	D-O warming						
D-O 19	GS					no data	cool, wet
	GI						warm, wet
	D-O warming						

6.2 Impact of abrupt climate change in the tropical southeast Atlantic during Marine Isotope Stage (MIS) 3

Ines Hessler[a*], *Stephan Steinke*[a], *Jeroen Groeneveld*[b], *Lydie Dupont*[a], *Gerold Wefer*[a]

[a] MARUM - Center for Marine Environmental Sciences, University of Bremen, 28359 Bremen, Germany

[b] Alfred Wegener Institute for Polar and Marine Research 27568, Bremerhaven, Germany

[*] Corresponding Author: Tel.: +49 (0) 421 - 218 65682, Email: ihessler@marum.de

Submitted to Paleoceanography

6.2.1 Abstract

High resolution planktonic foraminifera Mg/Ca paleotemperature and oxygen isotope reconstructions of Ocean Drilling Program (ODP) Site 1078 (off Angola) reveal insight into the behaviour of the Angola Current (AC), the Angola-Benguela Front (ABF), and the Benguela Current (BC) during the last glacial (50-23.5 ka BP). Special emphasis is put on North Atlantic Heinrich Stadials (HS), which are thought to lead to an accumulation of heat in the South Atlantic due to a reduction of the Atlantic Meridional Overturning Circulation (AMOC). A warming of the surface waters during austral summer in association with HS is recorded in the Mg/Ca record of *Globigerinoides ruber* (pink) which supports the hypothesis of a bipolar seesaw during HS. In contrast, the Mg/Ca temperatures and d18O values of *Globigerina bulloides*, representing the surface water conditions of the BC upwelling regime during austral winter, show no response to the North Atlantic HS in the study area. We suggest that the expected warming during HS in the BC upwelling regime is most likely mitigated by enhanced upwelling and cooling coincident with HS.

6.2.2 Introduction

The tropical southeast Atlantic surface circulation is dominated by a wind-driven current system that is crucial in the cross-equatorial heat and salt transport (Gordon, 1986; Peterson and Stramma, 1991). The BC represents an important component of the upper level warm water route of the thermohaline circulation, car-

rying heat northward across the equator. The warm surface waters, coming from the Agulhas Leakage, are driven offshore by coastal upwelling (Gordon, 1986). Reconstructing the history of upwelling, links to major oceanographic, atmospheric and biological issues (e.g. current pattern, wind stress; water mass mixing, carbon cycle, productivity) can be made (Waldron et al., 1992; Summerhays et al., 1995; Berger and Wefer, 2002; Kim et al., 2003). The northern boundary of the Benguela system is defined by the occurrence of a sharp thermal front, the Angola-Benguela Front (ABF), situated at present day between 15°-17°S off southwest Africa (Shannon et al., 1987; Kostianoy and Lutjeharms, 1999; Lass et al., 2000). Separating the cold, productive waters of the BC from the warm nutrient-limited waters of the Angola Current (AC), the ABF represents an essential feature of the regional ocean circulation off Namibia and Angola (Shannon et al., 1987). Seasonal variations in the position and characteristics of the ABF are controlled by the pressure gradient driven by the South Atlantic Anticyclone (Kostianoy and Lutjeharms, 1999; Colberg and Reason, 2006). The intensity of the ABF, expressed in its horizontal thermal gradient, and its position is suggested to be sensitive to changes in the position and intensity of the trade winds (Kim et al., 2003; Colberg and Reason, 2006). Enhanced trade winds lead to an intensified Benguela upwelling which results in a cooling of the surface waters south of the ABF. North of the ABF intensified trade winds result in a stronger intrusion of AC waters, hence leading to a warming of the surface waters (Kim et al., 2003).

An intensification of the BC during the last glacial due to intensified trade winds has been suggested by several studies (Diester-Haas, 1985; Summerhays et al., 1995; Scheider et al., 1996; Mix and Morey, 1996; Little et al., 1997; Kirst et al., 1999, Kim et al., 2003; Farmer et al., 2005; Kucera et al., 2005). In addition, it is assumed that an increase in the upwelling intensity and an expansion of the Southern Ocean cold water sphere during the last glacial resulted in a cooling of the surface water in the Benguela upwelling region (Niebler et al., 2003).

Contradicting results exist concerning the glacial position and intensity of the ABF. Kim et al. (2003) proposed an enhanced temperature gradient due to intensified trade winds together with a steady position of the ABF as inferred from alkenone-based SST records. In contrast, a strong northward shift of the ABF during the last glacial is suggested by Jansen et al. (1996). The authors conclude that the entire southeast Atlantic Current system was latitudinally displaced due to a shift of the Subpolar and Subtropical Front during the last glacial. (Kirst et al., 1999) suggest a reduction of the SST gradient over the front due to the southward penetration of warm waters associated with "Benguela Ninos" rather than a northward shift of the ABF during the last glacial.

Millennial-scale climate changes associated with the North Atlantic Heinrich events, the so-called Heinrich Stadials (HS), have been found in records from various places around the globe including the tropics (e.g. Leuschner and

Sirocko, 2000; Dupont et al., 2008; González et al., 2008; Tjallingii et al., 2008; Zhou et al., 2008). Based on the bipolar seesaw concept it has been suggested that a reduction in the strength of the Atlantic meridional overturning circulation (AMOC) would have led to a cooling of the North Atlantic realm and an accumulation of heat in the South Atlantic realm during HS (Broecker, 1998; EPICA members, 2006; Barker et al., 2009). In contrast to a cooling in the northern Hemisphere during HS, SST records from the southeast South Atlantic reveal a warming during HS in the Southern Ocean as a consequence of the reduction of the AMOC and a potential intensification of the Agulhas Leakage (Barker et al., 2009).

However, very little is known about changes associated with HS in the tropical southeast Atlantic, especially on the Benguela coastal upwelling system, the strength and position of the ABF, and the intensity of the AC. Records from the northern Benguela upwelling system document intense upwelling events controlled by an increased intensity and zonality of the trade winds in connection with HS (Little et al., 1997). In contrast, a decrease in the SST gradient across the ABF was reconstructed and attributed to weaker trade winds during HS1 causing a decrease in upwelling intensity (Kim et al., 2003). Due to the decrease in trade wind intensity a weakening of the AC is assumed, leading to a reduction of warm tropical water transport towards the north of the ABF (Kim et al., 2003). A warming of the Benguela Current region during HS1 was also observed in an alkenone based temperature record from the eastern Angolan Basin (Kim et al., 2002). In contrast to these findings, Farmer et al. (2005) found a brief but significant cooling of 1.5°-2°C together with an increase in upwelling intensity of the Benguela current system that most likely corresponds to HS1.

These partly inconsistent results concerning the potential impact of HS on the oceanography (e.g. the AC, ABF, and BC) off southwest Africa complicate the understanding of the climatic and oceanographic development during the last glacial in such an important region. Moreover, the temporal resolution of the existing records is either too low to detect a possible impact of HS on the tropical southeast Atlantic, or the records are too short to cover more than one HS. To draw more general conclusions about the regional impact of HS, we need a high resolution record covering several HS. Here, we present high-resolution *G. bulloides* and pink-pigmented *G. ruber* Mg/Ca-based SST records (ca. 200 year sample spacing) along with δ^{18}O values of *G. bulloides* from the tropical southeast Atlantic (Ocean Drilling Program Site 1078, off Angola) in order to reconstruct the behaviour of the AC, ABF and BC during the last glacial (50-23.5 ka BP) with special emphasis on HS.

6.2.3 Modern Oceanographic Setting

The modern oceanography in the southeast Atlantic is dominated by the seasonally varying trade wind system. As one of the four major eastern boundary currents, the BC, is the main oceanographic feature controlling the regional surface water circulation patterns (Figure 13)

(Nelson and Hutchings, 1983; Shannon, 1985; Stramma and Peterson, 1989; Peterson and Stramma, 1991). The water is formed at the subtropical convergence zone between 30° and 40°S at a depth of 100 to 300 m. The contribution of Agulhas waters to the BC appears to be small but continuous (Nelson and Hutchings, 1983). The remaining water is subantarctic surface water which is added at the Subtropical Front, or intermediate water that enters the South Atlantic through the Drake Passage (Nelson and Hutchings, 1983, Stramma and Peterson, 1989).

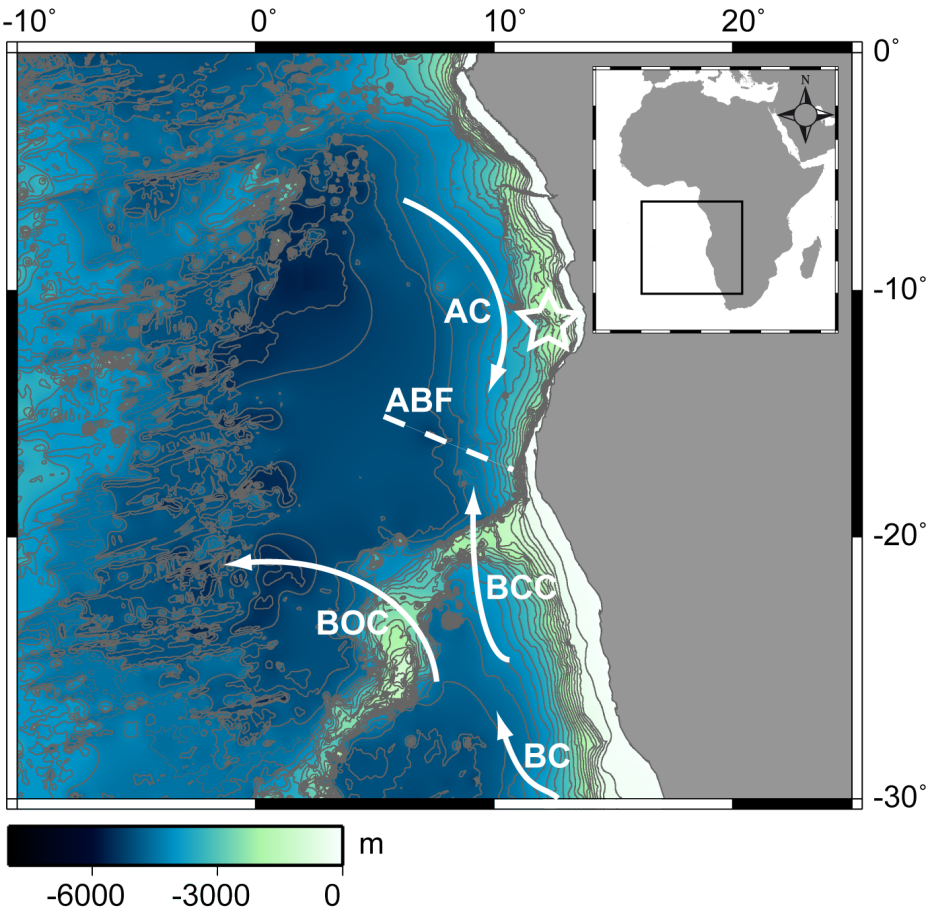

Figure 13: Modern southeast Atlantic bathymetry and surface water oceanography. AC = Angola Current; ABF = Angola-Benguela Front; BCC = Benguela Coastal Current; BOC = Benguela Ocean Current; BC = Benguela Current. Star indicates location of ODP Site 1078.

The Benguela Current system flows north-northwest along the coast of southwest Africa, dividing around 25°S into the coastal oriented Benguela Coastal Current (BCC) and the northwestward flowing Benguela Ocean Current (BOC) (Figure 13). Seasonal components of

the BC extend up to 12°-13°S which define the northernmost boundary (Figure 14) (Moroshkin et al., 1970). Atmospheric conditions over the BC region are mainly influenced by the semi-permanent South Atlantic high pressure cell and a low pressure system developing over southern Africa during the austral summer. Prevailing winds from the south and south-east induce coastal upwelling of cold, nutrient rich water which are characterised by spatial and temporal variations (Nelson and Hutchings, 1983; Shannon, 1985; Stramma and Peterson, 1989). In general, wind-induced upwelling is restricted to the area between the ABF and the Agulhas Bank (Lutjeharms and Meeuwis, 1987). The annual position and intensity of the BC upwelling varies as a consequence of seasonal shifts in the position and intensity of the South Atlantic High and changes in the atmospheric pressure over the African subcontinent. Although coastal upwelling takes place throughout the year, the peak season is the austral winter (July-September). The upwelling is weaker during the rest of the year. Two regionally fixed centres of intense upwelling (26°S= Lüderitz cell and 29°S = Namaqua cell) split the BC region into a northern and southern regime, which are located between the northern and southern boundary of the SE trade winds (Hagen et al., 2001). This results in an opposite pattern in the upwelling intensity between the seasons. Pronounced upwelling maxima occur in the northern Benguela region (north of 25°S) during austral winter, while very little upwelling takes place in the southern regime south of 30°S. The central (25°-30°S) and the northernmost part of the BC, however, seem to be unaffected by obvious periods of upwelling relaxation (Shannon and Nelson, 1996). The upwelling extends to its northernmost position at about 12°-13°S during austral winter which is coupled to the position of the ABF (Figure 14). The warm and high-saline AC that is fed by the south-eastern branch of the South Atlantic Counter Current flows southwards along the shelf of Angola (Moroshkin et al., 1970). At approximately 17°S, the waters of the AC encounter the upwelling waters of the BC that result in the development of a sharp thermal front (temperature drop from 27° to 20.5 °C, Schlitzer, 2010), the Angola-Benguela Front (ABF) (Figure 13). This shallow (upper 50-75 m water depth) front is E-W oriented and extends to a distance of about 150 km offshore (Shannon et al., 1987). A meridional migration of the ABF is induced by the seasonally varying wind system. Between July and September the ABF reaches its northernmost position of 12°-13°S which is coupled to the equatorward extension of the coastal upwelling zone (Figure 14). During this time of the year, the ABF is less well defined leading to a regular southward intrusion of warm saline Angolan waters as far south as 22°S. Highest convergence between the AC and BC occurs between January and March when the ABF is located at about 17°S (Shannon et al., 1987.

6.2.4 Strategy and proxy variables

Two different planktonic species of foraminifera, *G. bulloides* and *G. ruber* (pink), were selected to reconstruct variations in sur-

face water conditions in the tropical eastern Atlantic during the last glacial. Temperature variations of near surface waters were estimated by using Mg/Ca in *G. bulloides*, an asymbiotic species often related to upwelling environments (Hemleben et al., 1989). In addition, we measured the Mg/Ca of *G. ruber* (pink), a warm-water and symbiont-bearing species (Hemleben et al., 1989). Due to the rarity of *G. ruber* (pink) specimens in the samples, no δ^{18}O measurements were performed. The spatial distribution of planktonic foraminifera depends largely on water temperatures, thermal stratification and nutrients (Bé and Tolderlund, 1971; Hemleben et al., 1989).

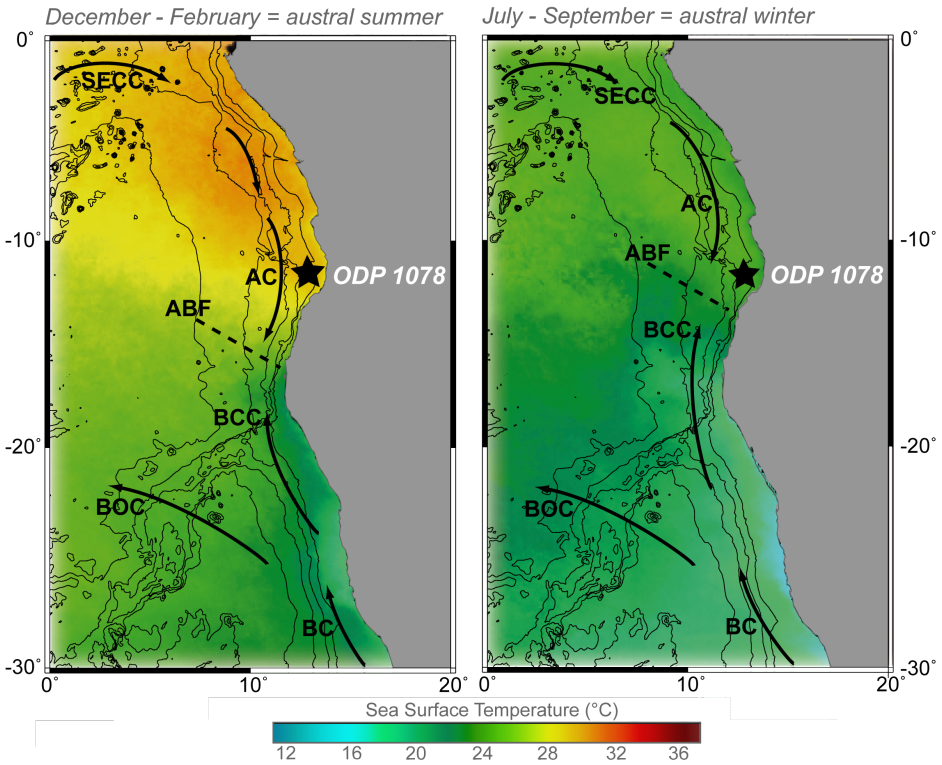

Figure 14: Seasonal SST pattern and location of oceanographic features off south-west Africa. Location of ODP Site 1078 is indicated by a black star.

The occurrence of *G. bulloides* is strongly related to poorly stratified eutrophic waters in subpolar and upwelling regions (Hemleben et al., 1989; Ufkes et al., 1998). Accordingly, its abundance in the south-eastern Atlantic is highest in the ABF and BC (Ufkes et al., 1998; Jansen et al., 1996). In contrast, *G. ruber* (pink), typical for oligotrophic warm tropical waters, mainly occurs in the warm waters of the AC (Jansen et al., 1996; Ufkes et al., 1998). The seasonal shift of the ABF provides a dominant control on the temporal distribution pattern and composition of planktonic foraminifera assemblages in our research area.

Sediment trap studies on *G. bulloides* and *G. ruber* (pink) from different regions of the world oceans confirm that both species become important components of the foraminiferal population during seasons with different environmental conditions (Zaric et al., 2005; Wilke et al., 2009). It has been shown that during periods of upwelling, high productivity and cool surface waters, fluxes of *G. bulloides* are highest as demonstrated for several upwelling regions (Zaric et al., 2005; Wilke et al., 2009). The ambient waters of ODP Site 1078 are increasingly influenced by the ABF and BC due to their northernmost position during austral winter. During austral summer when surface water temperatures are highest and the upper water column is strongly stratified, *G. ruber* (pink) becomes an important part of warm water assemblages (Thompson et al., 1979; Zaric et al., 2005; Wilke et al., 2009). The ABF and BC are at their southernmost position during austral summer giving way for the AC to penetrate further south into the southeast Atlantic (Figure 2). *G. ruber* (pink) is most common in the upper 25 m but occur in lesser abundance down to 50 m water depth as shown by plankton tow studies in the Bight of Angola (Oberhänsli et al., 1992). In the Benguela upwelling system, *G. bulloides* occurs mainly in the upper 50 m of the water column but was also found in lesser abundance in a water depth of 100-150 m (Oberhänsli et al., 1992).

The different ecological and seasonal preferences of the planktonic foraminifera species used in this study enable us to derive seasonal SST estimates for the tropical southeast Atlantic. Thus, the *G. ruber* (pink) based Mg/Ca temperatures allow to reconstruct changes of the AC during austral summer. *G. bulloides* based Mg/Ca SST estimates allow to monitor the Benguela upwelling system during austral winter.

6.2.5 Material and Methods

Site description and age model

The planktonic foraminifera tests used in this study were obtained from sediments of ODP Site 1078 Hole C situated inside the Bight of Angola (11°55'S, 13°24'E) in 426 m water depth (Figure 13). The sediment is predominately composed of moderately bioturbated olive-grey silty clay with varying amounts of nannofossils and planktonic and benthic foraminifera (Wefer et al., 1998).

The chronostratigraphy of the studied depth interval of ODP Site 1078 is based on six AMS-^{14}C measurements on foraminifera and molluscs tests (Dupont et al., 2008). All radiocarbon ages were corrected with an average oceanic reservoir age of 400 yr (Hughen et al., 2004) and were calibrated using the Fairbanks0107 calibration data set (Fairbanks et al., 2005). In the following all ages refer to calibrated ka before present (cal ka BP).

Based on our age model, the Mg/Ca SST records of *G. bulloides* and *G. ruber* (pink) cover the time period between 50 and 23.5 cal ka BP. The average temporal resolution is 200 years. However, the age model for the period between 50 and 40 ka needs to be considered with caution because of large uncertainties in the ^{14}C calibration curve beyond ~ 40 ka.

Analytical methods

Samples (n = 155) for both species were taken for Mg/Ca analysis with a sampling interval of 2 cm and a volume of 10 cm^3. 40 specimens of *G. bulloides* (250-315 μm) and 15 to 40 specimens of *G. ruber* (pink) (250-400 μm) were picked, gently crushed, and cleaned following the cleaning protocol of Barker et al. (2003). Clays were removed by rinsing the samples five times with distilled deionized water and two times with methanol (Ultrapure) while after each rinse samples were briefly ultrasonicated. Samples were then oxidised with alkali buffered 1% H_2O_2 solution and heated for 10 minutes to remove organic matter. Possible gaseous build-ups were released by tapping the micro-tubes every 2.5 minutes, while after 5 minutes micro-tubes have been briefly placed in an ultrasonic bath to maintain the contact between reagent and sample. This step was repeated after renewing the oxidation solution to ensure the removal of all organic matter. After removing the oxidation solution, rinsing with distilled deionized water (Seralpur), and transferring the samples into new clean micro-tubes a weak acid leach with 250 μl 0.001 M HNO_3 was applied including a 30 seconds of ultrasonic treatment. This step was repeated to remove any re-absorbed ions on the test fragments. After two rinses with distilled deionised water the samples were dissolved in 0.075 M HNO_3 and placed in the ultrasonic bath to support the dissolution. After dissolution, any remaining solids were removed by centrifuging the samples for 10 minutes and transferring the supernatant into clean micro-tubes. Samples were measured with an ICP-OES Perkin Elmer Optima 3300 RL with autosampler and ultrasonic nebulizer (U-5000 AT Cetac Technologies Inc., Department of Geosciences, University of Bremen). Instrumental precision of the ICP-OES was ensured by analysis of an in-house standard solution (Mg/Ca = 2.92 mmol/mol) every fifth sample. In order to allow for interlaboratory comparison an international limestone standard (ECRM752-1) with a specified Mg/Ca of 3.75 mmol/mol (Greaves et al., 2008) was routinely analysed twice before each batch of 50 samples. To monitor the efficiency of the cleaning Al/Ca, Fe/Ca and Mn/Ca were measured additionally. Mg/Ca were converted to SST by means of the species-specific calibration for *G. bulloides* developed by Mashiotta et al. (1999) and for *G. ruber* (pink) using the calibration developed by Anand et al. (2003).

For the oxygen isotope measurements *G. bulloides* tests were picked from the same samples as for Mg/Ca analysis. Depending on the availability of material, between 6 and 12 specimens were picked out from the size fraction 250-315 μm. Stable oxygen isotope analyses were performed using a Finnigan MAT 251 mass spectrometer with an automated carbonate preparation device at the MARUM, University of Bremen. The external standard error of the stable oxygen isotope analyses is < 0.06‰. Values are reported relative to the Vienna Pee Dee Belemnite (VPDB), calibrated by using the National Bureau of Standards (NBS) 18, 19, and 20 standards.

6.2.6 Results

The Mg/Ca of range between 2.8 and 4.2 mmol/mol (Figure 15). Between 50 and ~40 ka BP values are usually lower (2.8-3.7 mmol/mol) whereas the period between ~ 40 and 23.5 ka BP is marked by higher ratios fluctuating between 3.4 and 4.2 mmol/mol. The Mg/Ca of *G. ruber* (pink) varies between 3.5 and 4.0 mmol/mol. The Mg/Ca exceed 4.0 mmol/mol between 36.5 and 38.5 ka BP. Maximum values of up to 4.5 mmol/mol are recorded around 38 ka BP (Figure 15).

G. bulloides based Mg/Ca-temperatures, calibrated according to Mashiotta et al. (1999), range between 17° and 20 °C ± 0.7°C (95% confidence level at max. 22°C, Mashiotta et al., 1999) over the investigated time period (Figure 15). SSTs are in average cooler (17-19°C) during the period 50-40 ka BP and changes are of higher amplitude than during the period 40-23.5 ka BP (Figure 15). *G. bulloides* temperatures range between 17° and 19°C whereas coldest temperatures are recorded around 42-44 ka BP. Higher temperatures (19°-20°C) are observed for the period 40-23.5 ka BP. Temperature fluctuations during this period appear to be more frequent.

The Mg/Ca temperature record of pink-pigmented *G. ruber* (Figure 15) differs considerably from that of *G. bulloides*. Throughout the covered time period, the temperature ranges between 25° and 27°C. Highest temperatures occur between 40 and 37 ka BP. The general trend during the period 50-40 ka BP is increasing (25°-26.5°C) whereas *G. ruber* temperatures decrease again (27°-25°C) between 37 and 23.5 ka BP (Figure 3).

Values of δ^{18}O calcite of *G. bulloides* vary between 1.1 and 0.4 ‰ (Figure 15). Local δ^{18}O seawater estimates for ODP Site 1078 vary between 1.4 and 0.5‰. Similar to the Mg/Ca temperature record of *G. bulloides* the δ^{18}O record reveals two distinct phases. Between 50 and 37 ka BP pronounced high amplitude variations occur, while the general trend is decreasing.

6.2.7 Discussion

Dissolution is known to affect the Mg/Ca of planktonic foraminifera in a systematic way, with increasing dissolution causing a progressive decrease in the Mg/Ca (Barker et al., 2005). We exclude an effect of carbonate dissolution on our foraminiferal Mg/Ca ratios because of the shallow location of ODP Site 1078 (426 m water depth) and well-preserved planktonic foraminifera tests. In the following we first discuss the Mg/Ca record of *G. ruber* (pink), which represents SST estimates of the AC during austral summer. The *G. bulloides* derived SST estimates are used to discuss the glacial development of the BC during austral winter.

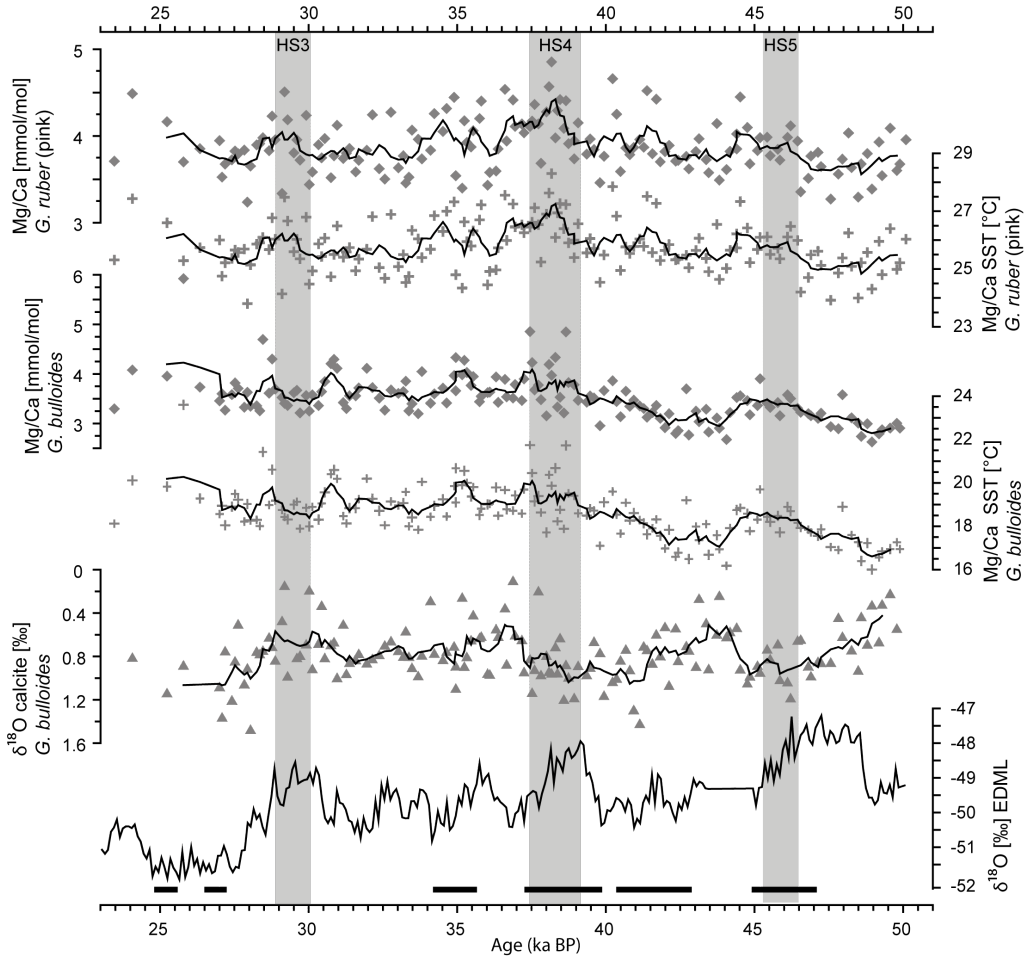

Figure 15: Mg/Ca of *G. ruber* (pink) in mmol/mol, Mg/Ca SST of *G. ruber* (pink) calibrated after Anand et al., (2003). Mg/Ca of *G. bulloides* in mmol/mol, Mg/Ca SST of *G. bulloides* calibrated after Mashiotta et al. (1999). δ^{18}O of *G. bulloides* calcite given in per mil. HS are after Sarnthein et al. (2001) and adjusted within dating uncertainties of the age model of ODP 1078. Dating intervals are shown as black bars at the bottom of the figure. EDML δ^{18}O is given in per mil.

The Angola Current System

Temperature reconstructions of the glacial southeast Atlantic surface waters indicate a lowering of SST that vary between 3.5°C and 5°C (Schneider et al., 1995; Kirst et al.; 1999, Kim et al., 2003; Farmer et al., 2005), most likely due to changes in the continental ice coverage, orbital parameters, atmospheric CO_2, and sea level, and global mean temperatures (e.g. Broccoli, 2000).

Our Mg/Ca temperatures for *G. ruber* (pink) represent southern hemisphere summer SST for the area of the AC. The reconstructed glacial temperatures are lower by up to 4°C than today, which is consistent with other glacial temperature reconstructions (e.g.

Schneider et al., 1995; Farmer et al., 2005). The *G. ruber* (pink) Mg/Ca based SST record reveals significantly increased temperatures around 46 ka, 38 ka and 29.5 ka that are most likely associated with the North Atlantic HS. Most pronounced is a warming around 38.5 and 37 that is coincident with HS4 (Figure 15). This increase in SST during HS can presumably be attributed to mode shifts in the Atlantic heat transport regime associated with changes in the intensity of the AMOC. A slow down or reduction in the intensity of the AMOC during HS caused a warming in the South Atlantic while the temperature in the North Atlantic decreases, the so-called bipolar seesaw concept (Stocker, 1998; Broecker, 1998; Seidov and Maslin, 2001; Barker et al., 2009). A linear dependency between the duration of stadials in the north Atlantic region with warming events in the southern hemisphere is further suggested by the EPICA members (2006). The authors argue that the duration of a warming period in the Southern Ocean due to a reduced AMOC determines the amount of heat accumulated in the Southern Ocean, supporting the concept of a thermal bipolar seesaw.

The warming of the South Atlantic due to thermal anti-phase behaviour seems to be strongest off the coast of west and/or southwest Africa where modelling experiments indicate the formation of a warm water pool (Rühlemann et al., 2003; Prange et al., 2004). Simulated SST reveal an increase of about 2°C for meltwater perturbation experiments (Prange et al., 2004). This is consistent with our results that show a 1°-2°C increase in SST during periods of HS (Figure 15). A rapid and intense warming of intermediate waters during HS1 at ODP Site 1078 is indicated also by benthic foraminiferal oxygen isotopes (Rühlemann et al., 2003). The authors suggest that the warming occurs due to a reduced ventilation of cold intermediate and deep waters in conjunction with a downward mixing of heat from the thermocline. Similarly, a *G. bulloides* Mg/Ca based SST record from the southeast South Atlantic reveals warming during HS 1 as a consequence of a reduced AMOC (Barker et al., 2009).

The Angola Benguela Front and the Benguela Upwelling System

Comparable to the summer season SST reflected by Mg/Ca of *G. ruber* (pink), temperatures of *G. bulloides*, which are indicative for water masses of the ABF and BC during the southern hemisphere winter season, show significantly cooler average temperatures than today. The Mg/Ca temperatures of *G. bulloides* vary between 17° and 20°C and are therefore 2°-5°C below modern temperatures (Figure 15). There are several possibilities for the strong cooling of the BC and ABF water masses. Firstly, the temperature of the upwelled waters of the Benguela coastal current might has been cooler during the last glacial. Compared to present day conditions the Antarctic winter sea ice is reconstructed to expand about 10° in latitude reaching up to 47°S during the last glacial (Gersonde et al., 2005). As a consequence the Southern Ocean frontal system, including the Polar Front, Subantarctic Front and Subtropical Front would

have been shifted northwards, giving way to a northward expansion of the Antarctic cold water realm (Keeling and Stephens, 2001; Gersonde et al., 2005). A northward shift of the Subtropical Front could have also cut of the warm water route via the Agulhas Leakage leading to a reduced supply of warm waters to the Benguela Current (Gersonde et al., 2003, 2005). However, contradicting results are given by Matsumoto et al. (2001) arguing against a glacial migration of the Southern Ocean Polar Front. This study not only indicates a largely unchanged position of the Southern Ocean Fronts but generally little change in the overall Southern Ocean hydrography. Secondly, Jansen et al. (1996) suggest that a northward shift of the South Atlantic Fronts results in a more northward position of the ABF. Hence, the ABF would have moved closer to our core location or even passed over it towards a more northerly position resulting in significantly lower SST. In contrast to the results of Jansen et al. (1996), a relatively stable glacial position and a more pronounced temperature gradient across the ABF due to increased SE trade winds and upwelling are reported by Kim et al. (2003). The assumption of a stable and intensified ABF in relation to enhanced SE trade-winds during glacial times is supported by modelling studies (Colberg and Reason, 2006). As a third possibility, the intensification of the Benguela upwelling during the last glaciation as a consequence of enhanced trade winds would lead to lowered SST and has been proposed by several studies (Diester-Haas, 1985; Mix et al., 1986; Summerhays et al., 1995; Scheider et al., 1996; Mix and Morey, 1996; Little et al., 1997; Kirst et al., 1999, Kim et al., 2003; Farmer et al., 2005; Kucera et al., 2005). An intensification of the BC system would result in a cold water intrusion further to the north, influencing the ambient waters of ODP Site 1078 more directly and/or extend the duration of the cold water influence from the south. Both, Kirst et al. (1999) and Schneider et al. (1996) indicate that the upwelling intensity was at its maximum between 50 and 35 ka. Hence, coolest temperatures were recorded during this period (Schneider et al., 1996; Kirst et al., 1999). This is in good agreement with our *G. bulloides* Mg/Ca-based temperature record (Figure 16).

We suggest that the significantly decreased austral winter SSTs in the study area during the last glacial reflect the combined effects of an intensification of the Benguela coastal upwelling, and enhanced northward intrusion of cold Benguela Current waters and a decreased inflow of warm waters via the Agulhas Leakage due to changes in glacial boundary conditions. This inference, however, should be explored further with a broader geographical coverage of surface water temperature records that span the last glaciation.

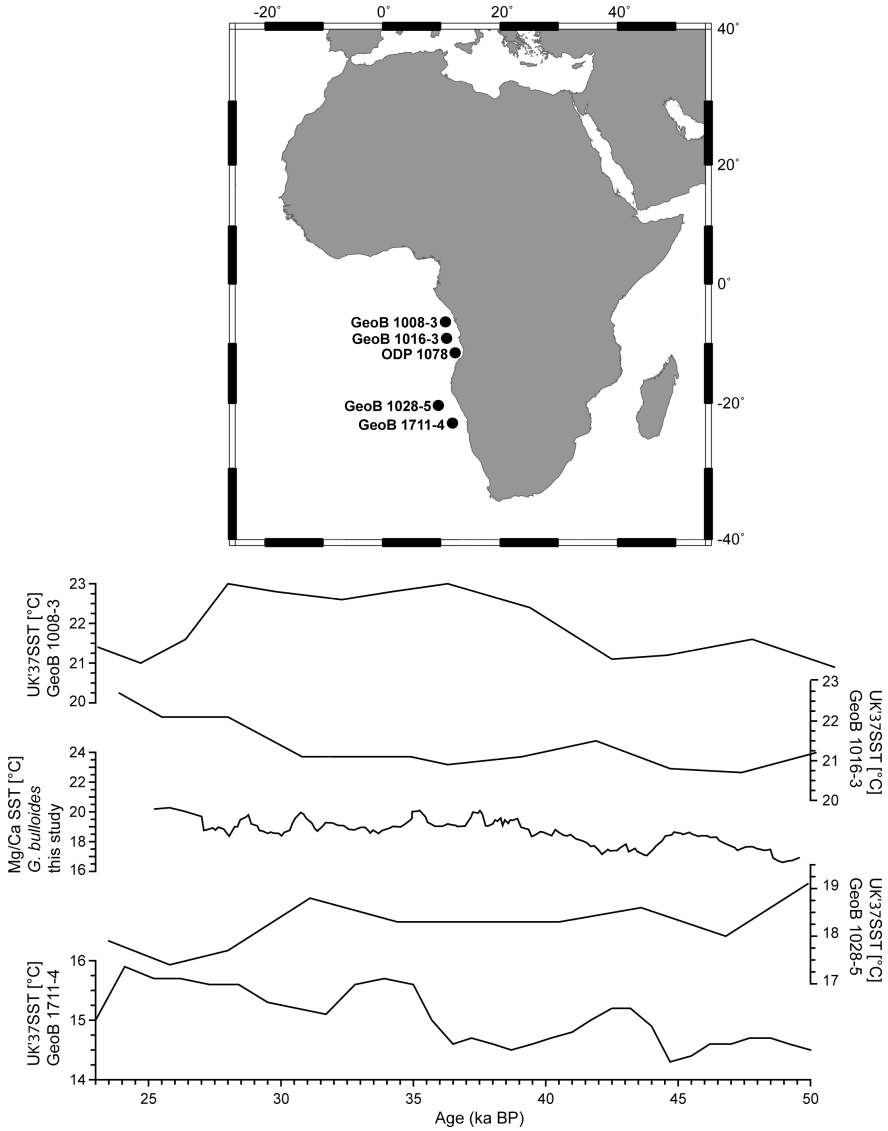

Figure 16: Comparison of SST records from the southeast Atlantic covering the investigated time frame(50-23.5 ka BP). Records are arranged from north to south.: alkenone-based SST record of GeoB 1008-3 [Schneider et al., 1995], GeoB 1016-3 (Schneider et al., 1995), Mg/Ca SST of *G. bulloides*, alkenone-based SST records of GeoB 1028-5 (Schneider et al., 1995), GeoB 1711-4 (Kirst et al., 1999).

Why is the HS signal subdued in the northern Benguela Upwelling System?

While our austral summer/AC (*G. ruber* (pink)) derived SST record yield abrupt SST changes associated with HS, our austral winter/BC (*G. bulloides*) SST record yield no changes associated with HS. In good agreement with our Mg/Ca temperature and δ^{18}O record of G. bulloides covering the period between 23.5 and 50 ka there is no indication for abrupt climate

changes associated with HS in the δ^{18}O record of *G. bulloides* obtained from centre of the Benguela upwelling system at 25°S (Romero et al., 2003). On the other hand, periods of high abundances of left coiling *Neogloboquadrina pachyderma* in the northern Benguela upwelling system, the so-called PS (pachyderma sinistral)-events, correlate with North Atlantic HS and indicate increased intensity and zonality of SE trade winds (Little et al., 1997). These PS events or periods of intensified upwelling are further interpreted to be the primary control on the SST patterns in the northern Benguela region during HS. A *G. bulloides* Mg/Ca-based SST record of ODP Site 1084B (~ 25°S) reveal a brief cooling that is interpreted to reflect an intensification of upwelling during HS1 (Farmer et al., 2005). These and our results support the finding of Little et al. (1997). We speculate that an intensification of upwelling associated with an increased equatorward advection of cold waters from the subtropical convergence during the HS (Little et al., 1997) most likely masked or subdued increasing SST in the study area as expected from the bipolar seesaw concept.

In contrast, alkenone-based SST records from the Walvis Ridge region indicate a (continuous) warming during HS1 due to a decrease in the strength of the SE trade winds and upwelling intensity (Kim et al., 2002, 2003). We suggest that discrepancies between the alkenone and our Mg/Ca record could be due to differences in the seasonality of *G. bulloides* and alkenone-producing algae. The alkenone-derived SSTs of Kim et al. (2002, 2003) reflect the annual mean temperatures of the upper 10 m of the water column (Müller et al., 1998). In contrast, the Mg/Ca temperatures of *G. bulloides* indicate winter season temperatures of the upper 50 to maximum 100 m water depth. Therefore, the SST derived from our *G. bulloides* Mg/Ca measurement would reflect a different season and the influence of possibly a different water mass compared to the alkenone-derived SST. Moreover HS1 is not completely comparable to other HS. The background conditions during HS1 with, for example, increasing sea level, temperature, insolation, sea ice extent and atmospheric CO_2 are very different from the one during all the other HS where full glacial conditions prevailed. Although the mitigation of the South Atlantic warming associated with North Atlantic HS by abrupt upwelling events and cooling of the surface waters seems to be a likely candidate to explain the absence of changes associated with HS in the *G. bulloides* temperature record, the exact mechanisms involved need to be further investigated.

6.2.8 Conclusions

The *G. ruber* (pink) and *G. bulloides* derived Mg/Ca SST records of ODP Site 1078 off Angola indicate significant differences in the response to abrupt climate perturbations in the AC and BC between 23.5 and 50 ka BP. Due to its seasonal and ecological preferences Mg/Ca of pink-pigmented *G. ruber* reflects austral summer surface water temperatures of the AC. The *G. ruber* Mg/Ca-SST record shows warming events during HS with considerably increasing SST but rather gradual in

nature. This is in good agreement with the general nature of the southern hemisphere signal (Barker et al., 2009) and the concept of the bipolar seesaw (Broecker, 1998, EPICA members, 2006; Barker et al., 2009). In contrast, in the BC our representative for the Benguela upwelling regime during austral winter, *G. bulloides*, records significant cooler SST but no temperature response to HS. The general colder SST during the investigated interval in the BC seem to result from an intensification of the coastal upwelling due to enhanced trade winds combined with an increase in the northward intrusion of cold BC waters and a decreased inflow of warm waters via the Agulhas Leakage. The occurrence of brief periods of intensified upwelling and cooling coinciding with HS (Little et al., 1997, Farmer et al., 2005) appear to be a highly probable mechanism to subdue increasing SST in the study area, as suggested by the bipolar seesaw hypothesis, and result in the non-existence of HS in our *G. bulloides* temperature record. However, further investigations are necessary to detect and evaluate the exact mechanisms involved.

Acknowledgment

We thank the Ocean Drilling Program for providing samples. This study was funded by the Deutsche Forschungsgemeinschaft (ACCAT) and by the Deutsche Forschungsgemeinschaft as part of the DFG-Research Center - Cluster of Excellence "The Ocean in the Earth System". We thank Stefan Mulitza and Mahyar Mohtadi for the discussions and their suggestions which clearly improved the manuscript. Isotope measurements have been conducted by Monika Segl at the MARUM, University of Bremen.

6.3 Masked millennial-scale climate variations in southwest Africa during the last glaciation

Ines Hessler[a*], *Lydie Dupont*[a], *Ute Merkel*[a], *Dian Handiani*[a], *Gerold Wefer*[a]

[a] MARUM - Center for Marine Environmental Sciences, University of Bremen, 28359 Bremen, Germany

[*] Corresponding Author: Tel.: +49 (0) 421 - 218 65682, Email: ihessler@marum.de

Planned to be submitted to Climate of the Past

6.3.1 Abstract

Large and abrupt shifts between extreme climatic conditions characterise the last glacial and deglacial period and are thought to be transmitted by the atmospheric and oceanic circulation. Abrupt shifts associated with North Atlantic Heinrich Stadials (HS) are closely related to a reduction of the Atlantic meridional overturning circulation (AMOC) leading to an accumulation of heat in the South Atlantic and a southward shift of the Intertropical Convergence Zone (ITCZ). Due to linkage between ocean and atmosphere it is thought that HS influence the vegetation composition in the tropics. To address the issue of the connection between tropical African vegetation development and high-latitude climate change we present a high-resolution marine pollen record off Angola (ODP Site 1078) covering the interval 50-10 ka BP. Although several tropical African vegetation climate reconstructions indicate an impact of HS on the African subcontinent, our vegetation record shows no response. Model simulations conducted with two Earth System Climate models including a dynamical vegetation component support the assumption that the vegetation response during HS is masked by mechanisms that cancel out each other.

6.3.2 Introduction

The last glacial period and the subsequent deglaciation are characterised by abrupt climate perturbations on a millennial and centennial time scale. Millennial-scale climate variability such as the northern hemisphere Heinrich Stadials (HS = contains a Heinrich event but is not equivalent to it) are thought to be recorded globally due to their transmission through both the atmosphere and ocean circu-

lation (e.g. Alley et al., 1999; Hoestler et al., 1999; Broecker, 1996). Ice core records from Greenland and Antarctica reveal a contrasting temperature response during HS, with cold conditions in the northern hemisphere and warm temperatures in the South Atlantic (EPICA members, 2006). This anti-phase behaviour is suggested to result from a reduction in the strength of the Atlantic meridional overturning circulation (AMOC) leading to the cooling in the north and a accumulation of heat in the south due to the bipolar seesaw (Broecker, 1998; EPICA members, 2006; Barker et al., 2009).

In the tropics, the southward shift of the Intertropical Convergence Zone (ITCZ) is a persistent feature of the slowdown of the AMOC and plays an important role in the atmospheric transmission of the northern hemisphere signal (Vellinga and Wood, 2002; Mulitza et al., 2008). Model simulations indicate that such southward shift in the migration pattern of the ITCZ causes particularly large precipitation anomalies over South America and Africa (Vellinga and Wood, 2002). Tropical South American vegetation records reflect these precipitation anomalies by an opposing vegetation development north and south of the recent position of the ITCZ during periods of abrupt climate change (Hessler et al., 2010). During HS the South American vegetation north of the modern position of the ITCZ indicates drier conditions with abrupt expanding salt marsh vegetation (González et al., 2008; González and Dupont, 2009). South of the modern position of the ITCZ a southward shift during HS results in more humid conditions and expansion of forests (Dupont et al., 2010). Similarly, arid conditions north of the ITCZ (e.g. Mulitza et al., 2008) and wetter conditions south of it (Dupont et al., 2008; Collins et al., 2010) have been indicated for the African continent providing further evidence for the link between the North Atlantic and tropical environmental conditions via the atmosphere and ocean circulation. However, especially in tropical Africa south of the equator the nature of response to North Atlantic HS varies significantly on a regional scale and between the different HS (e.g. Gasse et al., 2008; Hessler et al., 2010). In general, processes that control climate in the tropics are poorly understood, reflecting the highly complex atmospheric pattern and relationship between ocean and atmosphere.

We present a high-resolution marine pollen record of ODP Site 1078 to reconstruct the vegetation and climate development of Angola and the southern Congo Basin between 50 and 10 ka BP focusing on HS. In order to get insight into atmospheric and oceanographic processes affecting the regional vegetation during HS, modelling simulations have been performed using a Community Climate System Model Version 3 (CCSM3). Experiments performed by the UVic Earth System Climate Model (UVic ECSM) including a dynamical vegetation and land surface component allow comparison between the reconstructed and modelled vegetation under glacial conditions with special emphasis on HS.

6.3.3 Study Area

Modern regional climate and oceanic conditions

The climate of the African tropics is strongly influenced by the latitudinal position of the Intertropical Convergence Zone (ITCZ), the trade winds and the monsoon. The ITCZ, a low pressure belt of warm, moist air develops as a consequence of the trade wind convergence. Due to a strong linkage between variations in atmospheric and oceanic conditions the position of the ITCZ follows an annual cycle, with a shift to its northernmost position during austral winter and to its southernmost one during austral summer.

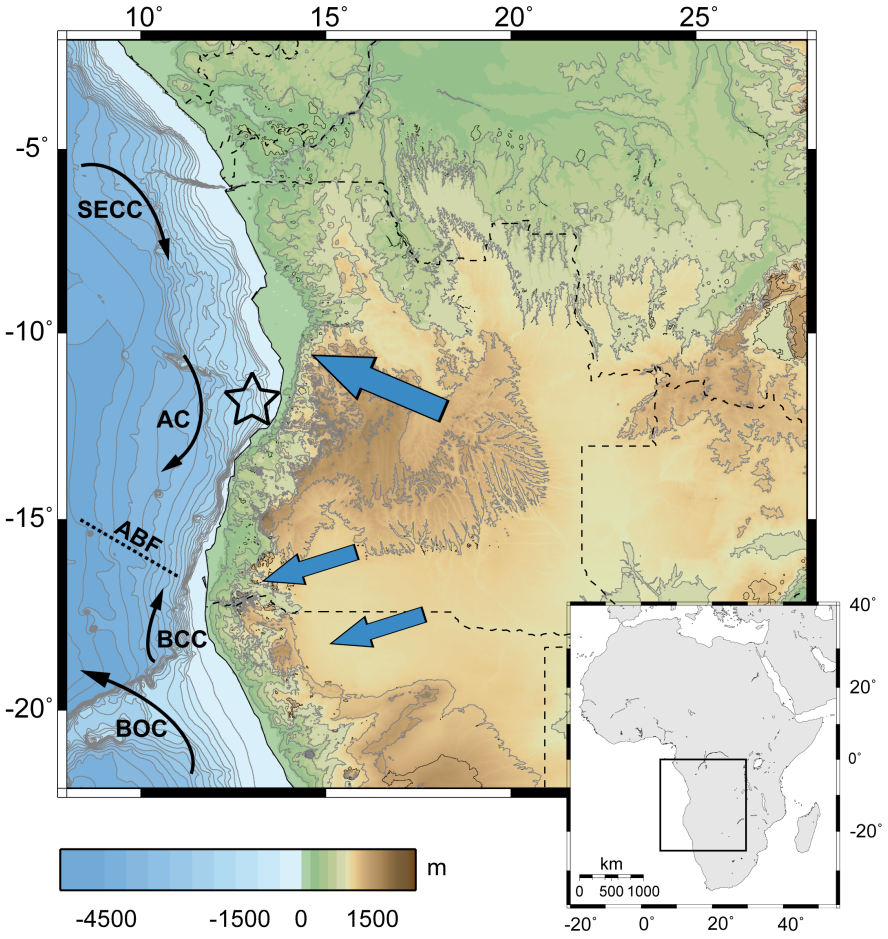

Figure 17: Modern regional climate and oceanic conditions. Black arrows indicate ocean current. SECC = South equatorial counter current, AC = Angola Current, BCC = Benguela Coastal Current, BOC = Benguela Ocean Current. Dashed line indicates Angola-Benguela Front (ABF). ODP Site 1078 is marked by black star. Blue arrows indicate main wind direction during austral winter (June-August).

The latitudinal transition of the ITCZ to its northernmost position at 15°-18°N also indicates the beginning of the summer monsoon and hence rainy season (Sultan and Janicot, 2003). During austral summer when a strong tropical trough is developed over central Africa (Angola Low, ~ 22°E-15°S) the ITCZ lies at 5°-6°N in the west and at 15°-20°S in the east (Gasse et al., 2008). The E-W asymmetry of the ITCZ position and zonal atmospheric pattern is generated by oceanic and topographic features south of the equator (Gasse et al., 2008). The variation in the position of the ITCZ also affects the rainfall distribution in equatorial and tropical regions, resulting in alternating wet and dry seasons.

Although, being a dominant feature of the tropical atmosphere, the ITCZ is not the only process producing precipitation. Moisture is also brought from the Atlantic Ocean into tropical Africa by the eastwards penetrating West African Monsoon and trade winds (Gasse et al., 2008; Nicholson, 2000) (Figure 17). To the east the inland flow of moisture laden air-masses is limited by the highlands of East Africa as well as the surface position of the Congolian Air Boundary, a low pressure area and southern branch of the ITCZ (Leroux, 1983).

The position of the ITCZ, intensity of trade winds and monsoon are also related to sea surface temperature and the oceanic circulation system. One of the most prominent ocean current systems in the south-eastern Atlantic is the broad northward flowing Benguela Current (BC) (Stramma and Peterson, 1989) (Figure 17). At around 24°-30°S the main BC separates into the westward directed Benguela Ocean Current and the northward flowing Benguela Coastal Current (BCC) (Shannon and Nelson, 1996). The BC and the coastal upwelling zone of the eastern South Atlantic are driven by the south-east trade winds. Resulting from the convergence of the BCC with the southward directed Angola Current (AC) the Angola-Benguela Frontal Zone (ABF) emerges, separating the tropical Angolan waters from the cold Benguela upwelling regime (Figure 17). Similar to the seasonal shifts of the ITCZ the ABF reaches its northernmost position in austral winter (20°S) and is farthest south during austral summer (16°S) (Shannon et al., 1987).

Recent southwest African vegetation composition

ODP Site 1078 is situated in close proximity to the African continent with a potential pollen source area that covers several vegetation zones (Figure 18). According to the trajectory model of Dupont and Wyputta (2003), which was used to reconstruct the aeolian pathways of terrigenous input to the south-east Atlantic Ocean, the potential pollen source area for ODP Site 1078 is Angola and the southern Congo Basin (Figure 17). The prevailing wind pattern during spring may also cause the transport of terrestrial particles from the northern Namib Desert into the Angolan Basin. Fluvial transport is also important as ODP Site 1078 is located off the mouth of Balombo River which collects pollen from several vegetation

zones. The vegetation pattern of south-west Africa is strongly influenced by the above described near shore ocean system, elevation and the dominant rainfall regime, which is related to the regional frontal system. The coastal vegetation of Angola is directly influenced by the offshore oceanic systems, particularly by the cold BCC and the related upwelling area that reduces convection and hence minimise precipitation (Nicholson and Entekhabi, 1987).

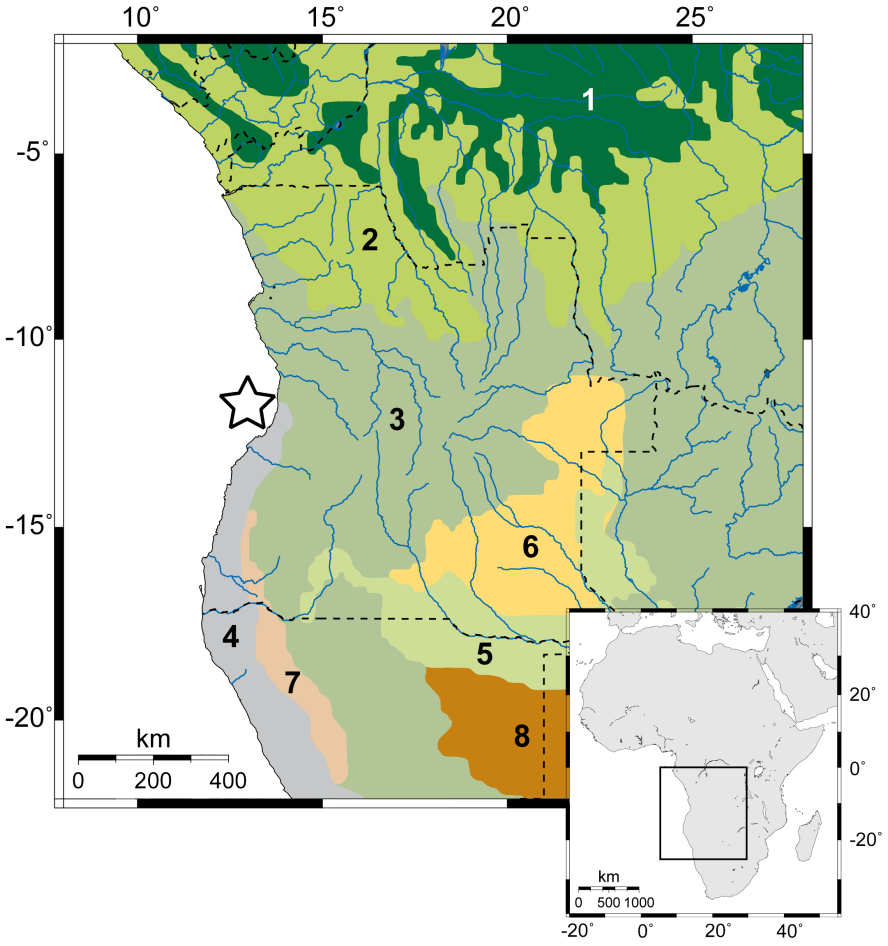

Figure 18: Simplified vegetation types after White (1983) of the Pollen source area of ODP Site 1078 (marked with a black star). 1 = Tropical forest of the Guineo-Congolian phytogeographical region; 2 = Transition between tropical forest and Dryforst/savannah; 3 = Dryforest/savannah of the Zambezian phytogeographical region, wetter Miombo woodland above 1000 m altitude, *Podocarpus* above 1500 m altitude; 4 = Desert and Semidesert of the Nama-Haroo phytogeographical region; 5 = Deciduous forest; 6 = Grassland and Miombo woodland; 7 = Woody shrubland; 8 = Dry deciduous forest and savannah of the Kalahari. Blue lines indicate major rivers.

White (1983) divided the prevalent vegetation of Angola and the southern Congo Basin into five phytogeographical regions (Figure 18). The vegetation of the Congolian Region consists of a few undisturbed tropical seasonal forest remains, secondary grassland and extensive forest regrowth, while above 1000 m bushland and thicket occur. To the south, the Congolian-Zambezian transition zone is a mosaic of grassland, wooded grassland, and dry evergreen forest. The majority of Angola is occupied by vegetation that belongs to the Zambezian Region, which is characterised by a highly diverse flora ranging from closed semi-deciduous forests in the north to broad-leaved savannah types in the south. On the relatively nutrient-poor soils of the Angolan highlands and its flanking escarpment a distinctive type of savannah woodland named Miombo woodland grows dominated by the tree species of the genus *Brachystegia*. Afromontane forests including the conifer tree *Podocarpus* exist in only a few high mountain sites in Angola. The semi-desert and desert vegetation of the southern Angolan coastal areas belong to the Karoo-Namib Region characterised small shrubs and succulents. To the east the Kalahari-Highveld transition zone represents a complex vegetation pattern of bushland and savannah including trees of the *Acacia* genus.

6.3.4 Material and Methods

Site description and age model

The sediments analysed in this study originate from ODP Site 1078 Hole C that is situated outside the Bight of Angola (11°55'S, 13°24'E) in 426 m water depth (Figure 17, 18). Lithologically, the material is composed of moderately bioturbated olive-grey and dark olive-grey silty clay with varying amounts of nanofossils and foraminifers (Wefer et al., 1998).

The chronostratigraphy used in this study (50-10 ka cal BP) was established by linear interpolation of accelerator mass spectrometry (AMS) radiocarbon dates determined on planktonic foraminiferal tests and molluscs fragments (Kim et al., 2003; Rühlemann et al., 2004; Dupont et al., 2008). Fourteen radiocarbon dates are within the investigated time interval and have been calibrated after Stuiver et al. (1998), Hughen et al. (2004) and Fairbanks et al. (2005). The radiocarbon dates were corrected with a reservoir age of 400 years reflecting the present day global average (Hughen et al., 2004). Temporal variations in reservoir ages are not taken into consideration since they are difficult to reconstruct (e.g. Bard et al., 1994) and, for pre-Holocene records are exceeded by the uncertainties in the radiocarbon dating (Fairbanks et al., 2005). Model simulations also show that temporal fluctuations in the marine reservoir age are of minor importance in the tropical Atlantic (Hughen et al., 2004; Franke et al., 2008). Only the oldest AMS ^{14}C date (<45 ka) exceeds the actual limit of radiocarbon dating. However, the time frame 50-40 ka needs to be considered with caution resulting from large uncertainties in the calibration curve beyond ~ 40 ka. All ages given here are in 1000 years calibrated before present (ka cal BP).

Analytical methods

For pollen analysis samples were taken every 2 to 7 cm resulting in a average temporal resolution of about 300 years. All samples were prepared using standard palynological procedures (Faegri and Iversen, 1989), which include the decalcification with diluted HCl (~ 10%) and the removal of silicate with HF (~ 40%). During the decalcification two *Lycopodium clavatum* tablets were added to determine pollen concentrations (grain/cm^3) and pollen influx (grains/cm^2/yr) (Stockmarr, 1971). To remove particles < 10 μm the samples were sieved over an 8 μm mesh using ultrasonic treatment. For identification of pollen grains, spores and other palynomorphs the samples were mounted in glycerine and microscopically examined at a magnification of 400 and 1000 times. About 300 grains of pollen and spores were counted for each sample. Only in a few samples 100-250 grains were counted due to a low pollen concentration in the sediments. The different types of pollen, spores and palynomorphs were distinguished using the reference collection of University of Göttingen, Department of Palynology and Climate Dynamics, the African Pollen Database (http://medias.obs-mip.fr/pollen/) and several publications (Bonnefille and Riollet, 1980; Maley, 1970; Sowunmi, 1973; 1995; Ybert, 1979). The percentages are calculated on the basis of the pollen sum including terrestrial pollen taxa, aquatics (mainly Cyperaceae and *Typha*) and spores (mainly ferns). Identified pollen and spores have been summarized into the groups tropical seasonal forest, mountain vegetation, Miombo woodland, dryforest/savannah, and semi-desert following the climatic and ecological preferences of the pollen taxa related plants (supplementary information).

Models and experiments

In our study we used two models, the comprehensive Community Climate System Model Version 3 (CCSM3; Collins et al., 2006) and the University of Victoria Earth System Climate Model (UVic ESCM version 2.8; Weaver et al., 2001) coupled with a dynamic vegetation (TRIFFID; Cox, 2001) and a land surface component (MOSES 2; Cox et al., 1999).

The UVic ESCM is an earth system model of intermediate complexity, thus allows transient simulations without huge amounts of CPU time, and comprising representations of the atmosphere, biosphere, hydrosphere and continental ice (Weaver et al., 2001). Coupled to the UVic ESCM is the TRIFFID model (Top-down Representation of Interactive Foliage and Flora Including Dynamics), a dynamic global vegetation model (Cox, 2001). The TRIFFID defines the state of the terrestrial biosphere in terms of soil carbon, and the structure and coverage of five plant functional types (broadleaf tree, needleleaf tree, C_3 grass, C_4 grass and shrub) (Cox, 2001). The land surface scheme MOSES 2 (Met Office Surface Exchange Scheme) calculates the surface to atmosphere fluxes of heat and water, updates the surface and subsurface variables that affect these fluxes, and calculates the vegetation to atmosphere fluxes of CO_2 (Cox et al., 1999). The simulation design and boundary conditions are described in detail in

Handiani et al. (in prep.). In summary, two equilibrium simulations at two time periods have been accomplished, a pre-industrial and LGM simulation. The pre-industrial climate experiment serves as control run, whereas the LGM experiment was compared to the control run. Heinrich-like climate conditions (HS1) have been forced by adding fresh water to the North Atlantic under glacial boundary conditions. The major vegetation composition has been calculated in terms of mega-biomes classified in BIOME6000 (Harrison and Prentice, 2003) and compared to our palaeovegetation record.

The comprehensive Community Climate System Model Version 3 (CCSM3) includes components representing the atmosphere, ocean, sea ice, and land surface and is designed to produce realistic simulations over a wide range of spatial resolutions (Collins et al., 2006). To allow longer integration times, the model experiments have been performed with the low resolution CCSM3 model set-up (Yeager et al., 2006). The experimental framework consists of two glacial climate simulations, one LGM simulation and one for HS1 conditions. Both experiments with their boundary conditions and key diagnostics are in detail described in Merkel et al. (2010).

6.3.5 Results

Pollen data

The diagram presented in Figure 19 shows percentages of identified pollen taxa, grouped according to the ecological preferences of the associated plants (supplementary information) as well as a selection of pollen taxa for the interval 50-10 cal ka BP. Based on the relative abundance of pollen groups and taxa three pollen zones (PZ1, PZ2, and PZ3) are distinguished. Figure 19 also includes the concentration values for the same groups and taxa. The different curves of vegetation groups and single pollen taxa are in contrast to the pollen percentages independent from each other. Podocarpus is excluded from its group "mountain vegetation" in the pollen percentages and pollen concentration values and shown separately to avoid biasing the record due to the over-representation of *Podocarpus* pollen within the group of mountain vegetation. For the same reason,values of Poaceae (grass) are not included in any vegetation group and shown separately in the diagram.

PZ 1 (50-32 ka BP) is dominated by Poaceae (grass) pollen reaching percentages up to 60 %. Pollen of the vegetation groups tropical forest (max. 2%), Miombo woodland (max. 3%), and mountain vegetation (max. 8.5%), excluding the conifer *Podocarpus* (max. 11.5%), show low values. The concentration of Poaceae pollen is are highly abundant (12,000-4000 grains/ml) during PZ 1, while that of *Podocarpus* is low (2000-400 grains/ml). Pollen taxa summarised in the mountain and semi-desert vegetation group reach their maximum concentration at the beginning of PZ 1 (mountain max. 1100 grains/ml; semi-desert max. 1000 grains/ml). Towards the end of PZ 1 the concentration values of both groups start to decline.

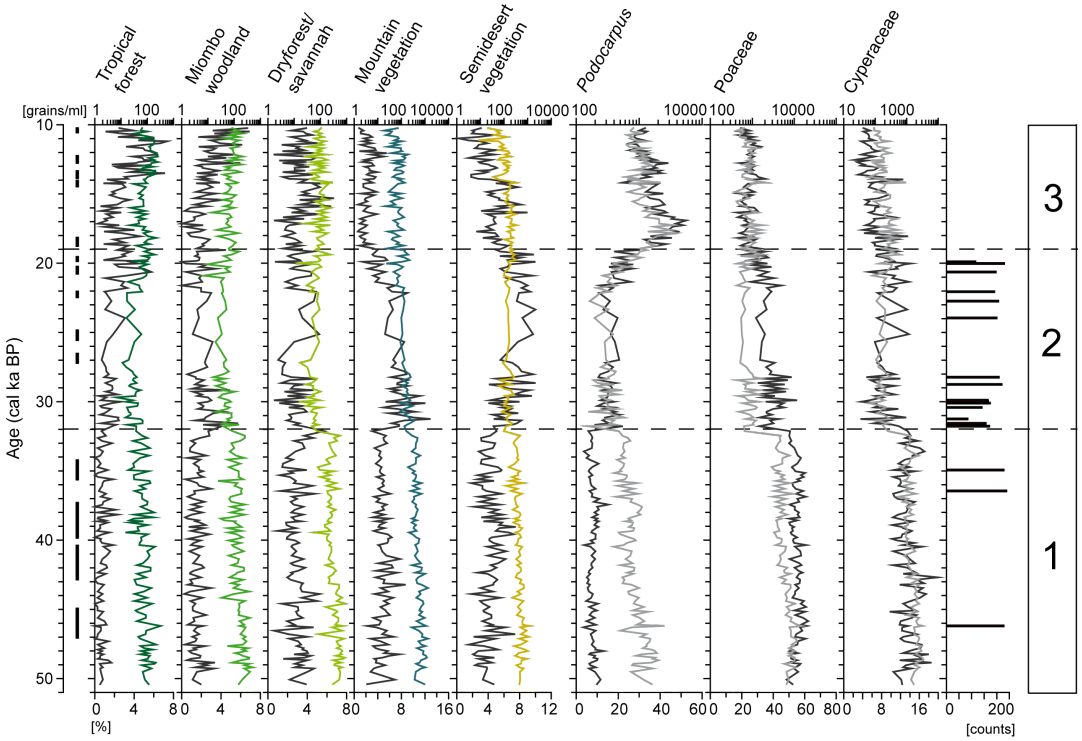

Figure 19: Pollen percentages (dark grey) and pollen concentrations of vegetation groups (coloured) and selected pollen taxa (lightgrey). Black vertical lines indicate calibrated ^{14}C age ranges (1 sigma range) according to Kim et al. (2003) and Rühlemann et al. (2004) for the period 10-22 ka BP and according to Dupont et al. (2008) for 22-<45 ka BP. Samples with less than 250 pollen grains counted are indicated on right. Concentrations are given in log10 grains/ml, note different scales. Pollen zones 1 to 3 (PZ) are separated by dashed lines.

Spanning the period 32-19 ka BP **PZ 2** is characterised by an early decline of grass pollen from about 44% to 32%. Pollen percentages of sedges (Cyperaceae) which are widespread in swamps and along riversides but not restricted to it (Dupont and Agwu, 1991) decrease during the same period to values between 13-4%. The group of semi-desert pollen including taxa from the coastal deserts and xerophytic shrubland doubles its percentages from about 5% at the beginning of PZ 2 to about 10% towards the end. Pollen of the group of mountain vegetation increases significantly just at the beginning of PZ 2 from about 4% to 10-12%. However, following a maximum between 31-29 ka BP, pollen percentages of this group start to decline to minimum values of 2% at about 19 ka BP. Relatively stable, however, with 20% about twice as high as during PZ 1, pollen of the Afromontane *Podocarpus* occur. Percentages of tropical forest reach a first maximum with 6% between 21 and 20 ka BP and subsequently decline. However, the pollen concentration values (Figure 19) of *Podocarpus*, semi-desert, and mountain vegetation do not increase during PZ 2. Indeed, all vegetation

groups show at least a slight decrease in their pollen concentrations. *Podocarpus* concentrations are even on the lowest level (1000-200 grains/ml) during PZ 2.

A strong increase of *Podocarpus* pollen percentages is recorded directly at the onset **of PZ 3**, reaching its maximum value of 52% at circa 17 ka BP (see also Dupont et al., 2006; Dupont et al., 2008). Following this maximum, pollen percentages of *Podocarpus* decrease continuously towards 30% at 10 ka BP. Similarly, relative abundances of grass, mountain, semi-desert, and dryforest/savannah pollen decline continuously until they reach minimum values at 10 ka BP. Pollen percentages of both Miombo woodland and tropical forest reach a maximum value of 7% at 10 ka BP. A comparable pattern as in the pollen percentages of *Podocarpus* can be seen in the concentration diagram with a steep increase (from 1000 to 4000 grains/ml) at the beginning of PZ 3 followed by decreasing values (down to about 700 grains/ml). Poaceae, mountain, and semi-desert pollen concentrations continue with a downward trend starting already in PZ 2. Only the concentration values of tropical forest (100 to 250 grains/ml) and Miombo woodland (60 to 200 grains/ml) increase slightly towards the end of PZ 3.

Model experiments

Modelling experiments show several changes in the oceanic and terrestrial parameters between LGM and HS simulation (Figure 20-23). Applying the UVic ESCM, the modelled vegetation distribution grouped in mega-biomes indicates only a minimal extension of the forest biome during HS compared to LGM conditions (Figure 20). Model simulations conducted with the CCSM3 illustrate the seasonal and annual-mean differences between HS and LGM conditions (Figure 21-23). Annual-mean surface temperatures indicate increasing SST of up to 2°C during HS off south-west Africa, while on the adjacent continent no temperature changes are indicated (Figure 23). Similarly, annual-mean precipitation (0.6-1.2 mm/day) and evaporation (0.5-1 mm/day) is enhanced over the ocean close to the coast, while on the continent only minor changes occur (Figure 21). In the seasonal model output surface temperatures are increased all year around off the coast of southwest Africa with a maximum values (2.5°C) between June and August. Between September and November the area of maximum surface heating shifts towards the north, with the developed warm-pool off west and south-west Africa having its greatest extension (Figure 23). On the African subcontinent no distinct temperature changes occur. During HS all year round a band of increased precipitation (up to 3 mm/day) exist in the equatorial Atlantic, being most distinct in spring and autumn. Only minimal to no changes have been simulated for tropical Africa south of the equator (Figure 21). Also only minor changes are indicated for evaporation rates during HS on the African subcontinent (Figure 22). Evaporation is consistently increased off southwest Africa with highest values occurring between June and August (Figure 22).

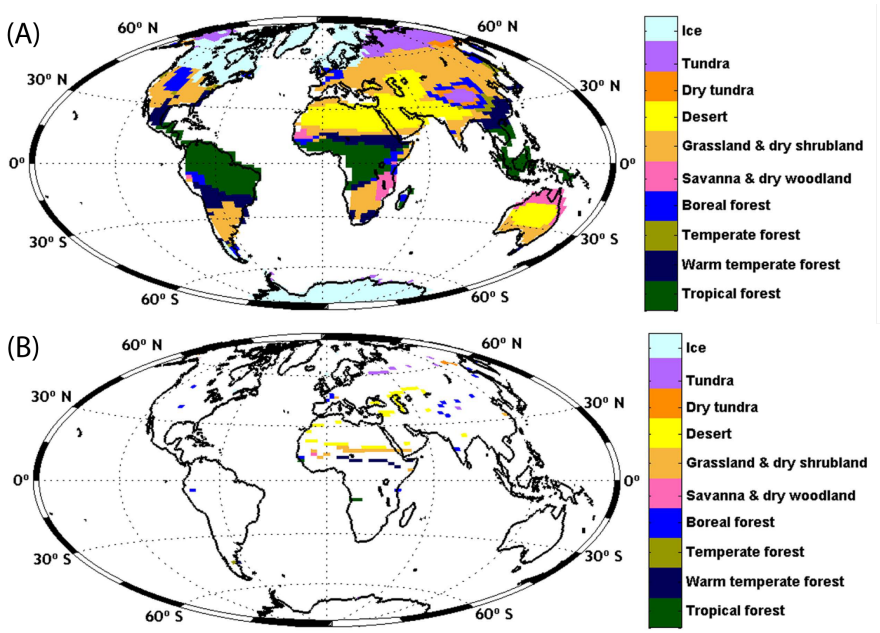

Figure 20: Model experiments of UVic ECSM with a dynamic vegetation component. Vegetation is grouped into mega-biomes according to Harrison and Prentice (2003). (A) Scenario for HS. (B) Difference between HS conditions and LGM.

6.3.6 Discussion

Combining palynological results published by Dupont et al. (2006) and Dupont et al. (2008) with our newly obtained pollen data for the period 50-30 ka BP the tropical African vegetation history of the last glacial up to the end of the deglaciation (50-10 ka BP) becomes more complete and distinct. Although there are several records in Africa south of the equator providing evidence for an impact of North Atlantic Heinrich events in southern hemisphere Africa (e.g. Vincens et al., 2007; Brown et al., 2007; Kim et al., 2003; Johnson et al., 2002; Stager et al., 2002; Vincens et al., 1991), our high-resolution vegetation record of Angola and the southern Congo Basin shows no response to HS. Vegetation changes coinciding with HS1 seem to be not tied to the duration of the HS 1 stadial (14.6-16.3 ka BP according to Greenland Ice Core Chronology 2005; Skinner, 2008; Wolff et al., 2010).

Therefore, we will discuss which mechanisms or a combination of them that might be responsible for the stability of southwest African vegetation, although several records from surrounding regions show a clear impact of HS. We further want to address the issue which are possible mechanisms that influence the vegetation development in tropical southwest Africa during the last glacial.

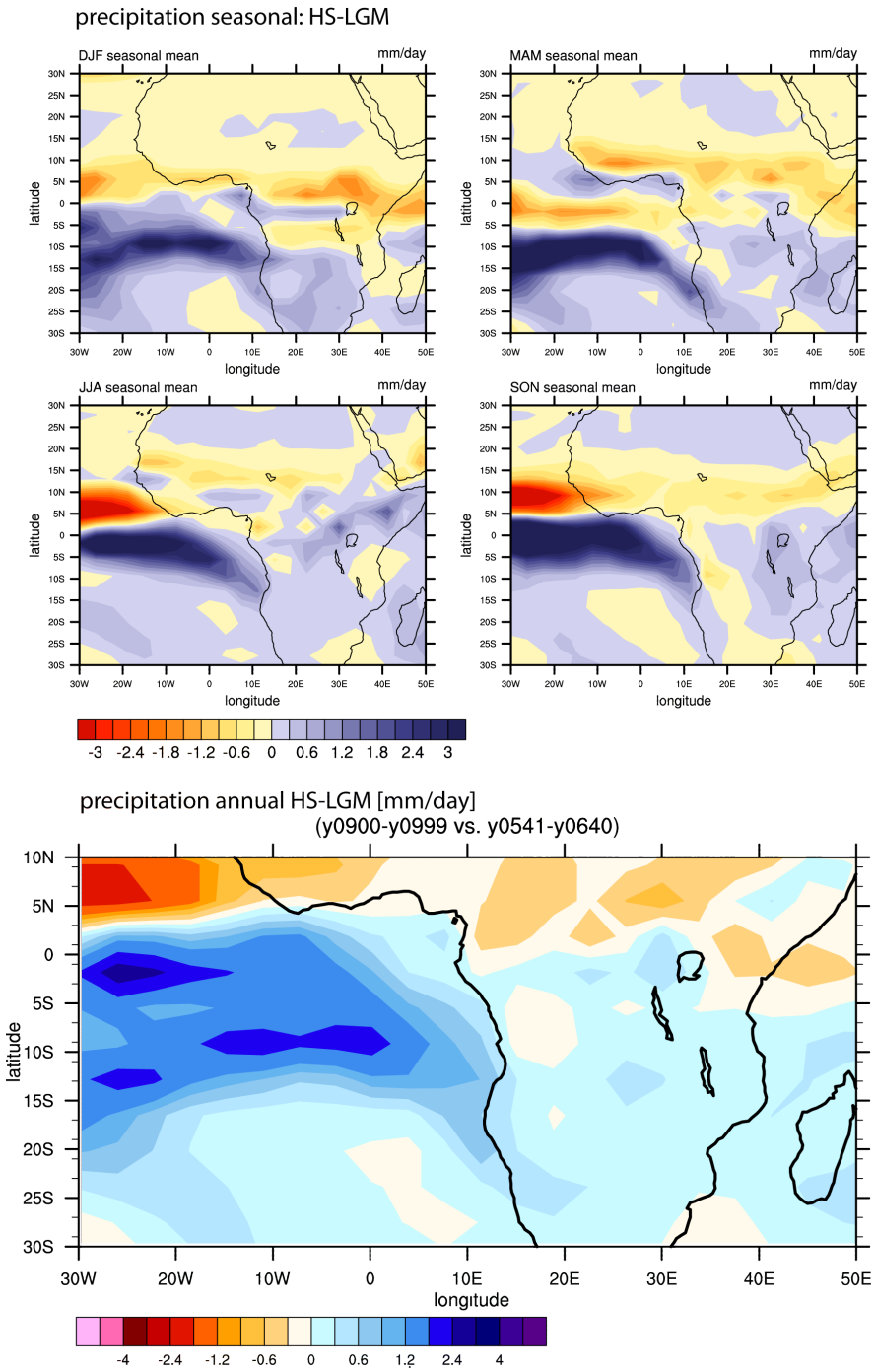

Figure 21: Annual and seasonal mean response of precipitation [mm/day] using the CCSM3 Model. Difference between HS and LGM conditions are shown.

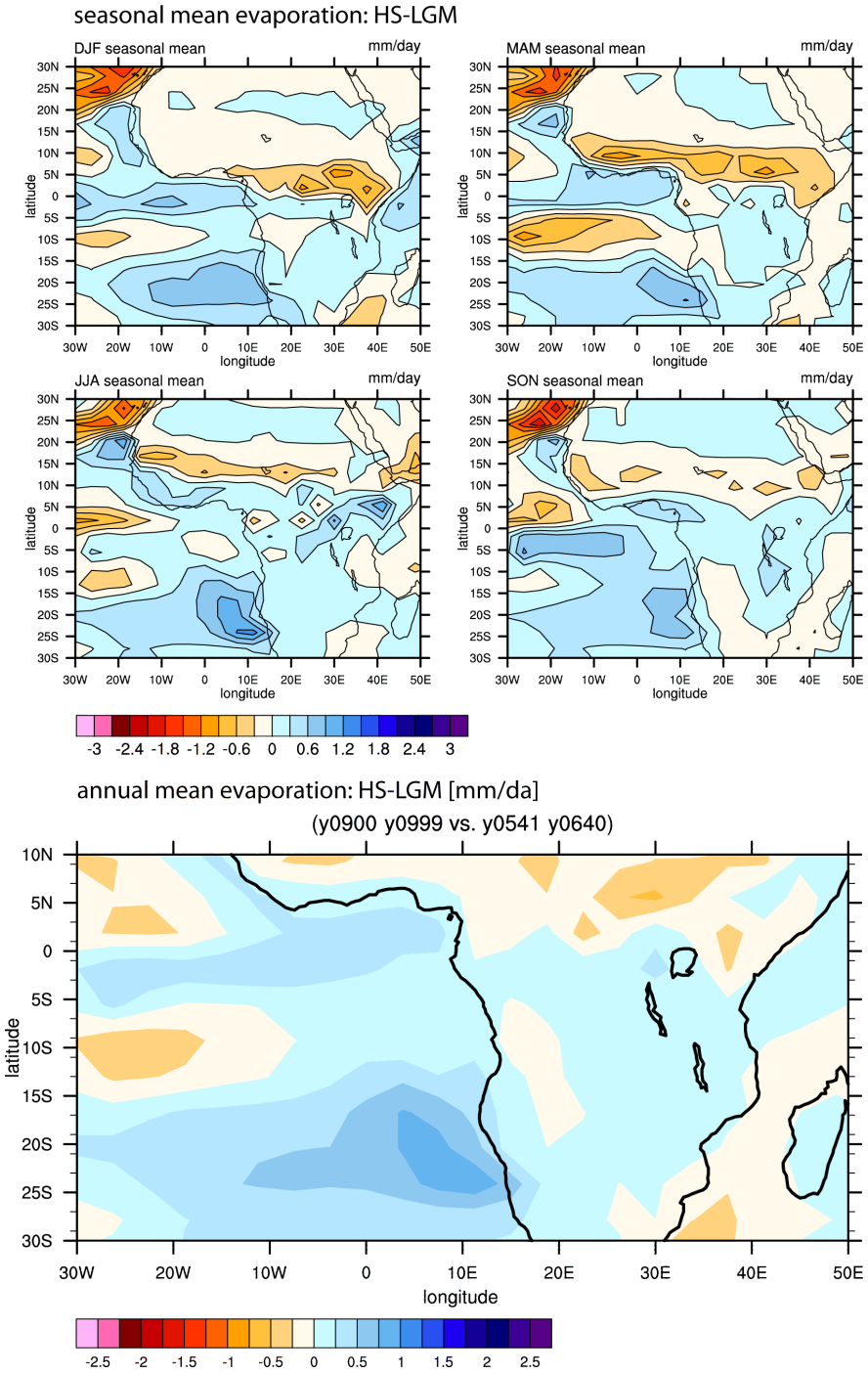

Figure 22: Annual and seasonal mean response of evaporation [mm/day] using the CCSM3 Model. Difference between HS and LGM conditions are shown.

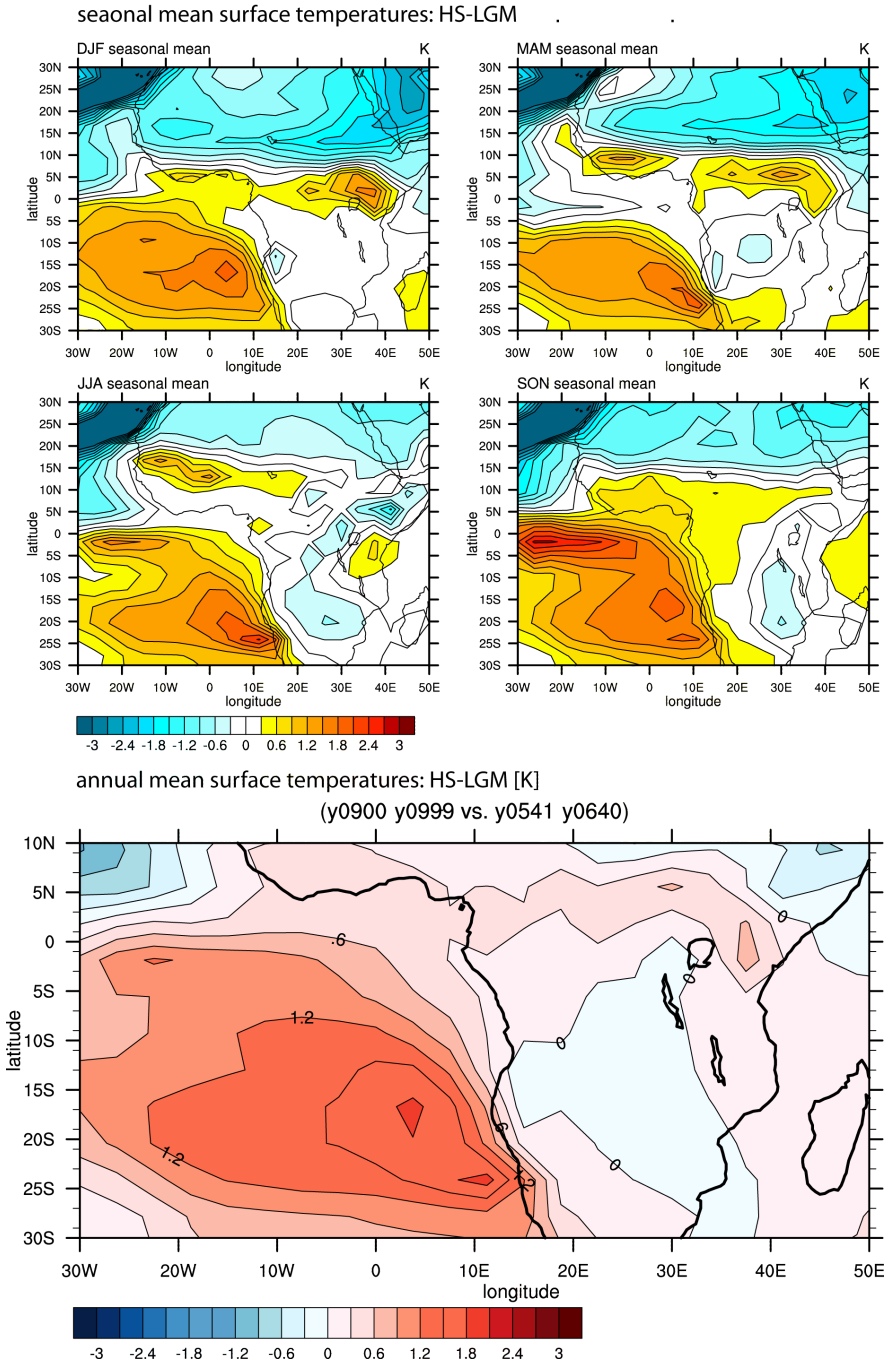

Figure 23: Annual and seasonal mean response of surface temperature [mm/day] using the CCSM3 Model. Difference between HS and LGM conditions are shown.

Masked millennial-scale climate changes

The assumption of a masked or mitigated impact of northern hemisphere abrupt climate perturbation on the tropical south-western African vegetation is based on the modelling experiments conducted with an UVic ESCM including a dynamical vegetation component and CCSM3 results with a seasonal resolution (Fig.4-7). The modelled SST shows the establishment of a warm-pool off the coast of southwest Africa under HS conditions, that extends between September and November north into the Gulf of Guinea. These results are consistent with the concept of bipolar seesaw during HS (Broecker, 1998; EPICA members, 2006; Barker et al., 2009) and SST reconstructions from the eastern South Atlantic (Kim et al., 2002; Hessler et al., submitted). A band of significantly increased precipitation rates during HS is simulated for the tropical Atlantic between 0° and 20°S. However, this pattern can not be detected over the continent where only minor changes in the precipitation rates are recorded. The band of locally enhanced precipitation might be due to a southward shifted ITCZ which is postulated in connection with a reduced AMOC strength during HS (Vellinga and Wood, 2002; Mulitza et al., 2008). However, the spatial limitation of enhanced precipitation over the tropical Atlantic might be due to the fact that the manifestation of the ITCZ is generally more distinct over the ocean than over the continent (Hastenrath, 1992). A southward shift of the ITCZ during HS (e.g. Mulitza et al., 2008) would also lead to the expectation that the moisture availability in the southern low-latitude African tropics is higher and hence the vegetation more lush. Since this is not the case there must be a mechanism or a combination of them that counteract. Due to the increased surface temperatures off south-west Africa evaporation rates increase in this region as well (Figure 22, 23). Increasing evaporation rates would lead to a reduction or compensation of the higher precipitation rates which in turn results in a net-freshwater supply not very different from LGM or glacial conditions. Consequently, a change in vegetation composition can not be expected since the influence of the net-freshwater supply on tropical vegetation is higher than the effect of temperature. In the UVic ESCM model experiments simulating vegetation anomalies based on biomes between HS-like conditions and LGM conditions, only a minor increase of the forest biomes become apparent. This is consistent with our reconstructed vegetation composition where especially around HS1 the representation of Podocarpus, a conifer tree, increases (Figure 20).

Further limiting factors for tropical vegetation development during last glacial

A further important factor that needs to be considered as a limitation to the glacial vegetation development in tropical Africa is the low (190-200 ppmv; e.g. Petit et al., 1999) CO_2 concentration of the atmosphere. Both model experiments and data indicate that the concentration of atmospheric CO_2 influences the global distribution of vegetation due to the different carbon dioxide fixation strategies of

plants (C_3, $C4_4$/CAM) (Ehleringer and Monson, 1993; Polley et al., 1995; 1996; Ward et al., 1999). Plants using the C_3 photosynthetic pathway (most woody species) are less competitive than C_4/CAM plants (mainly grasses and succulents) under low CO_2 concentrations and the growth of tree taxa would be reduced (Johnson et al., 1993; Street-Perrott et al., 1997). Therefore, it is suggested that vegetation types representing the C_4/CAM pathway (grassland, shrubland, savannah) were more important and widespread during the glacial than today (Prentice et al., 2000).

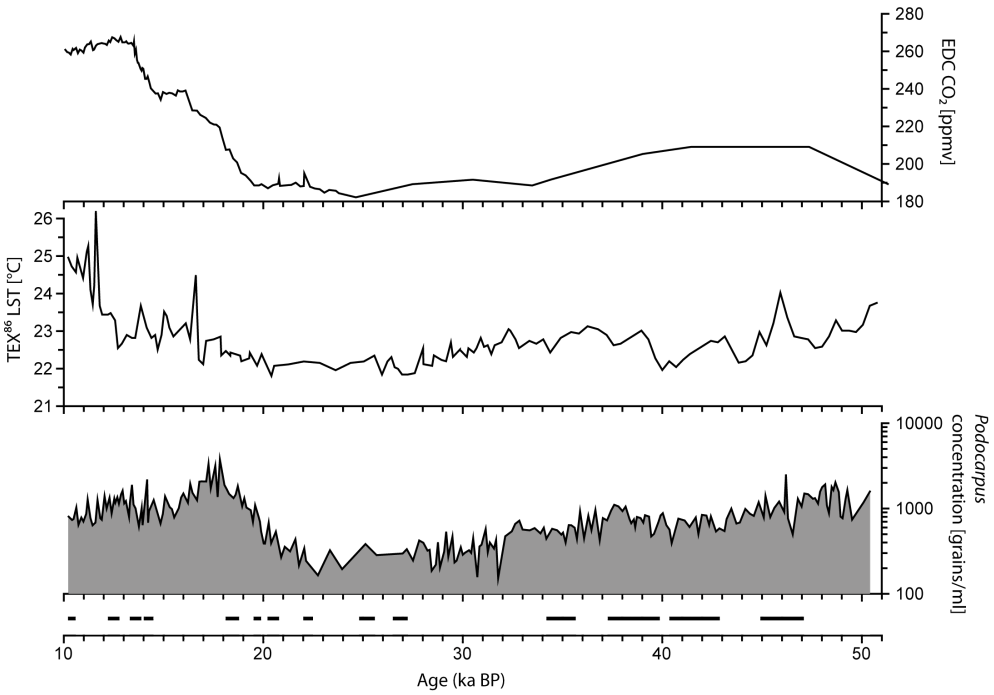

Figure 24: Concentrations of *Podocarpus* representing C_3 vegetation. Concentrations are given on log10 scale in [grains/ml]. Black lines indicate radiocarbon dating intervals. Land-surface temperature (LST) is according to Tierney et al. (2008). The atmospheric CO_2 concentration (Monnin et al., 2001; Petit et al., 1999) is plotted on the EDC3 timescale (EPICA members, 2006).

Model simulations produced by Harrison and Prentice (2003) also suggest that regions of actual or potential tropical forest today are being occupied by more drought tolerant biomes at the LGM. An even larger reduction of forested areas in the tropics is simulated if physiological effects of low atmospheric CO_2 concentrations (200 ppm) are considered (Harrison and Prentice, 2003). The deglaciation is marked by an increasing CO_2 level which favours C_3 species by shifting the competitive balance in their direction due to increasing plant productivity and water use efficiency (Pearcy and Ehleringer, 1984; Chapin et al., 1990; Johnson et al., 1993; Cowling and Sykes, 1999; Ward et al., 1999). These results are in good agreement with our

data, since under full glacial conditions the Angolan vegetation is dominated by grassland (Figure 19) while during the deglaciation tree taxa become more important (Figure 19, 24). We assume that a substantial fraction of the vegetation changes in southern hemisphere Africa during the last glacial and deglaciation is due to the physiological response to low CO_2 concentrations.

The increase of *Podocarpus* (conifer) about 3000 years before the increase in atmospheric CO_2 may be rather related to rising temperatures as indicated from southeast African and Antarctic temperature records (Monnin et al., 2001; Tierney et al., 2008) than CO_2. In general, our *Podocarpus* record follows the reconstructed temperature development for southern hemisphere Africa very well (Figure 24), which may indicate that temperature is the dominant limitation factor for Afromontane *Podocarpus* in southern Africa during the last glacial.

During the last glacial the intensity of the African monsoon circulation was weaker relative to today due to a reduced solar insolation and presence of large ice sheets leading to an increased surface albedo (e.g. Revel et al., 2010; Braconnot et al., 2000; Janicot, 2009). The cooler temperatures leading to a reduction in evaporation which in combination with a reduced monsoon circulation and decreased moisture supply in the ITCZ results in less precipitation and drier conditions (Braconnot et al., 2000). Generally drier conditions are reflected in our pollen record by high pollen percentages of grasses (Poaceae) and the corresponding low values of tree taxa representing groups (tropical seasonal forest, *Podocarpus*, Miombo woodland) (Figure 19).

Although we suggested several approaches to explain the glacial and deglacial vegetation development in Africa south of the equator there are a number of factors and feedbacks including the effect of elevation, the feedback of evaporation upon ecosystems, varying thresholds, species-depend respond to varying CO_2 concentrations etcetera , that are still poorly understood and need further investigation (e.g. Gasse et al., 2008).

6.3.7 Conclusion

High-resolution pollen studies using marine sediments provide an important contribution for the understanding of vegetation and climate development on the adjacent continent. The here presented high-resolution glacial vegetation record of tropical south-west Africa (Angola) gives insight into the climate and vegetation evolution of a region where high-quality terrestrial records are lacking. Throughout the last glacial grassland and savannah taxa dominate the pollen source area indicating an open vegetation type as a result of reduced moisture availability and low atmospheric CO_2 concentrations. During the deglaciation when the monsoon strengthens and CO_2 concentrations are rising tree taxa (excluding *Podocarpus*) dominated biomes become more widespread. Although, there are several existing tropical records that show an impact of HS in the Southern Hemisphere our high-resolution vegetation record with its pollen source area in Angola

and the southern Congo Basin provides no evidence for an impact of climate change during HS. Indeed, millennial-scale climate changes such as HS seem to be disguised by mechanisms that chancel out each other as indicated by model simulation.

Acknowledgement

We thank the Ocean Drilling Program for providing samples. This study was funded by the Deutsche Forschungsgemeinschaft (grant DU221/3, ACCAT) and by the Deutsche Forschungsgemeinschaft as part of the DFG-Research Center/Cluster of Excellence "The Ocean in the Earth System"

Supplement

Table 6: Assignment of identified pollen taxa to vegetation groups

Vegetation group	Pollen taxa	Family
Tropical forest	Adenium, Alchornea	Apocynaceae, Euphorbiaceae
	Blighia-type, Bosqueia	Sapindaceae, Moraceae
	Celastraceae/Hippocrateaceae, Celtis	Celastraceae, Ulmaceae
	Cissus, Coffea-type	Vitaceae, Rubiaceae
	Cola cordifolia, Cola nitida-type	Sterculiaceae
	Crossopteryx, Cuviera	Rubiaceae
	Daniellia-type, Duparquetia orchidacea	Caesalpiniaceae/Leguminosae
	Elaeis guineensis, Entada-type	Arecaceae/Palmae, Mimosaceae/Leguminosae
	Funtumia-type, Gaertnera	Apocynaceae, Rubiaceae
	Holoptelea grandis, Iodes	Ulmaceae, Icacinaceae
	Ixora-type, Khaya-type	Rubiaceae, Meliaceae
	Klaineanthus, Leea	Euphorbiaceae, Leeaceae
	Lophira, Mallotus-type	Ochnaceae, Euphorbiaceae
	Manilkara, Martretia	Meliaceae, Euphorbiaceae
	Melochia, Mezoneuron-type	Sterculiaceae, Caesalpiniaceae/Leguminosae
	Moraceae, Morinda	Moraceae, Rubiaceae
	Mussaenda, Pentaclethra	Rubiaceae, Mimosaceae/Leguminosae
	Phyllanthus, Psydrax parviflora	Euphorbiaceae, Rubiaceae
	Pycnanthus angolensis, Sabicea	Myristicaceae, Rubiaceae
	Sauvagesia, Schefflera	Ochnaceae, Araliaceae
	Sherbournea, Sorindeia-type	Rubiaceae, Anacardiaceae
	Stereospermum, Sysygium	Bignoniaceae, Myrtaceae
	Tamarindus/Cryptosepalum	Caesalpiniaceae/Leguminosae
	Tapinanthus-type, Tessmannia	Loranthaceae, Caesalpiniaceae/Leguminosae
	Tetrorchidium, Urticaceae (Africa)	Euphorbiaceae, Urticaceae
Mountain	Chionanthus-type, Chrysophyllum	Oleaceae, Sapotaceae
	Erica (Africa), Geranium	Ericaceae, Geraniaceae
	Ilex cf. I. mitis, Myrica (Africa)	Aquifoliaceae, Myricaceae
	Myrsine africana, Ocimum	Myrsinaceae, Lamiaceae
	Olea (Africa), Olea capensis	Oleaceae
	Restionaceae, Anthospermum	Restionaceae, Rubiaceae
Miombo woodland	Afzelia, Afzelia tetrade	Caesalpiniaceae/Leguminosae
	Berlinia-type, Brachystegia	Caesalpiniaceae/Leguminosae
	Paramacrolobium	Caesalpiniaceae/Leguminosae
	Pericopsis, Uapaca	Fabaceae/Leguminosae, Euphorbiaceae
Dryforest/ savannah	Acalypha, Adansonia	Euphorbiaceae, Bombacaceae
	Allophylus, Annonaceae	Sapindaceae, Annonaceae
	Antidesma, Tarchonanthus/Artemisia afra	Euphorbiaceae, Asteraceae
	Balanites, Baphia-type	Balanitaceae, Fabaceae/Leguminosae
	Bauhinia-type, Blepharis-type	Caesalpiniaceae/Leguminosae, Acanthaceae
	Bombax, Boscia-type	Bombacaceae, Capparaceae
	Bridelia, Burkea	Euphorbiaceae, Caesalpiniaceae/Leguminosae
	Butyrospermum, Canthium	Sapotaceae, Rubiaceae
	Capparis, Cardiospermum	Capparaceae, Sapindaceae
	Cassia-type, Ceiba pentandra	Caesalpiniaceae/Leguminosae, Bombaccaeae

	Clematis-type, Cnestis-type	Ranunculaceae, Conneraceae
	Coccinia, Cocos nucifera	Cucurbitaceae, Arecaceae/Palmae
	Colophospermum mopane, Croton-type	Caesalpiniaceae/Leguminosae, Euphorbiaceae
	Cussonia, Dalbergia	Araliaceae, Fabaceae/Leguminosae
	Detarium, Dialium-type	Caesalpiniaceae/Leguminosae
	Dombeya, Erythrina	Sterculiaceae, Fabaceae/Leguminosae
	Flacourtia, Garcinia	Flacourtiaceae, Clusiaceae/Guttiferae
	Grewia, Hugonia	Tiliaceae, Linaceae
	Hymenocardia, Hypoestes-type	Euphorbiaceae, Acanthaceae
	Jasminum/Schrebera, Kohautia	Oleaceae, Rubiaceae
	Lannea-type, Luffa	Anacardiaceae, Cucurbitaceae
	Maesa lanceolata-type, Maytenus-type	Myrsinaceae, Celastraceae
	Mimosa pigra, Nyctaginaceae undiff.	Mimosaceae/Leguminosae, Nyctaginaceae
	Olax, Ormocarpum	Olacaceae, Fabaceae/Leguminosae
	Papilionoideae, Piliostigma	Fabaceae/Leguminosae, Caesalpiniaceae/Leguminosae
	Protea, Pseudocedrela	Proteaceae, Meliaceae
	Psydrax-type subcordata, Pterocarpus-type	Rubiaceae, Fabaceae/Leguminosae
	Rubiaceae monade, Rytigynia-type	Rubiaceae
	Sclerocarya-type birrea, Sesbania-type	Anacardiaceae, Fabaceae/Leguminosae
	Securinega, Spathodea	Euphorbiaceae, Bignoniaceae
	Spermacoce-type, Sterculia-type	Rubiaceae, Sterculiaceae
	Stipularia africana, Strychnos	Rubiaceae, Loganiaceae
	Tarenna, Teclea	Rubiaceae, Rutaceae
	Triapsis, Buxus-type madagascaria	Malphigiaceae, Euphorbiaceae
	Zanthoxylum	Rutaceae
Semidesert	Gazania-type, Gomphrena-type	Asteraceae, Amaranthaceae
	Heliotropium, Hermannia	Boraginaceae, Sterculiaceae
	Hermannia stricta-type, Indigofera-type	Sterculiaceae, Fabaceae/Leguminosae
	Ipomoea-type, Justicia/Monechma	Convolvulaceae, Acanthaceae
	Kalanchoe, Maerua-type	Crassulaceae, Capparaceae
	Malvaceae (Africa), Merremia	Malvaceae, Convolvulaceae
	Neurada-type, Nitraria	Neuradaceae/Rosaceae, Zygophyllaceae
	Parkinsonia, Pelargonium	Fabaceae/Leguminosae, Geraniaceae
	Pentzia-type, Petalidium	Asteraceae, Acanthaceae
	Phoenix, Phyla nodiflora	Arecaceae/Palmae, Verbenaceae
	Plantago, Rhynchosia-type	Plantaginaceae, Fabaceae/Leguminosae
	Salvadora persica, Solanum (Africa)	Salvadoraceae, Solanaceae
	Stoebe-type, Tephrosia	Asteraceae, Fabaceae/Leguminosae
	Thymelaeaceae (Africa), Tribulus	Thymelaeaceae, Tribulaceae/Zygophyllaceae
	Walafrida, Welwitschia	Scrophulariaceae, Welwitschiaceae
	Zygophyllum	Zygophyllaceae

7 Summary and conclusion

The results presented in this thesis document,

- the tropical vegetation response to abrupt climate variability typical for the last glaciation in tropical Africa and South America, and

- a local study of changes in the terrestrial and marine environment in southern hemisphere Africa during the last glacial with special emphasis on periods associated with Heinrich Stadials.

The compilation of high-resolution pollen records from the circum-Atlantic tropics covering the last glacial reveals the response of the vegetation from both South America and Africa to abrupt climate fluctuations such as Dansgaard-Oeschger (D-O) cycles and Heinrich Stadials (HS) (Chapter 6.1). Although the pollen records from tropical Africa do register HS, a response to D-O variability has only been detected in records from South America. In general, abrupt climate variations appears to have left a stronger signal in the South American records compared to the African ones. The hypothesis of a southward shift in the migration pattern of the ITCZ is corroborated by the pollen records from tropical South America, which show an opposing vegetation development north and south of the modern position of the ITCZ. North of the present-day limit of the ITCZ the vegetation becomes more open during abrupt climate change indicating drier conditions, while at the southern limit of the modern ITCZ the vegetation cover increases denoting wetter circumstances. The lack of high-resolution pollen records from the northern African tropics hinders the determination if this pattern is mirrored on the African continent. However, HS in tropical Africa are marked by an increase in arboreal taxa, possibly indicating an increase in moisture availability.
When combined with other records from northern Africa that suggest drier conditions during HS (e.g. Peck et al., 2004; Mulitza et al., 2008; Collins et al., 2010) the observed changes are still consistent with the hypothesis that tropical climate changes are associated with a shift in the migration pattern of the ITCZ due to a reduction in the strength of the AMOC. At sites where multiple HS are registered the vegetation response differs between different HS events. Since the atmospheric configuration over Africa, including the ITCZ and the Congolian Air Boundary, is highly complex, a different behaviour of this system during different HS events is not surprising. The hypothesis that the tropics play a key role in generating abrupt climate variations cannot be supported by the observed vegetation changes in tropical Africa and South America.

The development of the surface water condition in the tropical southeast Atlantic during the last glacial (50 to 23.5 ka BP) was investigated using the Mg/Ca and oxygen isotope ratios of planktonic foraminifera obtained from ODP Site 1078 (Chapter 6.2). Considering the seasonal and ecological preferences of the foraminifera species used, the Mg/Ca of *G. ruber* (pink) represents the warm waters of the Angola Current (AC) during austral summer while the Mg/Ca of *G. bulloides* reflects the austral winter surface water temperatures in the Benguela upwelling system (BC). For the investigated time period significant differences in the thermal response to abrupt climate variations were reconstructed for the regions of the AC and BC. In the AC the Mg/Ca temperatures of pink-pigmented G. ruber indicate increasing SST during HS, which is in good agreement with the concept of the bipolar seesaw (Broecker et al., 1998; EPICA members, 2006; Barker et al., 2009). However, in the BC significantly cooler SSTs and no response to HS are recorded. We suggest the cooler SSTs between 50 and 23.5 ka BP reflect the combined effect of an intensification of the Benguela coastal upwelling, an enhanced northward intrusion of cold BC waters and a decreased inflow of warm waters through the Agulhas Leakage due to a northward shift of the South Atlantic frontal system. Brief periods of intensified upwelling and cooling that coincide with HS (Little et al., 1997; Farmer et al., 2005) appear to be a highly probable mechanism that counteract the warming in the study area during HS as predicted by the bipolar seesaw hypothesis.

A high-resolution pollen record from tropical southwest Africa gained from marine sediments of ODP Site 1078 provides insight into the general climate trends in the region and the vegetation development on the adjacent continent during the period 50 to 10 ka BP (Chapter 6.3). During the last glacial the dominance of grassland and savannah taxa indicates an open vegetation type prevailing in southern hemisphere Africa. The low glacial atmospheric CO_2 values combined with the reduced strength of the African monsoon are assumed to be the main factors influencing the tropical African vegetation. During the last deglaciation when the monsoon strengthened and the CO_2 concentration began to rise, percentages of arboreal taxa increase indicating the expansion of forests. Although several tropical African vegetation records do show an impact of millennial-scale climate variations such as HS (Chapter 6.1), the vegetation in Angola and the southern Congo Basin is surprisingly stable and shows no response to HS. Model simulations conducted with a Earth System Climate Model including a dynamic vegetation component suggest that the vegetation response during HS is subdued by mechanisms that cancel out each other.

8 Prospect for future research

The work presented here contributed to shed light on the glacial development of a region with a highly complex atmospheric and oceanographic setting. Previous studies of past southwest African vegetation (Dupont et al., 2006; 2007; 2008) convincingly showed a sensitivity to millennial-scale climate variations. This study has found the response of tropical African vegetation to millennial-scale climate variations to be less predictable and unexpectedly stable during some periods of abrupt climate change (Chapter 6.3). The marine realm off the coast of southwest Africa is dominated by three macro-scale oceanographic features, the Angola Current (AC), the Angola Benguela Front (ABF) and Benguela Current (BC). Although, the AC register the influence of abrupt climate change in this region, the BC seems to be influenced by other mechanisms (Chapter 6.2). However, changes in the SST are not reflected in the vegetation on the adjacent continent, suggesting a less direct connection between land and sea in this part of the world.
Due to the obviously complex environmental situation several questions remained unsolved, providing various opportunities for future research.
Here two studies currently underway are introduced. Following in the subsection "Further Research" a selection of possible future research avenues are suggested.

8.1 Dinoflagellate Cysts

The reconstruction of past sea surface conditions is crucial for the understanding of climatic change. The assemblages and morphology of planktonic organisms, including dinoflagellates, are thought to reflect environmental conditions and such as can be useful for determining past sea surface conditions (e.g. Hays et al., 2005). Dinoflagellates are a large group of flagellate bearing protists and represent one of the main groups of phytoplankton in the aquatic environment. Approximately 10 to 20% of the living marine dinoflagellate species produce organic-walled cysts during various stages of their complex lifecycle. A macromolecular and highly resistant organic compound (dinosporin) comparable to sporopollenin (Fensome et al., 1993), forms or partly forms their walls, meaning the cysts can be well preserved in sediments. The identification of the cyst species is determined through the tabulation and/or paratabulation pattern, and the presence of an archaeophyle and cingulum. Morphological features such as size and shape of cyst, structure and ornamentation of cyst walls, and the form and length of the cyst processes may also be highly diagnostic (Matthiessen et al., 2005). Changes in the assemblage composition and/or morphology can be attributed to changes in environmental conditions like temperature, salinity and nutrient content (Dale, 1996, Dale et al., 2002). Although the fossil dinoflagellate cyst record might be biased by transport and preservation issues (Dale and Dale,

2002; Zonneveld et al., 2008) dinoflagellate cysts are considered to be a useful tool to reconstruct past environmental changes in marine surface waters.

Although, the reconstruction of late Quaternary marine environmental variations using organic-walled dinoflagellate cysts has been widely applied to temperate and high-latitude sediments (e. g. Marret et al., 2001; Mudie et al., 2002; deVernal et al., 2005), only a few studies focus on tropical areas (e. g. Zonneveld et al., 1997; Marret and Turon, 1994; González et al., 2008).

In order to contribute to the study of variations in the marine surface conditions in the tropics during the last glaciation, counts of dinoflagellate cysts originating from ODP 1078 (off Angola) have been generated for the period 50 to 28 ka BP. The assignment of the 28 identified taxa and their assemblage to specific environmental variables (e.g. productivity, salinity, temperature) or oceanographic features (AC, ABF, BC) would allow changes of these paleoceanographic parameters to be placed in the context of (abrupt) climate change. Combining the dinoflagellate cyst record with the record of Mg/Ca of planktonic foraminifers reveals a comprehensive picture of the oceanographic development of the tropical southeast Atlantic in the last glacial. Including unpublished dinoflagellate cyst counts from Lydie Dupont, which have also been obtained from ODP Site 1078, the record can be extended up to Holocene times. This high-resolution record covering the last 50 ka would provide a valuable insight into the behaviour of the tropical eastern Atlantic under glacial, deglacial and interglacial conditions.

8.2 Data-Model Comparison

The analysis and interpretation of the data obtained during this project clearly contributed to improve the understanding of (abrupt) climate variations in the African tropics during the last glacial. This study also provides insight into the nature of climate change in the terrestrial and marine realm. However, many unanswered questions emerge about the role and interactions of the atmosphere, ocean and terrestrial environment during (abrupt) climate fluctuations in the tropics.

The issues and scientific questions addressed in this thesis using proxy analysis have also been part of a modelling project conducted by Dian Handiani at the Department of Geoscience, University of Bremen. The modelling work based on the University of Victoria (Uvic) Earth System Climate Model (ESCM) includes several components such as the atmosphere, biosphere, hydrosphere, and land-ice. The land-surface and dynamic vegetation component is based on the MOSES and TRIFFID models and allows the study of feedbacks between climate and vegetation. Based on the incorporation of these components in the model the response of SST,

precipitation and vegetation of tropical Africa to changes in the AMOC can be experimentally determined. Within the dynamic vegetation model plant functional types (PFTs) have been defined, relying on the phenomena of functional convergence between unrelated plants growing in similar physical environments (e.g. Prentice and Webb, 1998). Using the output of the dynamic vegetation model and additional climatic constraints biomes (here simplified as broad physiognomic vegetation classes) can be defined. Plant species can be assigned to PFTs using easily recognisable physiognomic and bioclimatic criteria, while biomes are defined combining the most dominant PFTs (e.g. Prentice et al., 1992). Paleovegetation records can then be compared to vegetation patterns resulting from modelling experiments.

In this context, pollen taxa identified in the sediments of ODP Site 1078 will be assigned to PFTs and then to biomes, allowing the comparison of changes in the pattern of palynologically reconstructed and modelled vegetation. However, since the definition of model-PFTs is usually based on climatic and physical parameters while the definition of plant-PFTs follows physiognomic and bioclimatic parameters, a common definition needs to be established. Similar issues need to be addressed when defining the biomes. The definition of both PFTs and biomes needs to be adjusted to tropical African flora (high diversity, low sampling representation of e.g. tropical forest taxa) and environmental conditions.

Finally, by comparing the mapped precipitation, temperature and vegetation pattern generated with the UVic ESCM with the classically reconstructed SW African vegetation and SST, distinct progress in the comprehension of the following issues is expected:

- the response of precipitation, temperature and vegetation to changes in the strength of the AMOC, with a special emphasis on millennial-scale climate variations
- the feedback and interactions between atmosphere, ocean and land during the last glacial
- the evaluation of the impact of changes in precipitation and/or temperature on tropical vegetation during the last glacial

Eventually, results of the coupled ocean-atmosphere model can be evaluated and if necessary improved.

8.3 Further Research

- High resolution assemblage counts of *G. bulloides* specimens would be useful to reconstruct changes in the Benguela upwelling intensity during the last glacial. Especially concerning abrupt climate change contradictory results exist regarding the intensity of

upwelling (Little et al., 1997; Kim et al., 2003). However, while the existing two records are high-resolution enough to record millennial-scale climate variability, they are not sufficient to draw general conclusions. Therefore, an additional high resolution reconstruction of changes in the Benguela upwelling intensity would be important.

- In order to trace shifts of the ABF, the Mg/Ca analyses from an additional two or more cores from within the ABF and south of the ABF would be required. Similar to the intensity of the BC, contradictory results exist concerning the glacial position of the ABF (Jansen et al., 1996; Kim et al., 2003).

- To place the results of this study in a transregional context, these data should be compared with other tropical high-resolution palynological and geochemical records covering the last glacial. General issues such as the position of the ITCZ during (abrupt) climate change, possible differences in the regional impact and manifestation of (abrupt) climate variations, and the role of the tropics during (abrupt) climate change could be addressed.

9 Acknowledgements

First of all, I sincerely thank Prof. Dr. Gerold Wefer for giving me the opportunity to realise my PhD at the MARUM, his interest and support for my work.

I owe my deepest gratitude to Dr. Lydie M. Dupont who shared with me her knowledge and time; supported, inspired, and encouraged me throughout these three years. Everything she did for me makes it difficult to find strong enough words to express my respect and thankfulness.

I would like to thank Dr. André Paul for his challenging questions and discussion which influenced and changed some of my perspectives.

I also thank Dr. Stefan Mulitza who, although not my official supervisor or directly involved in my project, always took his time to answer my question, gave me advice and support.

Possibly unaware of his significant contribution to my PhD thesis might be Dr. Frank J. C. Peeters, who suggested during one of these ordinary hallway talks to additionally include Mg/Ca analysis in my project. The promising results and the related publication can be read in Chapter 6.2 of this document.

The Bremen Graduate School "Global Change in a marine Realm" (GLOMAR) gave me the opportunity to further educate myself by attending courses with various topics. GLOMAR, furthermore, supported me financially giving me the chance to present my work during international meeting and hence played an important role for my career planning. Special thank goes to Uta Brathauer and Carmen Murken, the good spirits of GLOMAR, who always took their time to solve problems and answer questions.

At the University of Liverpool where I accomplished my three month research stay I was warmly welcomed by Dr. Fabienne Marret and introduced in the world of dinoflagellate cysts.

My former and current office mates I want to thank for their comradeship, patience, and all the little chats in between that made the days always a bit friendlier. Particular thank to Nick Rackebrandt my office mate and friend who I not just shared scientific thoughts and ideas with but also the frustrations, dreams and anxieties of the daily life of PhD students.

Without my friends and colleagues Cata, Cyril, Dave, Flo, Hiske, Inka, Jan-Berend, Jeroen,

Kathrin, Mahyar aka Marco, Marcos, Marius, Markus E., Markus R., Matthias, Petra, Stephan, Stijn, Ulli (note the alphabetical order) life and work in Bremen would have been less beneficial.

Ulli, my dear friend, I thank you so much for your friendship, patience, warmth, support, fun and advice. I miss you.

Without my beloved parents, Petra and Michael, I would certainly not be where I am today. Thank you for all your support and assistance.

At the end and most of all I want to thank my partner for everything you did and mean for me. Thank you so much for your support, patience and understanding not only at times when I wrote my thesis.

I thank the Ocean Drilling Program for providing samples. This study was funded by the Deutsche Forschungsgemeinschaft (ACCAT) and by the Deutsche Forschungsgemeinschaft as part of the DFG-Research Center - Cluster of Excellence "The Ocean in the Earth System"

10 References

Agwu, C.O.C., Beug, H.-J., 1982. Palynological studies of marine sediments off the West African coast. Meteor Forschungsergebnisse, Deutsche Forschungsgemeinschaft, Reihe C Geologie und Geophysik, Gebrüder Bornträger, Berlin, Stuttgart, C36, 1-30.

Alley, R.B., 1998. Icing the North Atlantic. Nature 392, 335-337.

Alley, R.B., Clark, P.U. Keigwin, L.D., Webb, R.S., 1999. Making sense of millennial scale climate change, in P.U. Clark, R.S.Webb and L.D. Keigwin (eds.), Mechanisms of Global Climate Change at Millennial Time Scales, Geophysical Monograph Vol. 112, American Geophysical Union, Washington, pp. 385-394.

Anand, P., H. Elderfield, Conte, M. H., 2003. Calibration of Mg/Ca thermometry in planktonic foraminifera from a sediment trap time series, Paleoceanography, 18, 1050.

Ansari, M. H., Vink, A., 2007. Vegetation history and palaeoclimate of the past 30 kyr in Pakistan as inferred from the palynology of continental margin sediments off the Indus Delta. Review of Palaeobotany and Palynology 145, 201-216.

Arz, H. W., Pätzold, J., Wefer, G., 1998. Correlated Millennial-Scale Changes in Surface Hydrography and Terrigenous Sediment Yield Inferred from Last-Glacial Marine Deposits off Northeastern Brazil. Quaternary Research 50, 157-166.

Bard, E., Arnold, M., Mangerud, J., Paterne, M., Labeyrie, L., Duprat, J., Mélières, M.-A., Sønstegaard, E., Duplessy, J.-C., 1994. The North Atlantic atmosphere-sea surface ^{14}C gradient during the Younger Dryas climatic event. Earth and Planetary Science Letters 126, 275-287.

Bard, E., Rostek, F., Turon, J.-L., Gendreau, S., 2000. Hydrological Impact of Heinrich Events in the Subtropical Northeast Atlantic. Science 289, 1321-1324.

Barker, S., M. Greaves, Elderfield, H., 2003. A study of cleaning procedures used for foraminiferal Mg/Ca paleothermometry, Geochem. Geophys. Geosyst., 4, 8407.

Barker, S., I. Cacho, H. Benway, Tachikawa, K., 2005. Planktonic foraminiferal Mg/Ca as a proxy for past oceanic temperatures: a methodological overview and data compilation for the Last Glacial Maximum, Quaternary Science Reviews, 24, 821-834.

Barker, S., P. Diz, M. J. Vautravers, J. Pike, G. Knorr, I. R. Hall, Broecker, W. S., 2009. Interhemispheric Atlantic seesaw response during the last deglaciation, Nature, 457, 1097-1102.

Bé, A. W. H., Tolderlund, D. S., 1971. Distribution and Ecology of living planktonic foraminifera in surface waters of the Atlantic and Indian Oceans, in The Micropalaeontology of Oceans, B. M. Funnell, W. R. Riedel (Eds.), Cambridge University Press, Cambridge, pp. 105-149.

Behling, H., 1997. Late Quaternary vegetation, climate and fire history from the tropical mountain region of Morro de Itapeva, SE Brazil. Palaeogeography, Palaeoclimatology, Palaeoecology 129, 407Ű422.

Behling, H., Arz, H.W., Pätzold, J., Wefer, G., 2000. Late Quaternary vegetational and climate dynamics in northeastern Brazil, inferences from marine core GeoB 3104-1. Quaternary Science Reviews 19, 981-994.

Behling, H., Arz, H.W., Pätzold, J., Wefer, G., 2002. Late Quaternary vegetational and climate dynamics in southeastern Brazil, inferences from marine cores GeoB 3229-2 and GeoB 3202-1. Palaeogeography, Palaeoclimatology, Palaeoecology 179, 227-243.

Bemis, B. E., Spero, H. J., Bijma, J., Lea, D. W., 1998. Reevaluation of the oxygen isotopic composition of planktonic foraminifera: Experimental results and revised paeotemperature equations. Paleoceanography 13, 150-160.

Berger, W. H., 1970. Planktonic Foraminifera: Selective Solution and the Lysocline. Marine Geology 8, 111-138.

Berger, W. H., Wefer, G., 2002. On the reconstruction of upwelling history: Namibia upwelling in context, Marine Geology, 180, 3-28.

BIOME 4: http://pmip2.lsce.ipsl.fr/synth/biome4.shtml.

Blunier, T., Brook, E.J., 2001. Timing of Millennial-Scale Climate Change in Antarctica and Greenland During the Last Glacial Period Science 291, 109-112.

Bogotá-Angel, R.G., Groot, M.H.M., Hooghiemstra, H., Berrio, J.-C., in review. Late Pleistocene sediment infill of the Fúquene Basin (Colombian Andes) from 4 pollen records and global significance of the centennial-resolution climate change. Journal of Quaternary Science.

Bonan, G.B., 2008. Forests and Climate Change: Forcings, Feedbacks, and the Climate Benefits of Forests Science 320, 1444-1449.

Bond, G., Broecker, W., Johnsen, S., McManus, J., Labeyrie, L., Jouzel, J. and Bonani, G., 1993. Correlations between climate records from North Atlantic sediments and Greenland ice. Nature 365, 143-147.

Bond, G., Showers, W., Cheseby, M., Lotti, R., Almasi, P., deMenocal, P., Priore, P., Cullen, H., Hajdas, I., Bonani, G., 1997. A pervasive millennial-scale cycle in North Atlantic Holocene and glacial climates. Science 278, 1257-1266.

Bonnefille, R., Riollet, G., 1980. Pollens des savanes dŠAfrique orientale. CNRS Editions, Paris, pp. 140.

Bonnefille, R., Riollet, G., 1988. The Kashiru pollen sequence (Burundi). Palaeclimatic implications for the last 40,000 yr. B.P. in tropical Africa. Quaternary Research 30, 19-35.

Bonnefille, R., Chalié, F., Guiot, J., Vincens, A., 1992. Quantitative estimates of full glacial temperatures in equatorial Africa from palynological data; Climate Dynamics 6, 251-257.

Bonnefille, R., Chalié, F., 2000. Pollen-inferred precipitation time-series from equatorial mountains, Africa, the last 40 kyr BP. Global and Planetary Change 26, 25-50.

Boyle, E.A., 1981. Cadmium, zinc, copper, and barium in foraminifera tests Earth and Planetary Science Letters 53 (1), 11-35.

Boyle, E.A.,Keigwin, L.D., 1985. Comparison of Atlantic and Pacific paleochemical records for the last 215,000 years: changes in deep ocean circulation and chemical inventories Earth and Planetary Science Letters 76, 135-150.

Braconnot, P., Joussaume, S., de Noblet, N., Ramstein, G., 2000. Mid-Holocene and Last Glacial Maximum African monsoon changes as simulated within the Paleoclimate Modelling Intercomparison Project. Global and Planetary Change 26, 51-66.

Broccoli, A. J., 2000. Tropical Cooling at the Last Glacial Maximum: An Atmosphere-Mixed Layer Ocean Model Simulation, Journal of Climate, 13, 951-976.

Broecker, W. S., Bond, G., Klas, M., Bonani, G. and Wolfli, W., 1990. A Salt Oscillator in the glacial Atlantic? 1. The concept. Paleoceanography 5, 469-477.

Broecker, W.S., Bond, G.C., Klas, M., Clark, E., McManus, J.F., 1992. Origin of the northern Atlantic's Heinrich events. Climate Dynamics 6, 265-273.

Broecker, W. S., 1992. Upset for Milankovitch theory. Nature 359, 779-780.

Broecker, W.S., 1994. Massive iceberg discharges as triggers for global climate change. Nature 372, 421-424.

Broecker, W., 1996. Glacial Climate in the Tropics. Science 272, 1902-1904.

Broecker, W. S., 1998. Paleocean circulation during the last deglaciation: A bipolar seesaw?, Palaeoceanography, 13, 119-121.

Broecker, W.S., 2003. Does the Trigger for Abrupt Climate Change Reside in the Ocean or in the Atmosphere? Science 300, 1519-1522, doi: 10.1126/science.1083797.

Brown, S. J., Elderfield, H., 1996. Variations in Mg/Ca and Sr/Ca ratios of planktonic foraminifera caused by postdepositional dissolution: Evidence of shallow Mg-dependent dissolution. Paleoceanography 11, 543-551.

Brown, E.T, Johnson, T.C., Scholz, C.A., Cohen, A.S., King, J.W., 2007. Abrupt change in tropical African climate linked to the bipolar seesaw over the past 55,000 years. Geophysical Research Letters 34, 1-5.

Burbridge, R.E., Mayle, F.E., Killeen, T.J., 2004. Fifty-thousand-year vegetation and climate history of Noel Kempff Mercado National Park, Bolivian Amazon. Quaternary Research 61, 215-230.

Bush, M.B., Silman, M.R., Urrego, D.H., 2004. 48,000 Years of Climate and Forest Change in a Biodiversity Hot Spot. Science 303, 827-829.

Bush, M.B., Correa-Metrio, A., Hodell, D.A., Brenner, M., Ariztegui, D., Anselmetti, D., Gilli, A., Burton, C., Muller, A.D., in press. The Last Glacial Maximum: Central America. In: F. Vimeux, F. Sylvestre and M. Khodri (eds), Past climate variability from the Last Glacial Maximum to the Holocene in South America and surrounding regions. Springer, Paris.

Cane, M., Clement, A.C., 1999. Mechanisms of Global Climate Change at Millennial Time Scales. P. U. Clark, R. S. Webb, L. D. Keigwin, Eds. (Geophysical Monograph 112, American Geophysical Union, Washington, DC, 1999), pp. 373-383.

Chapin, F.S., Schulze, E.D., Mooney, H.A., 1990. The ecology and economics of carbon storage in plants. Annual Review of Ecology and Systematics 21, 423-447.

Chen, F. H., Bloemendal, J., Wang, J. M., Li, J. J., Oldfield, F., 1997. High-resolution multi-proxy climate records from Chinese loess: evidence for rapid climatic changes over the last 75 kyr. Palaeogeography, Palaeoclimatology, Palaeoecology 130, 323-335.

Chiang, J. C. H. and Koutavas, A., 2004. Climate change: Tropical flip-flop connections. Nature 432, 684-685.

Chmura, G.L., Smirnov, A., Campbell, I.D., 1999. Pollen transport through distributaries and depositional patterns in coastal waters. Palaeogeography, Palaeoclimatology, Palaeoecology 149, 257-270.

Clark, P.U., Hostetler, S.W., Pisias, N.G., Schmittner, A., Meissner, K., 2007. Mechanisms for an ~ 7-kyr Climate and Sea-Level Oscillation during Marine Isotope Stage 3. In: Ocean Circulation: Mechanisms and Impacts. A. Schmittner, J. C. H. Chiang and S. R. Hemming, American Geophysical Union. 173, 209 - 246.

Cohen, A.S., Stone, J.R., Beuning, K.R.M., Park, L.E., Reinthal, P.N., Dettman, D., Scholz, C.A., Johnson, T.C., King, J.W., Talbot, M.R., Brown, E.T., Ivory, S.J., 2007. Ecological consequences of early Late Pleistocene megadroughts in tropical Africa. Proceedings of the National Academy of Sciences 104 (42), 16422-16427.

Colberg, F., Reason, C. J. C., 2006. A model study of the Angola Benguela Frontal Zone: Sensitivity to atmospheric forcing, Geophys. Res. Lett., 33, L19608.

Colinvaux, P.A., De Oliveira, P.E., Moreno, J.E., Miller, M.C., Bush, M.B., 1996. A Long Pollen Record from Lowland Amazonia: Forest and Cooling in Glacial Times. Science 274. 85-88.

Collins, W. D., Bitz, C. M., Blackmon, M. L., Bonan, G. B., Bretherton, C. S., Carton, J. A., Chang, P., Doney, S. C., Hack, J. J., Henderson, T. B., Kiehl, J. T., Large, W. G., McKenna, D. S., Santer, B. D., Smith, R. D., 2006. The Community Climate System Model Version 3 (CCSM3). Journal of Climate 19, 2122-2143.

Collins, J. A., Schefusz, E., Heslop, D., Mulitza, S., Prange, M., Zabel, M., Tjallingii, R., Dokken, T. M., Huang, E., Mackensen, A., Schulz, M., Tian, J., Zarriess, M., Wefer, G., 2010. Interhemispheric symmetry of the tropical African rainbelt over the past 23,000 years. Nature Geoscience 4, 42-45.

Crowley, T.J., 1992. North Atlantic Deep Water cools the Southern Hemisphere. Paleoceanography 7 (4), 489-497.

Cowling, S.A., Sykes, M.T., 1999. Physiological Significance of Low Atmospheric CO_2 for Plant-Climate Interactions. Quaternary Research 52, 237-242.

Cox, P. M., Betts, R. A., Bunton, C. B., Essery, R. L. H., Rowntree, P. R., Smith, J., 1999. The impact of new land surface physics on the GCM simulation of climate and climate sensitivity. Climate Dynamics 15, 183-203-203.

Cox, P. M., 2001. Description of the TRIFFID dynamic global vegetation model Hadley Center technical note 24, 1-17.

Dahl, K. A., Broccoli, A. J. and Stouffer, R. J., 2005. Assessing the role of North Atlantic freshwater forcing in millennial scale climate variability: a tropical Atlantic perspective. Climate Dynamics 24, 325-346.

Dale, B. 1996. Dinoflagellate cyst ecology: modelling and geological applications. In: Jansonius, J. and McGregor, D.C. (Eds.), Palynology: Principles and Applications, vol. 3. American Association of Stratigraphic Palynologists, Dallas, Texas, 1249-1275.

Dale, B. and Dale, A.L. 2002. Environmental applications of dinoflagellate cysts and acritarchs. In: Haslett, S.K. (Ed.), Quaternary Environmental Micropalaeontology. Arnold, London, pp. 207-240.

Daniau, A. L., Sánchez-Goñi, M. F., Beaufort, L., Laggoun-Défarge, F., Loutre, M. F. and Duprat, J., 2007. Dansgaard-Oeschger climatic variability revealed by fire emissions in southwestern Iberia. Quaternary Science Reviews 26, 1369-1383.

Dansgaard, W., Johnson, S., Clausen, H. B., Dahl-Jensen, D., Gundestrup, N., Hammer, C. U. and Oeschger, H., 1984. North Atlantic climatic oscillations revealed by deep Greenland ice cores. In: J. E. Hansen and T. Takahashi (Eds.), Climate Processes and Climate Sensitivity. American Geophysical Union, Washington D. C., 288-298.

DeBusk, G.H., 1998. A 37,500-year pollen record from Lake Malawi and implications for the biogeography of afromontane forests. Journal of Biogeography 25, 479-500.

Dekens, P. S., Lea, D. W., Pak, D. K., Spero, H. J., 2002. Core top calibration of Mg/Ca in tropical foraminifera: Refining paleotemperature estimation. Geochemistry, Geophysics, Geosystems 3, 1-29.

de Vernal, A., Eynaud, F., Henry, M., Hillaire-Marcel, C., Londeix, L., Mangin, S., Matthiessen, J., Marret, F., Radi, T., Rochon, A., Solignac, S., Turon, J.-L., 2005. Reconstruction of sea-surface conditions at middle to high latitudes of the Northern Hemisphere during the Last Glacial Maximum (LGM) based on dinoflagellate cyst assemblages. Quaternary Science Reviews 24, 897-924.

Diester-Haass, L., 1985. Late Quaternary sedimentation on the Eastern Walvis Ridge, SE Atlantic (HPC 532 and four piston cores), Marine Geology, 65, 145-189.

Dittert, N., Henrich, R., 2000. Carbonate Dissolution in the South Atlantic Ocean: evidence from ultrastructure breakdown in Globigerina bulloides. Deep-Sea Research 47, 603-620.

Duffin, K.I., Bunting, M.J., 2008. Relative pollen production and fall speed estimates for southern African savanna taxa. Veget. Hist. Archaeobot. 17, 507-525.

Duplessy, J. C., Blanc, P. L., Bé, A. W. H., 1981. Oxygen-18 enrichment of planktonic foraminifera due to gametogenic calcification below the euphotic zone. Science 213. 1247-1250.

Duplessy, J. C., Labeyrie, L., Juillet-Leclerc, A., Maitre, F., Duprat, J., Sarnthein,M., 1991. Surface salinity reconstruction of the North Atlantic Ocean during the last glacial maximum. Oceanol Acta 14, 311-324.

Dupont, L., Beug, H.-J., Stalling, H., Tiedemann, R., 1989. First palynological results from site 658 at 21 °N off Northwest Africa: Pollen as climate indicators. In: W. Ruddiman, M.Sarnthein et al., Proceedings of the Ocean Drilling Program, Scientific Results, Vol. 108, 93-111.

Dupont, L.M., Agwu, C.O.C., 1991. Environmental control of pollen grain distribution patterns in the Gulf of Guinea and offshore NW-Africa. Geologische Rundschau 80 (3), 567-589.

Dupont, L.M., Agwu, C.O.C, 1992. Latitudinal shifts of forest and savanna in N.W. Africa during the Brunhes chron: further marine palynological results from site M 16415 (9°N 19°W). Vegetation History and Archaeobotany 1(3), 163-175.

Dupont, L., Weinelt, M., 1996. Vegetation history of the savanna corridor between the Guinean and the Congolian rain forest during the last 150,000 years. Vegetation History and Archaeobotany 5, 273-292.

Dupont, L., Marret, F., Winn, K., 1998. Land-sea correlation by means of terrestrial and marine palynomorphs from the equatorial East Atlantic: phasing of SE trade winds and the oceanic productivity. Palaeogeography, Palaeoclimatology, Palaeoecology 142, 51-84.

Dupont, L.M., 1999. Pollen and Spores in Marine Sediments from the East Atlantic- A View from the Ocean into the African Continent. In: G. Fischer, G. Wefer (Eds.), Use of Proxies in Paleoceanography: Examples from the South Atlantic. Springer Verlag Berlin Heidelberg, 523-546.

Dupont, L., Wyputta, U., 2003. Reconstructing pathways of aeolian pollen transport to the marine sediments along the coastline of SW Africa. Quaternary Science Reviews 22, 157-174.

Dupont, L., Behling, H., 2006. Land-sea linkages during deglaciation: High-resolution records from the eastern Atlantic off the coast of Namibia and Angola. Quaternary International 148, 19-28.

Dupont, L., Behling, H., Jahns, S., Marret, F., Kim, J.-H., 2007. Variability in glacial and Holocene marine pollen records offshore from west southern Africa Vegetation History and Archaeobotany 16, 87-100.

Dupont, L.M., Behling, H., Kim, J.-H., 2008. Thirty thousand years of vegetation development and climate change in Angola (Ocean Drilling Program Site 1078). Climate of the Past 4, 111-147.

Dupont, L., Schlütz, F., Ewah, C. T., Jennerjahn, T., Paul, A. and Behling, H., 2009. Two-step vegetation response to enhanced precipitation in Northeast Brazil during Heinrich event 1. Global Change Biology 16, 1647-1660.

Ehleringer, J. R., Monson, R. K., 1993. Evolutionary and Ecological Aspects of Photosynthetic Pathway Variations. Annu. Rev. Ecol. Syst. 24, 411-439.

Elderfield, H., Ganssen, G., 2000. Past temperature and δ^{18}O of surface ocean waters inferred from foraminiferal Mg/Ca ratios. Nature 405, 442-445.

Elenga, H., Schwartz, D., Vincens, A., 1994. Pollen evidence of late Quaternary vegetation and inferred climate changes in Congo. Palaeogeography, Palaeoclimatology, Palaeoecology 109, 345-356.

Emiliani, C., 1993. Milankovitch theory verified. Nature 364, 583-584.

EPICA Community Members, 2004. Eight glacial cycles from an Antarctic ice core. Nature 429, 623-628.

EPICA Community Members, 2006. One-to-one coupling of glacial climate variability in Greenland and Antarctica. Nature 444, 195-198.

Faegri, K., Iversen, J., 1989. Textbook of pollen analysis. IV Edition by Faegri, K., Kaland, P.E., Krzywinski, K.Wiley, New York.

Fairbanks, R. G., 1989. A 17,000-year glacio-eustatic sea level record: influence of glacial melting rates on the Younger Dryas event and deep-ocean circulation Nature 342 (6250), 637-642.

Fairbanks, R.G., Mortlock, R.A., Chiu, T.-C., Cao, L., Kaplan, A., Guilderson, T.P., Fairbanks, T.W., Bloom, A.L., 2005. Marine Radiocarbon Calibration Curve Spanning 10,000 to 50,000 Years B.P. Based on Paired ^{230}Th/^{234}U/^{238}U and ^{14}C Dates on Pristine Corals. Quaternary Science Reviews 24, 1781-1796.

Farmer, E. C., P. B. deMenocal, Marchitto, T. M., 2005. Holocene and deglacial ocean temperature variability in the Benguela upwelling region: Implications for low-latitude atmospheric circulation, Palaeoceanography, 20, PA2018.

Fensome, R.A., Taylor, F.J.R., Norris, G., Sarjeant, W.A.S., Wharton, D.I., Williams, G.L.,ă1993. A classification of fossil and living dinoflagellates. Micropaleontology Special Paper 7, 1-351.

Fischer, G., Arz, H., et al., 1996. Report and preliminary results of Meteor-Cruise M 34/4, Recife-Bridgetown, Berichte, Fachbereich Geowissenschaften, Universität Bremen, 80, pp.105.

Fletcher, W.J., Sánchez Goñi, M.F., Allen, J.R.M., Cheddadi, R., Combourieu-Nebout, N., Huntley, B., Lawson, I., Londeix, L., Magri, D., Margari, V., Müller, U.C., Naughton, F., Novenko, E., Roucoux, K., Tzedakis, P.C., 2010. Millennial-scale variability during the last glacial in vegetation records from Europe Quaternary Science Reviews 29, 2839-2864.

Flückiger, J., Knutti, R., White, J.W.C., 2006. Oceanic processes as potential trigger and amplifying mechanisms for Heinrich events. Paleoceanography 21, PA2014, pp. 11.

Foley, J.A., Levis, S., Prentice, C.I., Pollard, D., Thompson, S.L., 1998. Coupling dynamic models of climate and vegetation Global Change Biology 4, 561-579.

Franke, J., Paul, A., Schulz, M., 2008. Modeling variations of marine reservoir ages during the last 45000 years. Climate of the Past 4, 125-136.

Fredoux, A., Tastet, J.-P., 1993. Analyse pollinique d'une carotte marine au large de la Côte d'Ivoire. Variations de la végétation et du climat depuis 225 000 ans BP. Palynosciences 2, 173Ű188.

Gan, M.A., Kousky, V.E., Ropelewski, C.F., 2004. The South American monsoon circulation and its relationship to rainfall over West-Central Brazil. Journal of Climate 17, 47-66.

Gasse, F., 2000. Hydrological changes in the African tropics since the Last Glacial Maximum. Quaternary Science Reviews 19, 189-211.

Gasse, F., Chalié, F., Vincens, A., Williams, M.A.J., Williamson, D., 2008. Climatic pattern in equatorial and southern Africa from 30,000 to 10,000 years ago reconstructed from terrestrial and near-shore proxy data. Quaternary Science Reviews 27, 2316-2340.

Gersonde, R., A. Abelmann, U. Brathauer, S. Becquey, C. Bianchi, G. Cortese, H. Grobe, G. Kuhn, H. S. Niebler, M. Segl, R. Sieger, U. Zielinski, Fütterer, D. K., 2003. Last glacial sea surface temperatures and sea-ice extent in the Southern Ocean (Atlantic-Indian sector): A multiproxy approach, Paleoceanography, 18, 1061.

Gersonde, R., X. Crosta, A. Abelmann, Armand, L., 2005. Sea-surface temperature and sea ice distribution of the Southern Ocean at the EPILOG Last Glacial Maximum-a circum-Antarctic view based on siliceous microfossil records, Quaternary Science Reviews, 24, 869-896.

Giresse, P., 2008. Tropical and Sub-tropical West Africa: Marine and Continental Changes during the Late Quaternary. Elsevier Amsterdam. pp.386.

Goldberg, E.D., Arrhenius, G.O.S., 1958. Chemistry of Pacific pelagic sediments Geochimica et Cosmochimica Acta 13, 153-198, IN151, 199-212.

González, C., Dupont, L.M., Behling H, Wefer G., 2008. Neotropical vegetation response to rapid climate changes during the last glacial period: Palynological evidence from the Cariaco Basin. Quaternary Research 69, 217-230.

González, C., Dupont, L. M., Mertens, K. and Wefer, G., 2008. Reconstructing marine productivity of the Cariaco Basin during marine isotope stages 3 and 4 using organic-walled dinoflagellate cysts. Paleoceanography 23, 1-16.

González, C., Dupont, L.M., 2009. Tropical salt marsh succession as sea-level indicator during Heinrich events. Quaternary Science Reviews 28, 939Ű946.

Gordon, A. L., 1986. Interocean Exchange of Thermocline Water, J. Geophys. Res., 91, 5037-5046.

Gordon, A. L., 1996. Comment on the South AtlanticŠs Role in the Global Circulation. In: G. Wefer, W. H. Berger, G. Siedler, D. J. Webb (Eds). The South Atlantic: Present and Past Circulation. Springer-Verlag Berlin Heidelberg, pp 121-124.

Graham, N. E. and Barnett, T. P., 1987. Sea Surface Temperature, Surface Wind Divergence, and Convection over Tropical Oceans. Science 238, 657-659.

Greaves, M., N. Caillon, et al., 2008. Interlaboratory comparison study of calibration standards for foraminiferal Mg/Ca thermometry, Geochem. Geophys. Geosyst., 9, Q08010.

Grimm, E. C., Jacobson, G. L., Jr., Watts, W. A., Hansen, B. C. S., Maasch, K. A., 1993. A 50,000-Year Record of Climate Oscillations from Florida and Its Temporal Correlation with the Heinrich Events. Science 261, 198-200.

Grimm, E. C., Watts, W. A., Jacobson, J. G. L., Hansen, B. C. S., Almquist, H. R., Dieffenbacher-Krall, A. C., 2006. Evidence for warm wet Heinrich events in Florida. Quaternary Science Reviews 25, 2197-2211.

Groot, J.J., 1971. Distribution of Pollen and Spores in the Ocean. In: B.M. Funnell, W.R. Riedel (Eds.), The Micropalaeontology of Oceans, Cambridge University Press, Cambridge, 359-360.

Groot, J.J., Groot, C.R., 1971. Horizontal and Vertical Distribution of Pollen and Spores in Quaternary Sequences. In: B.M. Funnell, W.R. Riedel (Eds.), The Micropalaeontology of Oceans, Cambridge University Press, Cambridge, 493-504.

Haberle, S., Maslin, M.A., 1999. Late Quaternary Vegetation and Climate Change in the Amazon Basin Based on a 50,000 Year Pollen Record from Amazon Fan, ODP Site 932. Quaternary Research 51; 27-38.

Hagen, E., R. Feistel, J. J. Agenbag, Ohde, T., 2001. Seasonal and interannual changes in Intense Benguela Upwelling (1982-1999), Oceanologica Acta, 24, 557-568.

Hall, I.R., Moran, S.B., Zahn, R., Knutz, P.C., and Shen, C.C., Edwards, R.L., 2006. Accelerated drawdown of meridional overturning in the late-glacial Atlantic triggered by transient pre-H event freshwater pertubations. Geophysical Research Letters 33, L16616, pp. 5.

Hansen, B.C.S., Wright, Jr., H.E., Bradbury, J.P., 1984. Pollen studies in the Junín area, central Peruvian Andes. The Geological Society of America Bulletin 95, 1454-1465.

Harrison, S.P., Prentice, C.I., 2003. Climate and CO_2 controls on global vegetation distribution at the last glacial maximum: analysis based on palaeovegetation data, biome modelling and palaeoclimate simulations. Global Change Biology 9, 983-1004.

Hastenrath, S., 1982. On meridional heat transport in the world ocean. Journal of Physical Oceanography 12, 922-927.

Hastenrath, S., 1992. Climate and dynamics of the Tropics. Kluwer Academic Publisher, Dordrecht, pp. 328.

Hathorne, E.C., James, R. H., Lampitt, R. S., 2009. Environmental versus biomineralization controls on the intratest variation in the trace element composition of the planktonic foraminifera *G. inflata* and *G. sciluta.* Paleoceanography 24, PA4204.

Hays, G.C., Richardson, A.J. and Robinson, C., 2005. Climate change and marine plankton Trends in Ecology & Evolution 20 (6), 337-344.

Hays, J. D., Imbrie, J. and Shackleton, N., 1976. Variations in the Earth's Orbit: Pacemaker of the Ice Ages. Science 194, 1121-1132.

Heinrich, H., 1988. Origin and consequences of cyclic ice rafting in the northeast Atlantic Ocean during the past 130,000 years. Quaternary Research 29, 142-152.

Helmens, K.F., Kuhry, P., Rutter, N.W., van der Borg, K., De Jong, A.F.M., 1996. Warming at 18,000 yr B.P. in the tropical Andes. Quaternary Research, 45, 289-299.

Hemleben, C., M. Spindler, Anderson, O. R., 1989. Modern Planktonic Foraminifera, Springer Verlag New York-Berlin-Heidelberg-London-Paris-Tokyo.

Hessler, I., Dupont, L., Bonnefille, R., Behling, H., González, C., Helmens, K.F., Hooghiemstra, H., Lebamba, J., Ledru, M.-P., Lézine, A.-M., Maley, J., Marret, F., Vincens, A., 2009. Millennial-scale changes in vegetation records from tropical Africa and South America during the last glacial. Quaternary Science Reviews 29, 2882-2899.

Heusser, L.E., 1988. Pollen Distribution in Marine Sediments on the continental margin off northern California. Marine Geology 80. 131-147.

Hirst, A. C., Hastenrath, S., 1983. Atmosphere-Ocean Mechanisms of Climate Anomalies in the Angola-Tropical Atlantic Sector. Journal of Physical Oceanography 13, 1146-1157.

Hodell, D. A., Anselmetti, F. S., Ariztegui, D., Brenner, M., Curtis, J. H., Gilli, A., Grzesik, D. A., Guilderson, T. J., Müller, A.D., Bush, M.B., Correa-Metrio, A., Escobar, J., Kutterolf,

S., 2008. An 85-ka record of climate change in lowland Central America. Quaternary Science Reviews 27, 1152-1165.

Hooghiemstra, H., Agwu, C.O.C., 1986. Distribution of palynomorphs in marine sediments:A record for seasonal wind patterns over NW Africa and adjacent Atlantic. Geologische Rundschau 75/1, 81-95.

Hooghiemstra, H., 1988. Changes of major wind belts and vegetation zones in NW Africa 20,000-5000 yr B.P., as deduced from a marine pollen record near Cap Blanc. Review of Palaeobotany and Palynology 55(1-3), 101-140.

Hooghiemstra, H., Lezine, A.-M., Leroy, S.A.G., Dupont, L., Marret, F., 2006. Late Quaternary palynology in marine sediments: A synthesis of the understanding of pollen distribution patterns in the NW African setting Quaternary International 148, 29-44.

Hostetler, S. W., Clark, P. U., Bartlein, P. J., Mix, A. C., Pisias, N. J., 1999. Atmospheric transmission of North Atlantic Heinrich events. Journal of Geophysical Research 104, 3947-3952.

Hughen, K. A., M. G. L. Baillie, et al., 2004. MARINE04 Marine Radiocarbon Age Calibration, 0Ű26 CAL Kyr BP, Radiocarbon, 46, 1059-1086.

Hughen, K., Southon, J., Lehman, S., Bertrand, C., Turnbull, J., 2006. Marine-derived 14C calibration and activity record for the past 50,000 years updated from the Cariaco Basin. Quaternary Science Reviews 25, 3216-3227.

Hulme, M., Doherty, R., Ngara, T., New, M., Lister, D., 2001. African Climate Change: 1900-2100. Climate Research 17, 145-168.

Hüls, M. and Zahn, R., 2000. Millennial-scale sea surface temperature variability in the western tropical North Atlantic from planktonic foraminiferal census counts. Palaeoceanography 15, 659-678.

Imbrie, J., Boyle, E. A., Clemens, S. C., Duffy, A., Howard, W. R., Kukla, G., Kutzbach, J., Martinson, D. G., McIntyre, A., Mix, A. C., Molfino, B., Morley, J. J., Peterson, L. C., Pisias, N. G., Prell, W. L., Raymo, M. E., Shackleton, N. J. and Toggweiler, J. R., 1992. On the Structure and Origin of Major Glaciation Cycles 1. Linear Responses to Milankovitch Forcing, Paleoceanography 7, 701-738.

Imbrie, J., Berger, A., Boyle, E. A., Clemens, S. C., Duffy, A., Howard, W. R., Kukla, G., Kutzbach, J., Martinson, D. G., McIntyre, A., Mix, A. C., Molfino, B., Morley, J.

J., Peterson, L. C., Pisias, N. G., Prell, W. L., Raymo, M. E., Shackleton, N. J. and Toggweiler, J. R., 1993. On the Structure and Origin of Major Glaciation Cycles 2. The 100,000-Year Cycle. Paleoceanography 8, 699-735.

IPCC, 2007. Contribution of Working Groups 1, 2, and 3 to the Fourth Assessment Report of the Intergovernmental Panel on Climate Change. Core Writing Team, Pachauri, R.K. and Reisinger, A. (Eds.), Geneva, Switzerland, pp 104.

Ivanochko, T.S., Ganeshram, R.S., Brummer, G.-J.A., Ganssen, G., Jung, S.J.A., Moreton, S.G., and Kroon, D., 2005. Variations in tropical convection as an amplifier of global climate change at the millennial scale. Earth and Planetary Science Letters 235, 302-314.

Jahns, S., 1996. Vegetation history and climatic changes in West Equatorial Africa during the Late Pleistocene and the Holocene based on a marine pollen diagram from the Congo fan. Veg. Hist. Archaeobot. 5, 207-213.

Jahns, S., Huls, M., Sarnthein, M., 1998. Vegetation and climate history of west equatorial Africa based on a marine pollen record off Liberia (site GIK 16776) covering the last 400,000 years. Review of Palaeobotany and Palynology 102, 277-288.

Janicot, S., 2009. A comparison of Indian and African monsoon variability at different times scales. Comptes Rendus Geoscience 341, 575-590.

Jansen, J. H. F., E. Ufkes, Schneider, R. R., 1996. Late Quaternary Movements of the Angola-Benguela Front, SE Atlantic, and Implications for Advection in the Equatorial Ocean, in The South Atlantic: Present and Past Circulation, edited by G. Wefer, W. H. Berger, G. Siedler, D. J. Webb, pp. 553-575, Springer Verlag Berlin-Heidelberg.

Jennerjahn, T.C., Ittekot, V., Arz, H.W., Behling, H., Pätzold, J., Wefer, G., 2004. Asynchronous terrestrial and marine signals of climate change during Heinrich Events. Science 306, 2236-2239.

Jiménez-Moreno, G., Anderson, R.S., Desprat, S., Grigg, L.D., Grimm, E.C., Heusser, L.E., Jacobs, B.F., López-Martínez, C., Whitlock, C.L., Willard, D.A., 2010. Millennial-scale variability during the last glacial in vegetation records from North America Quaternary Science Reviews 29, 2865-2881.

Johnson, H.B., Polley, H.W., Mayeux, H.S., 1993. Increasing CO_2 and plant-plant interactions: effects on natural vegetation. Vegetatio 104/105, 157-170.

Johnson, T.C., Brown, E.T., McManus, J., Barry, S., Barker, P., Gasse, F., 2002. A High-resolution Paleoclimate Record Spanning the Past 25,000 Years in Southern East Africa. Science 296. 113-116.

Jolly, D., Haxeltine, A., 1997. Effect of Low Glacial Atmospheric CO2 on Tropical African Montane Vegetation. Science 276, 786-788.

Jolly, D., Prentice, I.C., Bonnefille, R., Ballouche, A., Bengo, M., Brenac, P., Buchet, G., Burney, D., Cazet, J.-P., Cheddadi, R., Edorh, T., Elenga, H., Elmoutaki, S., Guiot, J., Laarif, F., Lamb, H., Lézine, A.-M., Maley, J., Mbenza, M., Peyron, O., Reille, M., Reynaud-Farrera, I., Riollet, G., Ritchi, J.C., Roche, E., Scott, L., Ssemmanda, I., Straka, H., Umer, M., Van Campo, E., 1998. Biome reconstruction from pollen and plant macrofossil data for Africa and the Arabian peninsula at 0 and 6000 years. Journal of Biogeography 25, 1007-1027.

Jullien, E., Grousset, F., Malaizé, B., Duprat, J., Sanchez-Goni, M. F., Eynaud, F., Charlier, K., Schneider, R., Bory, A., Bout, V. and Flores, J. A., 2007. Low-latitude "dusty events" vs. high-latitude "icy Heinrich events". Quaternary Research 68, 379-386. Kaiser, J., Schefuß, E., Lamy,

Kaiser, J., Schefuß, E., Lamy, F., Mohtadi, M., Hebbeln, D., 2008. Glacial to Holocene changes in sea surface temperature and coastal vegetation in north central Chile: high versus low latitude forcing. Quaternary Science Reviews 27, 2064-2075.

Kaplan, J.O., Bigelow, N.H., Prentice, I.C., Harrison, S.P., Bartlein, P.J., Christensen, T.R., Cramer, W., Matveyeva, N.V., McGuire, A.D., Murray, D.F., Razzhivin, V.Y., Smith, B., Walker, D.A., Anderson, P.M., Andreev, A.A., Brubaker, L.B., Edwards, M.E., and Lozhkin, A.V., 2003. Climate change and arctic ecosystems II: Modeling, paleodata-model comparisons, and future projections. Journal of Geophysical Research 108 (D19), 8171, doi:10.1029/2002JD002559.

Keeling, R. F., Stephens, B. B., 2001. Antarctic sea ice and the control of Pleistocene climate instability, Paleoceanography, 16, 112-131.

Kim, S.-T., O'Neil, J. R., 1997. Equilibrium and nonequlibrium oxygen isotope effects in synthetic carbonates. Geochimica et Cosmochimica Acta 61. 3461-3475.

Kim, J.-H., R. R. Schneider, P. J. Müller, Wefer, G., 2002. Interhemispheric comparison of deglacial sea-surface temperature patterns in Atlantic eastern boundary currents, Earth and Planetary Science Letters, 194, 383-393.

Kim, J.-H., R. R. Schneider, S. Mulitza, Müller, P. J., 2003. Reconstruction of SE trade-wind intensity based on sea-surface temperature gradients in the Southeast Atlantic over the last 25 kyr, Geophysical Research Letters, 30, 1-4.

Kim, J.-H., Dupont, L., Behling, H. and Versteegh, G.J.M., 2005. Impacts of rapid sea-level rise on mangrove deposit erosion: application of taraxerol and Rhizophora records Journal of Quaternary Science 20 (3), 221-225.

Kirst, G. J., R. R. Schneider, P. J. Müller, I. von Storch, Wefer, G., 1999. Late Quaternary Temperature Variability in the Benguela Current System Derived from Alkenones, Quaternary Research, 52, 92-103.

Kostianoy, A. G., Lutjeharms, J. R. E., 1999. Atmospheric effects in the Angola-Benguela frontal zone, J. Geophys. Res., 104, 20963-20970.

Kucera, M., M. Weinelt, T. Kiefer, U. Pflaumann, A. Hayes, M. Weinelt, M.-T. Chen, A. C. Mix, T. T. Barrows, E. Cortijo, J. Duprat, S. Juggins, Waelbroeck, C., 2005. Reconstruction of sea-surface temperatures from assemblages of planktonic foraminifera: multi-technique approach based on geographically constrained calibration data sets and its application to glacial Atlantic and Pacific Oceans, Quaternary Science Reviews, 24, 951-998.

Lambert, F., Delmonte, B., Petit, J. R., Bigler, M., Kaufmann, P. R., Hutterli, M. A., Stocker, T. F., Ruth, U., Steffensen, J. P. and Maggi, V., 2008. Dust-climate couplings over the past 800,000 years from the EPICA Dome C ice core. Nature 452, 616-619.

Lass, H. U., M. Schmidt, V. Mohrholz, Nausch, G., 2000. Hydrographic and Current Measurements in the Area of the Angola-Benguela Front, Journal of Physical Oceanography, 30, 2589-2609.

Latorre, C., Betancourt, J. L. and Arroyo, M. T. K., 2006. Late Quaternary vegetation and climate history of a perennial river canyon in the Río Salado basin (22°S) of Northern Chile. Quaternary Research 65, 450-466.

Lea, D. W., Mashiotta, T. A., Spero, H. J., 1999. Controls on magnesium and strontium uptake in planktonic foraminifera determined by live cultering. Geochimica et Cosmochimica Acta, 63, 2369-2379.

Lea, D. W., Pak, D. K., Spero, H. J., 2000. Climate Impact of Late Quaternary Equatorial Pacific Sea Surface Temperature Variations. Science 289. 1719-1724.

Lebamba, J., Ngomanda, A., Vincens, A., Jolly, D., Favier, C., Elenga, H., Bentaleb, I., 2009. A reconstruction of Atlantic Central African biomes and forest succession stages derived from modern pollen data and plant functional types. Climate of the Past 5, 403-429.

Ledru, M. P., Soares Braga, P. I., Soubiés, F., Fournier, M., Martin, L., Suguio, K., Turcq, B., 1996. The last 50,000 years in the Neotropics (Southern Brazil): evolution of vegetation and climate. Palaeogeography, Palaeoclimatology, Palaeoecology 123, 239Ű257.

Ledru, M.-P., Ceccantini, G., Gouveia, S.E.M., Lopez-Saez, J.A., Pessenda, L.C.R., Ribeiro, A.S., 2006. Millenial-scale climatic and vegetation changes in a northern Cerrado (Northeast, Brazil) since the Last Glacial Maximum. Quaternary Science reviews 25, 1110-1126.

Ledru, M-P., Campello, R.C., Landim-Dominguez, J.M., Martin, L., Mourguiart, P., Sifeddine, A., Turcq, B., 2001. Late-Glacial cooling in Amazonia inferred from pollen at Lagoa do Caçó, Northern Brazil. Quaternary Research 55, 47-56.

Ledru, M.-P., Mourguiart, P., Riccomini, C., 2009. Related changes in biodiversity, insolation and climate in the Atlantic rainforest since the last interglacial. Palaeogeography, Palaeoclimatology, Palaeoecology 271, 140Ű152. Lenters, J.D., Cook, K.H., 1999. Summertime precipitation variability over South America: role of the Large-Scale circulation. Monthly Weather Review 127, 409-431.

Leroux, M., 1983. Le climat de L'Afrique tropicale (Texte et atlas). Champion, Paris, France.

Leuschner, D. C., Sirocko, F., 2000. The low-latitude monsoon climate during Dansgaard-Oeschger cycles and Heinrich Events, Quaternary Science Reviews, 19, 243-254.

Leyden, B.W., Brenner, M., Hodell, D.A., Curtis, J.H., 1994. Orbital and internal forcing of climate on the Yucatan Peninsula for the past ca. 36 ka. Palaeogeography, Palaeoclimatology, Palaeoecology 109, 193-210.

Lézine, A.-M., 1991. West African paleoclimates during the last climatic cycle inferred from an Atlantic deep-sea pollen record. Quaternary Research 35, 456-463.

Lézine A.M., Vergnaud-Grazzini C., 1993. Evidence of forest extension in West Africa since 22,000 BP: a pollen record from the Eastern Tropical Atlantic. Quaternary Science Reviews 12, 203-210.

Lézine A.M., Tastet, J.P., Leroux M., 1994. Evidence of atmospheric paleocirculation over the Gulf of Guinea since the Last Glacial Maximum. Quaternary Research 41, 390-395.

Lézine, A.M. and Denèfle, M., 1997. Enhanced anticyclonic circulation in the eastern North Atlantic during cold intervals of the last deglaciation inferred from deep-sea pollen records. Geology 25, 119-122.

Lézine, A.-M., Duplessy, J.-C., and Cazet, J.P., 2005. West African monsoon variability during the last deglaciation and the Holocene: Evidence from fresh water algae, pollen and isotope data from core KW31, Gulf of Guinea. Palaeogeography, Palaeoclimatology, Palaeoecology 219, 225-237.

Lézine, A-M., Cazet, J-P., 2005. High-resolution pollen record from core KW31, Gulf of Guinea, documents the history of the lowland forests of West Equatorial Africa since 40,000 yr ago. Quaternary Research 64, 432-443.

Lisiecky, L.E., Raymo, M.E., 2005. A Pliocene-Pleistocene stack of 57 globally distributed benthic ^{18}O records. Paleoceanography 20, PA1003.

Little, M. G., R. R. Schneider, D. Kroon, B. Price, C. P. Summerhayes, Segl,M., 1997. Trade Wind Forcing of Upwelling, Seasonally, and Heinrich Events as a Response to Sub-Milankovitch Climate Variability, Paleoceanography, 12, 568-576.

Liu, Z., Notaro, M., Kutzbach, J., Liu, N., 2006. Assessing Global Vegetation and Climate Feedbacks from Observations Journal of Climate 19, 787-814.

Lutjeharms, J. R. E., Meeuwis, J. M., 1987. The extent and variability of South-East Atlantic Upwelling, South African Journal of Marine Science, 5, 51-62.

Lutjeharms, J. R. E., Van Ballegooyen, R. C., 1988. The retroflection of the Agulhas Current. Journal of Physical Oceanography 18, 1570-1583.

Lynch-Stieglitz, J., Curry, W. B., Slowey, N., 1999. Weaker Gulf Stream in the Florida Straits during the Last Glacial Maximum. Nature 402, 644-648.

Maley, J., 1970. Contributions à l'étude du bassin tchadien. Atlas de pollens du Tchad. Bulletin du Jardin botanique national de Belgique 40, 29-48.

Maley, J., 1991. The African Rain Forest Vegetation and Paleoenvironments during Late Quaternary. Climatic Change 19, 79-98.

Maley, J., Brenac, P., 1998. Vegetation dynamics, palaeoenvironments and climatic changes in the forests of western Cameroon during the last 28,000 years BP. Review of Palaeobotany and Palynology 99, 157-187.

Marchant, R., Taylor, D., Hamilton, A., Late Pleistocene and Holocene History at Mubwindi Swamp, Soutwest Uganda. Quaternary Research 47, 316-328.

Marchant, R., Harrison, S.P., et al., 2009. Pollen-based biome reconstructions for Latin America at 0, 6000 and 18000 years. Climate of the Past Discussions 5, 369-461, accepted.

Marret, F., 1994. Evolution paléoclimatique et paléohydrologique de lŠAtlantique est-equatoriale et du proche continent au quaternaire terminal. Contribution palynologique (Kystes des dinoflagellés, pollen et spores). Thèse Université Bordeaux I, pp. 271.

Marret, F., Turon, J.-L. 1994. Paleohydrology and paleoclimatology off Northwest Africa during the last glacial-interglacial transition and the Holocene: Palynological evidences. Marine Geology 118, 107-117.

Marret, F., Scourse, J., Versteegh, G., Jansen, J.H.F., Schneider, R., 2001. Integrated marine and terrestrial evidence for abrupt Congo River palaeodischarge fluctuations during the last deglaciation. Journal of Quaternary Science 16 (8), 761-766.

Marret, F., Scource, J., Kennedy, H., Ufkes, U., Jansen, F.J.H., 2008. Marine production in the Congo-influenced SE Atlantic over the past 30,000 years: A novel dinoflagellate-cyst based transfer function approach Marine Micropaleontology 68, 198-222.

Martin, L., Bertaux, J., Correge, T., Ledru, M.-P., Mourguiart, P., Sifeddine, A., Soubies, F., Wirrmann, D., Suguio, K., Turcq, B., 1997. Astronomical forcing of contrasting rainfall changes in tropical South America between 12,400 and 8800 cal yr BP. Quaternary Research 47, 117-122.

Mashiotta, T. A., D. W. Lea, Spero, H. J., 1999. Glacial-interglacial changes in Subantarctic sea surface temperature and d18O-water using foraminiferal Mg, Earth and Planetary Science Letters, 170, 417-432.

Matsumoto, K., J. Lynch-Stieglitz, Anderson, R. F., 2001. Similar Glacial and Holocene Southern Ocean Hydrography, Paleoceanography, 16, 445-454.

Matthiessen, J., de Vernal, A., Head, M.J., Okolodkov, Y.B., Zonneveld, K.A.F., Harland, R., 2005. Modern organic-walled dinoflagellate cysts in Arctic marine environments and their (paleo)environmental significance. Paläontologische Zeitschrift 79, 3-51.

Mayle, F.E., Burbridge, R., Killeen, T.J., 2000. Millennial-Scale Dynamics of Southern Amazonian Rain Forest. Science 290, 2291-2294.

Mayle, F.E., Langstroth, R.P., Fisher, R.A., Meir, P., 2007. Long-term forest-savannah dynamics in the Bolivian Amazon: implications for conservation. Philosophical Transactions of the Royal Society B 362, 291-307.

McConnell, M. C., Thunell, R. C., 2005. Calibration of the planktonic foraminiferal Mg/Ca paleothermometer: Sediment trap results from the Guaymas Basin, Gulf of California. Paleoceanography 20, PA2016.

McIntyre, A., Ruddiman, W. F., Karlin, K. and Mix, A. C., 1989. Surface Water Response of the Equatorial Atlantic Ocean to Orbital Forcing. Paleoceanography 4, 19-55.

McIntyre, A., Molfino, B., 1996. Forcing of Atlantic Equatorial and Subpolar Millennial Cycles by Precession. Science 274, 1867-1870.

McManus, J.F., Francois, R., Gherardi, J.M., Keigwin, L.D., and Brown-Leger, S., 2004. Collapse and rapid resumption of Atlantic meridional circulation linked to deglacial climate changes. Nature 428, 834-837, doi:10.1038/nature02494.

Mekik, F., François, R., Soon, M., 2007. A novel approach to dissolution correction of Mg/Ca-based paleothermometry in the tropical Pacific. Paleoceanography 22; PA3217, 1-12.

Merkel, U., Prange, M., Schulz, M., 2010. ENSO variability and teleconnections during glacial climates. Quaternary Science Reviews 29, 86-100.

Milankovitch, M. 1920. Theorie Mathematique des Phenomenes Thermiques produits par la Radiation Solaire. Gauthier-Villars Paris.

Mix, A. C., W. F. Ruddiman, McIntyre, A., 1986. Late Quaternary Paleoceanography of the tropical Atlantic, 1: Spatial variability of annual mean sea surface temperatures, 0-20,000 years B.P, Paleoceanography, 1, 43-66.

Mix, A. C., Morey, A. E., 1996. Climate Feedback and Pleistocene Variations in the Atlantic South Equatorial Current, in The South Atlantic: Present and Past Circulation, edited by G. Wefer, W. H. Berger, G. Siedler, D. J. Webb, pp. 503 - 525, Springer-Verlag Berlin-Heidelberg.

Mommersteeg, H.J.P.M., 1998. Vegetation development and cyclic and abrupt climate change during the late Quaternary. PhD thesis, University of Amsterdam, 191 pp.

Mohtadi, M., Lückge, A., Steinke, S., Groeneveld, J., Hebbeln, D., Westphal, N., 2010. Late Pleistocene surface and thermocline conditions of the eastern tropical Indian Ocean Quaternary Science Reviews 29, 887-896.

Mommersteeg, H.J.P.M., Hooghiemstra, H., in review. Millennium scale climate variability and vegetation development in the tropical Andes from 85 ka pollen record Fúquene-7C (Colombia). Journal of Quaternary Science.

Monnin, E., Indermühle, A., Dällenbach, A., Flückiger, J., Stauffer, B., Stocker, T.F., Raynaud, D., Barnola, J.-M., 2001. Atmospheric CO_2 concentrations over the Last Glacial Termination. Science 291, 112-114.

Moroshki, K. V., Bubnov, V. A., Bulatov, R. P., 1970. Water circulation in the eastern South Atlantic-Ocean, Oceanology-USSR, 10, 27-34.

Morrison, M.E.S., 1968. Vegetation and Climate in the Uplands of South-Western Uganda during the Later Pleistocene Period: Muchoya Swamp, Kigezi District. Journal of Ecology 56, 363-384.

Mourguiart, P., Ledru, M.-P., 2003. Last Glacial Maximum in an Andean cloud forest (eastern Cordillera, Bolivia). Geology, 31, 195-198.

Mudie, P.J., Aksu, A.E. and Yasar, D. 2001. Late Quaternary dinoflagellate cysts from the Black, Marmara and Aegean seas: variations in assemblages, morphology and paleosalinity. Marine Micropaleontology 43, 155-178.

Mulitza, S., Dürkoop, A., Hale, W., Wefer, G., Niebler, H. S., 1997. Planktonic foraminifera as recorders of past surface-water stratification. Geology 25, 335-338.

Mulitza, S., Boltovskoy, D., Donner, B., Meggers, H., Paul, A., Wefer, G., 2003. Temperature: δ^{18}O relationships of palnktonic foraminifera colleted from surface waters. Palaeogeography, Palaeoclimatology, Palaeoecology 202, 143-152.

Mulitza, S., Prange, M., Stuut, J.-B.W., Zabel, M., von Dobeneck, T., Itambi, A.C., Nizou, J., Schulz, M., and Wefer, G., 2008. Sahel megadroughts triggered by glacial slowdowns of Atlantic meridional overturning. Palaeoceanography 23, 1-11.

Mumbi, C.T., Marchant, R., Hooghiemstra, H. and Wooller, M.J., 2008. Late Quaternary vegetation reconstruction from the Eastern Arc Mountains, Tanzania. Quaternary Research 69, 326Ű341.

Muller, J., 1959. Palynology of Rencent Orinoco Delta and Shelf Sediments: Reports of the Orinoco Shelf. Micropaleontology 5, 1-32.

Müller, P. J., G. Kirst, G. Ruhland, I. von Storch, Rosell-Melé, A., 1998. Calibration of the alkenone paleotemperature index U37K' based on core-tops from the eastern South Atlantic and the global ocean (60°N-60°S), Geochimica et Cosmochimica Acta, 62, 1757-1772.

Muller, J., Kylander, M., Wüst, R. A. J., Weiss, D., Martinez-Cortizas, A., LeGrande, A. N., Jennerjahn, T., Behling, H., Anderson, W. T. and Jacobson, G., 2008. Possible evidence for wet Heinrich phases in tropical NE Australia: the Lynch's Crater deposit. Quaternary Science Reviews 27, 468-475.

Naughton, F., Sanchez Goñi, M. F., Desprat, S., Turon, J. L., Duprat, J., Malaizé, B., Joli, C., Cortijo, E., Drago, T., Freitas, M.C., 2007. Present-day and past (last 25 000 years) marine pollen signal off western Iberia. Marine Micropaleontology 62, 91-114.

Nelson, G., Hutchings, L., 1983. The Benguela Upwelling Area, Progress In Oceanography, 12, 333-356.

NGRIP Community Members, 2004. High-resolution record of Northern Hemisphere climate extending into the last interglacial period. Nature 431, 147-151.

Nicholson, S.E., Entekhabi, D., 1987. Rainfall Variability in Equatorial and Southern Africa: Relationships with Sea Surface Temperatures along the Southwestern Coast of Africa. Journal of Climate and Applied Meteorology 26, 561-578.

Nicholson, S.E., 2000. The nature of rainfall variability over Africa on time scales of decades to millennia. Global Planetary Change 26, 137- 158.

Niebler, H. S., H. W. Arz, B. Donner, S. Mulitza, J. Pätzold, Wefer, G., 2003. Sea surface temperatures in the equatorial and South Atlantic Ocean during the Last Glacial Maximum (23-19 ka), Paleoceanography, 18, PA1069.

Nürnberg, D., Bijma, J., Hemleben, C., 1996. Assessing the reliability of magnesium in foraminiferal calcite as a proxy for water mass temperatures. Geochimica et Cosmochimica Acta, 60, 803-814.

Oberhänsli, H., C. Bénier, G. Meinecke, H. Schmidt, R. Schneider, Wefer, G., 1992. Planktonic Foraminifers as Tracers of Ocean Currents in the Eastern South Atlantic, Paleoceanography, 7, 607-632.

Paduano, G.M., Bush, M.B., Baker, P.A., Fritz, S.C., Seltzer, G.O., 2003. A Vegetation and Fire History of Lake Titicaca since the Last Glacial Maximum. Palaeogeography, Palaeoclimatology, Palaeoecology 194, 259-279.

Partridge, T., Scott, L. and Schneider, R., 2004. Between Agulhas and Benguela: responses of Southern African climates of the Late Pleistocene to Current Fluxes, Orbital Precession and the Extent of the Circum-Antarctic Vortex. In: R. W. Battarbee et al. (Eds.) Past Climate Variability through Europe and Africa, Springer, Dordrecht, The Netherlands, pp. 45-68.

Pearcy, R.W., Eherlinger, J., 1984. Comparative ecophysiology of C_3 and C_4 plants. Plant, Cell, and Environment 7, 1-13.

Peck, J.A., Green, R.R., Shanahan, T., King, J.W., Overpeck, J.T., Scholz, C.A., 2004. A magnetic mineral record of Late Quaternary tropical climate variability from Lake Bosumtwi, Ghana. Palaeogeography, Palaeoclimatology, Palaeoecology 215, 37-57.

Peterson, R. G., Stramma, L., 1991. Upper-level circulation in the South Atlantic Ocean, Progress In Oceanography, 26, 1-73.

Peterson, L.C., Haug, G.H., Hughen, K.A., and Röhl, U., 2000. Rapid Changes in the Hydrologic Cycle of the Tropical Atlantic during the Last Glacial. Science 290, 1947-1951.

Petit, J.R., Jouzel, J., Raynaud, D., Barkov, N.I., Barnola, J.-M., Basile, I., Bender, M., Chappellaz, J., Davis, M., Delaygue, G., Delmotte, M., Kotlyakov, V.M., Legrand, M., Lipenkov, V.Y., Lorius, C., Pépin, L., Ritz, C., Saltzman, E., Stievenard, M., 1999. Climate and atmospheric history of the past 420,000 years from the Vostok ice core, Antarctica. Nature 399, 429-436.

Peyron, O., Jolly, D., Braconnot, P., Bonnefille, R., Guiot, J., Wirrmann, D., Chalié, F., 2006. Quantitative reconstructions of annual rainfall in Africa 6000 years ago: Model-data comparison. Journal of Geophysical Reseach 111, D24110, 1-9.

Pokras, E. M. and Mix, A. C., 1985. Eolian evidence for spatial variability of late Quaternary climates in tropical Africa. Quaternary Research 24, 137-149.

Polley, H. W., Johnson, H. B., Mayeux, H. S., 1995. Nitrogen and water requirements of C_3 plants grown at glacial to present carbon dioxide concentrations. Functional Ecology 9, 86-96.

Polley, H. W., Johnson, H. B., Mayeux, H. S., Brown, D. A., White, J. W. C., 1996. Leaf and plant water use effeciency of C_4 species grown at glacial to elevated CO_2 concentrations. International Journal of Plant Sciences 157, 164-170.

Prange, M., G. Lohmann, V. Romanova, Butzin, M., 2004. Modelling tempo-spatial signatures of Heinrich Events: influence of the climatic background state, Quaternary Science Reviews, 23, 521-527.

Prell, W. L., Kutzbach, J. E., 1987. Monsoon Variability Over the Past 150,000 Years. Journal of Geophysical Research 92, 8411-8425.

Prentice, I.C, Cramer, W., Harrison, S.P., Leemans, R., Monserud, R.A., Solomon, A.M., 1992. Special Paper: A Global Biome Model Based on Plant Physiology and Dominance, Soil Properties and Climate. Journal of Biogeography 19, 117-134.

Prentice, C.I., Webb III, T., 1998. BIOME 6000: reconstructing global mid-Holocene vegetation patterns from palaeoecological records Journal of Biogeography 25, 997-1005.

Prentice, I.C., Heimann, M., Sitch, S., 2000. The carbon balance of the terrestrial biosphere: Ecosystem models and atmospheric observations, Ecol. Appl. 10, 1553Ű1573.

Prentice, I.C., Jolly, D., BIOME 6000 participants, 2000. Mid-Holocene and glacial-maximum vegetation geography of the northern continents and Africa. Journal of Biogeography 27, 507-519.

Rahmstorf, S., 2002. Ocean circulation and climate during the past 120,000 years. Nature 419, 207-214.

Raymo, M. E. and Nisancioglu, K., 2003. The 41 kyr world: Milankovitch's other unsolved mystery. Paleoceanography 18, 1011.

Raynor, G.S., Hayes, J.V., Ogden, E.C., 1974. Mesoscale Transport and Dispersion of Airborne Pollens. Journal of Applied Meteorology 13, 87-95.

Regenberg, M., Nürnberg, D., Steph, S., Groeneveld, J., Garbe-Schönberg, D., Tiedemann, R., Dullo, W.-C., 2006. Assessing the effect of dissolution on planktonic foraminiferal Mg/Ca ratios: Evidence from Caribbean core tops. Geochemistry, Geophysics, Geosystems 7, Q07P15, 1-23.

Reid, J. L., 1989. On the total geostrophic circulation of the South Atlantic Ocean: Flow patterns, tracers, and transports. Progress Oceanogr. 23, 149-244.

Reid, J.R., 1996. On the Circulation of the South Atlantic Ocean. In: G. Wefer, W. H. Berger, G. Siedler and D. J. Webb (Eds.), The South Atlantic: Present and Past Circulation, pp. 13-44. Springer-Verlag, Berlin-Heidelberg.

Revel, M., Ducassou, E., Grousset, F.E., Bernasconi, S.M., Migeon, S., Revillon, S., Mascle, J., Murat, A., Zaragosi, S., Bosch, D., 2010. 100, 000 Years of African monsoon variability recorded in sediments of the Nile margin. Quaternary Science Reviews 29, 1342-1362.

Romero, O., G. Mollenhauer, R. R. Schneider, Wefer, G., 2003. Oscillations of the siliceous imprint in the central Benguela Upwelling System from MIS3 through to the early Holocene: the influence of the Southern Ocean, Journal of Quaternary Science, 18, 733-743.

Rosenthal, Y., Boyle, E. A., 1993. Factors controlling the fluoride content of planktonic foraminifera: An evaluation of its paleoceanographic applicability. Geochimica et Cosmochimica Acta 57, 335-346.

Rosenthal, Y., Lohmann, G. P., Lohmann, K. C., Sherrell, R. M., 2000. Incorporation and preservation of Mg in Globigerinoides sacculifer: Implications for reconstructing the temperature and $^{18}O/^{16}O$ of seawater. Paleoceanography 15, 135-145.

Rosenthal, Y., Perron-Cashman, S., et al., 2004. Interlaboratory comparison study of Mg/Ca and Sr/Ca measurements in planktonic foraminifera for paleoceanographic research. Geochemistry, Geophysics, Geosystems 5, Q04D09, 1-29.

Ruddiman, W.F., 2001. Earth's Climate: Past and Future. W.H. Freeman and Company, New York; 464 pp.

Rühlemann, C., Mulitza, S., Müller, P.J., Wefer, G., Zahn, R., 1999. Warming of the tropical Atlantic Ocean and slowdown of thermohaline circulation during the last deglaciation. Nature 402, 511-514.

Rühlemann, C., S. Mulitza, G. Lohmann, A. Paul, M. Prange, Wefer, G., 2003. Abrupt Warming of Intermediate-Depth Atlantic Ocean in Response to Thermohaline Circulation Slowdown During the Last Deglaciation, PAGES News, 11.

Rühlemann, C., Mulitza, S., Lohmann, G., Paul, A., Prange, M., Wefer, G., 2004. Intermediate depth warming in the tropical Atlantic related to weakened thermohaline circulation: Combining paleoclimate and modeling results for the last deglaciation. Paleoceanography 19, PA1025.

Sarnthein, M., Winn, K., Jung, S.J.A., Duplessy, J.C., Labeyrie, L., Erlenkeuser, H., Ganssen, G., 1994. Changes in East Atlantic deep water circulation over the last 30,000 years: an eight time-slice record. Paleoceanography 9, 209-267.

Sarnthein, M., Stattegger, K., Erlenkeuser, H., Grootes, P., Haupt, B.J., Jung, S., Kiefer, T., Kuhnt, W., Pflaumann, U., Schäfer-Neth, C., Schulz, H., Schulz, M., Seidov, D., Simstich, J., van Kreveld, S., Vogelsang, E., Völker, A., and Weinelt, M., 2001. Fundamental Modes and Abrupt Changes in North Atlantic Circulation and Climate over the last 60ky - Concepts, Reconstruction and Numerical Modeling. The Northern North Atlantic: A Changing Environment. P. Schäfer, W. Ritzrau, M. Schlüter and J. Thiede (Eds.), Springer, Berlin, 365-410.

Sautter, L. R., Thunell, R. C., 1991. Seasonal variability in the δ^{18}O and δ^{13}C of planktonic foraminifera from an upwelling environment; Sediment trap results from the San Pedro Basin, Southern California. Paleoceanography 6, 307-314.

Schlitzer, R., 1996. Mass and Heat Transport in the South Atlantic derived from Historical Hydrographic Data. In: G. Wefer, W. H. Berger, G. Siedler, D. J. Webb (Eds). The South Atlantic: Present and Past Circulation. Springer-Verlag Berlin Heidelberg, pp 305-323.

Schlitzer, R., 2010. Ocean Data View, http://odv.awi.de.

Schmittner, A., Appenzeller, C., and Stocker, T.F., 2000. Enhanced Atlantic freshwater export during El Niño. Geophysical Research Letters 27 (8), 1163-1166.

Schneider, R. R., P. J. Müller, Ruhland, G., 1995. Late Quaternary Surface Circulation in the East Equatorial South Atlantic: Evidence from Alkenone Sea Surface Temperatures, Paleoceanography, 10, 197-219.

Schneider, R. R., P. J. Müller, G. Ruhland, G. Meinecke, H. Schmidt, Wefer, G., 1996. Late Quaternary Surface Temperatures and Productivity in the East-Equatorial South Atlantic: Response to Changes in Trade/Monsoon Wind Forcing and Surface Water Advection, in The South Atlantik: Present and Past Circulation, edited by G. Wefer, W. H. Berger, G. Siedler, D. J. Webb, pp. 527 Ű 551, Springer-Verlag Berlin-Heidelberg.

Seidov, D., M. Maslin, 2001. Atlantic ocean heat piracy and the bipolar climate see-saw during Heinrich and Dansgaard-Oeschger events, Journal of Quaternary Science, 16, 321-328.

Shackleton, N. J., 1974. Attainment of isotopic equilibrium between ocean water and the benthonic foraminifera genus Uvigerina: Isotopic changes in the ocean during the last glacial. Colloques Internationaux du C.N.R.S. 219, 203-209.

Shaffer, G., Olsen, S.M., Bjerrum, C.J., 2004. Ocean subsurface warming as a mechanism for coupling Dansgaard-Oeschger climate cycles and ice-rafting events. Geophysical Research Letters 31, pp.1-4.

Shannon, L. V., 1985. The Benguela Ecosystem Part 1: Evolution of the Benguela, physical features and processes, Oceanogr. Mar. Biol. Ann. Rev., 23, 105-182.

Shannon, L. V., J. J. Agenbag, Buys, M. E. L., 1987. Large- and Mesoscale features of the Angola-Benguela Front, South African Journal of Marine Science, 5, 11-34.

Shannon, L. V., Nelson, G., 1996. The Benguela: Large Scale Features and Processes and System Variability in The South Atlantik: Present and Past Circulation, edited by G. Wefer, W. H. Berger, G. Siedler, and D. J. Webb, pp. 163 - 210, Springer-Verlag Berlin Heidelberg.

Shaw, H. K. A., 1947. The vegetation of Angola. Journal of Ecology 35, 23-48.

Shi, N., Dupont, L., Beug, H.-J., Schneider, R., 1998. Vegetation and climate changes during the last 21 000 years in S.W. Africa based on a marine pollen record. Vegetation History and Archaeobotany 7, 127-140.

Shi, N, Dupont, L., 1997. Vegetation and climatic history of southwest Africa: A marine palynological record of the last 300,000 years. Vegetation History and Archaeobotany 6 (2), 117-131.

Skinner, L.C., 2008. Revisiting the absolute calibration of the Greenland ice-core age-scales. Climate of the Past 4, 295-302.

Sowunmi, M.A., 1973. Pollen grains of Nigerian plants. Grana 13, 145-186.

Sowunmi, M.A., 1995. Pollen of Nigerian plants 2. Woody species. Grana 34, 39-44.

Spero, H. J., Lea, D. W., 1993. Intraspecific stable isotope variability in the planktic foraminifera Globigerinoides sacculifer: Results from laboratory experiments. Marine Micropaleontology 22, 221-234.

Spero, H. J., Lea, D. W., 1996. Experimental determination of stable isotope variability in Globigerina bulloides: Implications for paleoceanographic reconstructions. Marine Micropaleontology 28, 231-246.

Spero, H. J., Bjima, J., Lea, D. W., Bemis, B. B., 1997. Effect of seawater carbonate concentration on foraminiferal carbon and oxygen isotopes. Nature 390, 497-500.

Stager, J.C., Mayewski, P.A., Meeker, L.D., 2002. Cooling cycles, Heinrich event 1, and the desiccation of Lake Victoria. Palaeogeography, Palaeoclimatology, Palaeoecology 183, 169-178.

Steinke, S., Chiu, H.-Y., Yu, P.-S., Shen, C.-C., Löwemark, L., Mii, H.-S., Chen, M.-T., 2005. Mg/Ca ratios of two *Globigerinoides ruber* (white) morphotypes: Implications for reconstructing past tropical/subtropical surface water conditions Geochem. Geophys. Geosyst. 6, Q11005.

Stocker, T. F., 1998. The Seesaw Effect, Science, 282, 61-62.

Stockmarr J., 1971. Tablets with spores used in absolute pollen analysis. Pollen Spores 13, 615Ű621.

Stott, L., Poulsen, C., Lund, S., Thunell, R., 2002. Super ENSO and Global Climate Oscillations at Millennial Time Scales Science 297, 222-226.

Stramma, L., Peterson, R. G., 1989. Geostrophic Transport in the Benguela Current Region, Journal of Physical Oceanography, 19, 1440-1448.

Stramma, L., England, M., 1999. On the water masses and mean circulation of the South Atlantic Ocean. Journal of Geophysical Research 104, 20863-20883.

Street-Perrott, F.A., Huang, Y., Perrott, R.A., Eglinton, G., Barker, P., Khelifa, L.B., Harkness, D.D., Olago, D.O., 1997. Impact of Lower Atmospheric Carbon Dioxid on Tropical Mountain Ecosystems. Science 278, 1422-1426.

Stuiver, M., Reimer, P.J., Bard, E., Beck, W., Burr, G.S., Hughen, K.A., Kromer, B., McCormac, G., van der Pflicht, J., Spurk, M., 1998. INTCAL98 radiocarbon age calibration, 24,000-0 cal BP. Radiocarbon 40, 1041-1083.

Stuut, J.-B. W. and Lamy, F., 2004. Climate variability at the southern boundaries of the Namib (southwestern Africa) and Atacama (northern Chile) coastal deserts during the last 120,000 yr. Quaternary Research 62, 301-309.

Sultan, B., Janicot, S., 2003. The West African Monsoon Dynamics. Part 2: The "‘Preonset"’ and "‘Onset"’ of the Summer Monsoon. Journal of Climate 16, 3407-3427.

Summerhayes, C. P., D. Kroon, A. Rosell-Melé, R. W. Jordan, H. J. Schrader, R. Hearn, J. Villanueva, J. O. Grimalt, Eglinton, G., 1995. Variability in the Benguela Current upwelling system over the past 70,000 years, Progress In Oceanography, 35, 207-251.

Takahara, H., Igarashi, Y., Hayashi, R., Kumon, F., Liew, P.-M., Yamamoto, M., Kawai, S., Oba, T. and Irino, T., 2010. Millennial-scale variability in vegetation records from the East Asian Islands: Taiwan, Japan and Sakhalin Quaternary Science Reviews 29, 2900-2917.

Taylor, D.M., 1990. Late Quaternary pollen records from two Ugandan mires:evidence for environmental change in the Rukiga Highlands of southwest Uganda. Palaeogeography, Palaeoclimatology, Palaeoecology 80, 283-300.

Thompson, P. R., A. W. H. Be, J.-C. Duplessy, Shackleton, N. J., 1979. Disappearance of pink-pigmented Globigerinoides ruber at 120,000 yr BP in the Indian and Pacific Oceans, Nature, 280, 554-558.

Tierney, J. E., Russell, J. M., Huang, Y., Damste, J. S. S., Hopmans, E. C., Cohen, A. S., 2008. Northern Hemisphere Controls on Tropical Southeast African Climate During the Past 60,000 Years. Science 322, 252-255.

Tjallingii, R., M. Claussen, J.-B. W. Stuut, J. Fohlmeister, A. Jahn, T. Bickert, F. Lamy, Röhl, U., 2008. Coherent high- and low-latitude control of the northwest African hydrological balance, Nature Geoscience, 1, 670-675.

Turney, C. S. M., Kershaw, A. P., Clemens, S. C., Branch, N., Moss, P. T. and Keith Fifield, L., 2004. Millennial and orbital variations of El Nino/Southern Oscillation and high-latitude climate in the last glacial period. Nature 428, 306-310.

Tyson, P. D., Preston-Whyte, R. A., (2000), The Weather and Climate of Southern Africa, Oxford University Press South Africa, Cape Town, pp.396.

Ufkes, E., J. H. Fred Jansen, Brummer, G.-J. A., 1998. Living planktonic foraminifera in the eastern South Atlantic during spring: Indicators of water masses, upwelling and the Congo (Zaire) River plume, Marine Micropaleontology, 33, 27-53.

Urey, H. C., 1947. The Thermodynamic Properties of Isotopic Substances. Journal of the Chemical Society, 562-581.

Van der Hammen, T., Hooghiemstra, H., 1995. The EL abra stadial, a younger dryas equivalent in Colombia. Quaternary Science Reviews 14, 841-851.

Van der Kaars, S., 2001. Pollen distribution in marine sediments from the south-eastern Indonesian waters. Palaeogeography, Palaeoclimatology, Palaeoecology 171, 341-361.

Van Geel, B., Van der Hammen, T., 1973. Upper Quaternary vegetational and climatic sequence of the Fúquene area (Eastern Cordillera, Colombia). Palaeogeography, Palaeoclimatology, Palaeoecology 14, 9-92.

Van't Veer, R., Islebe, G.A., Hooghiemstra, H., 2000. Climatic change during the Younger Dryas chron in northern South America: a test of the evidence. Quaternary Science Reviews 19, 1821-1835.

Vellinga, M., Wood, R.A., 2002. Global Climatic Impacts of a Collapse of the Atlantic Thermohaline Circulation. Climatic Change 54, 251-267-267.

Vidal, L., Labeyrie, L., Cortijo, E., Arnold, M., Duplessy, J. C., Michel, E., Becque, S., van Weering, T. C. E., 1997. Evidence for changes in the North Atlantic Deep Water linked to meltwater surges during the Heinrich events Earth and Planetary Science Letters 146, 13-27.

Vincens, A., 1991. Late Quaternary vegetation history of the South-Tanganyika Basin; Climatic implications in South Central Africa. Palaeogeography, Palaeoclimatology, Palaeoecology 86, 207-226.

Vincens, A., Chalié, F., Bonnefille, R., Guiot, J., Tiercelin, J-J., 1993. Pollen-derived rainfall and temperature estimates from Lake Tangayika and their implication for Late Pleistocene water levels. Quaternary Research 40, 343-350.

Vincens, A., Buchet, G., Williamson, D., Taieb, M., 2005. A 23,000 yr pollen record from Lake Rukwa (8°S, SW Tanzania): New data on vegetation dynamics and climate in Central Eastern Africa. Review of Palaeobotany and Palynology 137 (3-4), 147-162.

Vincens, A., Bremond, L., Brewer, S., Buchet, G., Dussouillez, P., 2006. Modern pollen-based biome reconstructions in East Africa expanded to southern Tanzania. Review of Palaeobotany and Palyonology 140, 187-212.

Vincens, A., Garcin, Y., Buchet, G., 2007. Influence of rainfall seasonality on African lowland vegetation during the Late Quaternary: pollen evidence from Lake Masoko, Tanzania. Journal of Biogeography 24, 1274-1288.

Voelker, A.H.L. and workshop participants, 2002. Global distribution of centennial-scale records for Marine Isotope Stage (MIS) 3: a database. Quaternary Science Reviews 21, 1185-1212.

Waelbroeck, C., L. Labeyrie, E. Michel, J. C. Duplessy, J. F. McManus, K. Lambeck, E. Balbon, Labracherie, M., 2002. Sea-level and deep water temperature changes derived from benthic foraminifera isotopic records, Quaternary Science Reviews, 21, 295-305.

Waldron, H. N., T. A. Probyn, J. R. E. Lutjeharms, Shillington, F. A., 1992. Corbon export associated with the Benguela Upwelling System, South African Journal of Marine Science, 12, 369-374.

Wang, Y.J., Cheng, H., Edwards, R.L., An, Z.S., Wu, J.Y., Shen, C.-C., Dorale, J.A., 2001. A high resolution absolute-dated late Pleistocene monsoon record from Hulu Cave, China. Science 294, 2345-2348.

Ward, J.K., Tissue, D.T., Thomas, R.B., Strain, B.R., 1999. Comparative responses of model C_3 and C_4 plants to drought in low and elevated CO2. Global Change Biology 5, 857-867.

Watts, W.A., Bradbury, J.P., 1982. Paleoecological studies at Lake Patzcuaro on the west-central Mexican Plateau and at Chalco in the basin of Mexico. Quaternary Research 17, 56-70.

Weaver, A. J., Eby, M., Wiebe, E. C., Bitz, C. M., Duffy, P. B., Ewen, T. L., Fanning, A. F., Holland, M. M., MacFadyen, A., Matthews, H. D., Meissner, K. J., Saenko, O., Schmittner, A., Wang, H., Yoshimori, M., 2001. The UVic earth system climate model: Model description, climatology, and applications to past, present and future climates. Atmosphere-Ocean 39, 361-428.

Wefer, G., Fischer, G., 1993. Seasonal patterns of vertical particle flux in equatorial and coastal upwelling areas of the eastern Atlantic. Deep-Sea Research 1, 40, 1613-1645.

Wefer, G., W. H. Berger, C. Richter, Party, S. S., 1998. Proceedings Ocean Drilling Program, Initial Report. Vol. 175, ODP, College Station TX.

Weldeab, S., Lea, D. W., Schneider, R. R. and Andersen, N., 2007. 155,000 Years of West African Monsoon and Ocean Thermal Evolution. Science 316, 1303-1307.

Weng, C., Bush, M.B., Curtis, J.H., Kolata, A.L., Dillehay, T.D., Binford, M.W., 2006. Deglaciation and Holocene climate change in the western Peruvian Andes. Quaternary Research 66, 87-96.

White, F. 1983. The vegetation of Africa. UNESCO/AETFAT/UNSO, Maps and Memoir, pp. 356.

Wilke, I., H. Meggers, and T. Bickert (2009), Depth habitats and seasonal distributions of recent planktic foraminifers in the Canary Islands region (29°N) based on oxygen isotopes, Deep Sea Research Part I: Oceanographic Research Papers, 56, 89-106.

Winograd, I. J., Coplen, T. B., Landwehr, J. M., Riggs, A. C., Ludwig, K. R., Szabo, B. J., Kolesar, P. T. and Revesz, K. M., 1992. Continuous 500,000-Year Climate Record from Vein Calcite in Devils Hole, Nevada. Science 258, 255-260.

Wolff, E.W., Chappellaz, J., Blunier, T., Rasmussen, S.O., Svensson, A., 2010. Millennial-scale variability during the last glacial: the ice core record. Quaternary Science Reviews 29, 2828-2838.

Wramneby, A., Smith, B., Samuelsson, P., 2010. Hot spots of vegetation-climate feedbacks under future greenhouse forcing in Europe. Journal of Geophysical Research 115 , D21119.

Ybert, J.P., 1979. Altas des pollens de Côte dŠIvoire. ORSTOM, Paris. Initiations Documentation Technique 40, pp.40.

Yeager, S. G., Shields, C. A., Large, W. G. and Hack, J. J., 2006. The Low-Resolution CCSM3. Journal of Climate 19 (11), 2545-2566.

Yu, J., Elderfield, H., Jin, Z., Booth, L., 2008. A strong temperature effect on U/Ca in planktonic foraminiferal carbonates. Geochimica et Cosmochimica Acta 72, 4988-5000.

Zaric, S., B. Donner, G. Fischer, S. Mulitza, Wefer, G., 2005. Sensitivity of planktic foraminifera to sea surface temperature and export production as derived from sediment trap data, Marine Micropaleontology, 55, 75-105.

Zeebe, R. E., 1999. An explanation of the effect of seawater carbonate concentration on foraminiferal oxygen isotopes. Geochimica et Cosmochimica Acta 63, 2001-2007.

Zhou, H., J. Zhao, Y. Feng, M. K. Gagan, G. Zhou, Yan, J., 2008. Distinct climate change synchronous with Heinrich event one, recorded by stable oxygen and carbon isotopic compositions in stalagmites from China, Quaternary Research, 69, 306-315.

Ziegler, M., Lourens, L. J., Tuenter, E., Hilgen, F., Reichart, G.-J. and Weber, N., 2010 a. Precession phasing offset between Indian summer monsoon and Arabian Sea productivity linked to changes in Atlantic overturning circulation. Paleoceanography 25, PA3213.

Ziegler, M., Tuenter, E. and Lourens, L. J., 2010 b. The precession phase of the boreal summer monsoon as viewed from the eastern Mediterranean (ODP Site 968). Quaternary Science Reviews 29, 1481-1490.

Zonneveld, K.A.F., 1997. New species of organic walled dinoflagellate cysts from modern sediments of the Arabian Sea (Indian Ocean). Review of Palaeobotany and Palynology 97, 319-337.

Zonneveld, K.A.F., Versteegh, G.J.M., Kodrans-Nsiah, M. 2008. Preservation and organic chemistry of Late Cenozoic organic-walled dinolfagellate cysts: a review. Marine Micropaleontology 68, 179-197.

11 Appendix

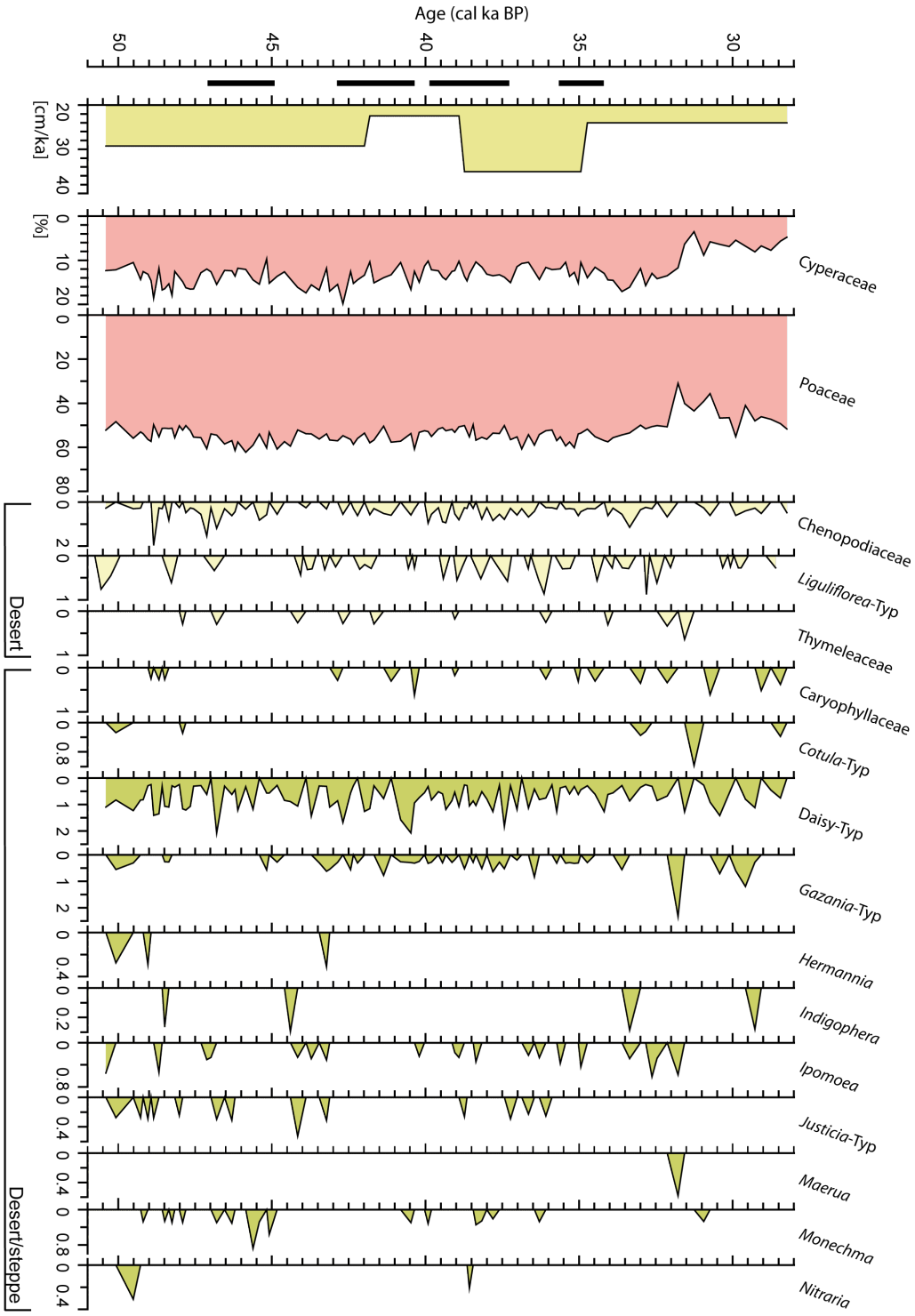

Figure 25: Relative abundance (%) of all pollen taxa from ODP Site 1078 and generated during this thesis. This diagram continuous on the following pages

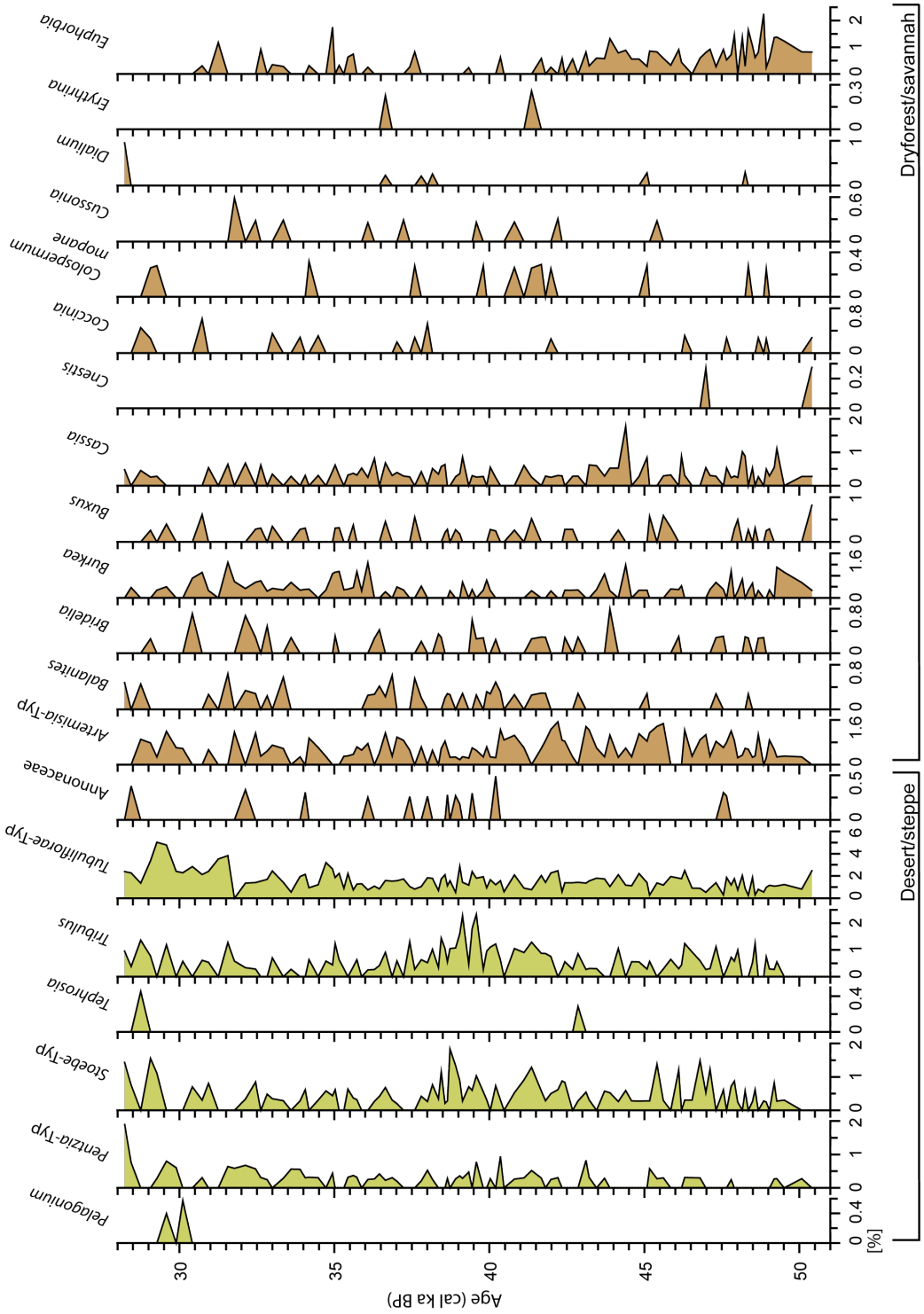
Euphorbia
Erythrina
Dialium
Cussonia
Colospermum mopane
Coccinia
Cnestis
Cassia
Buxus
Burkea
Bridelia
Balanites
Artemisia-Typ
Annonaceae
Tubuliflorae-Typ
Tribulus
Tephrosia
Stoebe-Typ
Pentzia-Typ
Pelagonium
0 0.4 0 1 2 0 1 2 0 0.4 0 2 0 4 6 0 0.5 0 1.6 0 0.8 0 0.8 1.6 0 1 0 2 0 0.2 0 0.8 0 0.4 0 0.6 0 1 0 3 0 1 2
[%]
Dryforest/savannah
Desert/steppe
30
35
40
45
50
Age (cal ka BP)

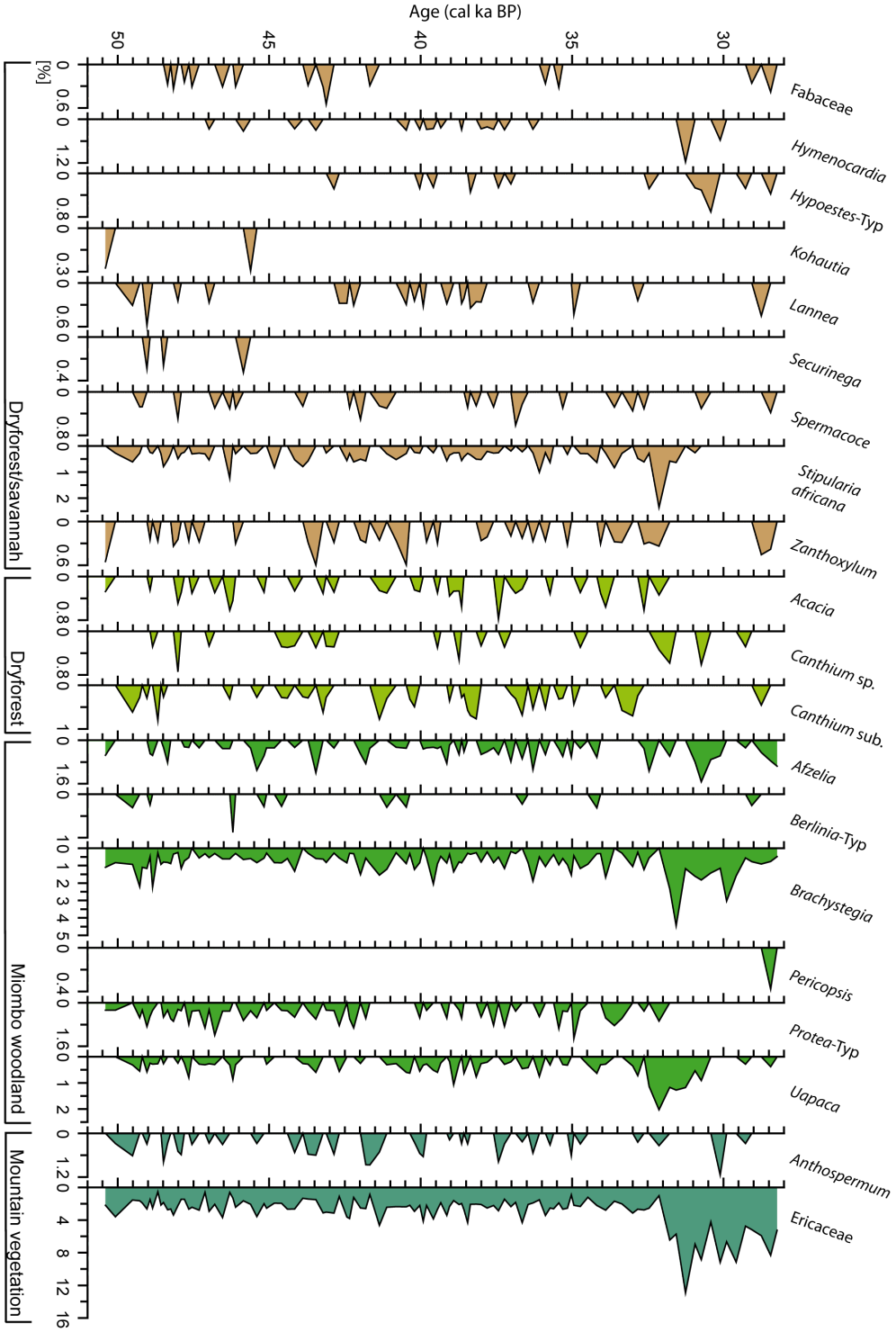
Age (cal ka BP)
50
45
40
35
30
[%]
Fabaceae
Hymenocardia
Hypoestes-Typ
Kohautia
Lannea
Securinega
Spermacoce
Stipularia africana
Zanthoxylum
Acacia
Canthium sp.
Canthium sub.
Afzelia
Berlinia-Typ
Brachystegia
Pericopsis
Protea-Typ
Uapaca
Anthospermum
Ericaceae
Dryforest/savannah
Dryforest
Miombo woodland
Mountain vegetation

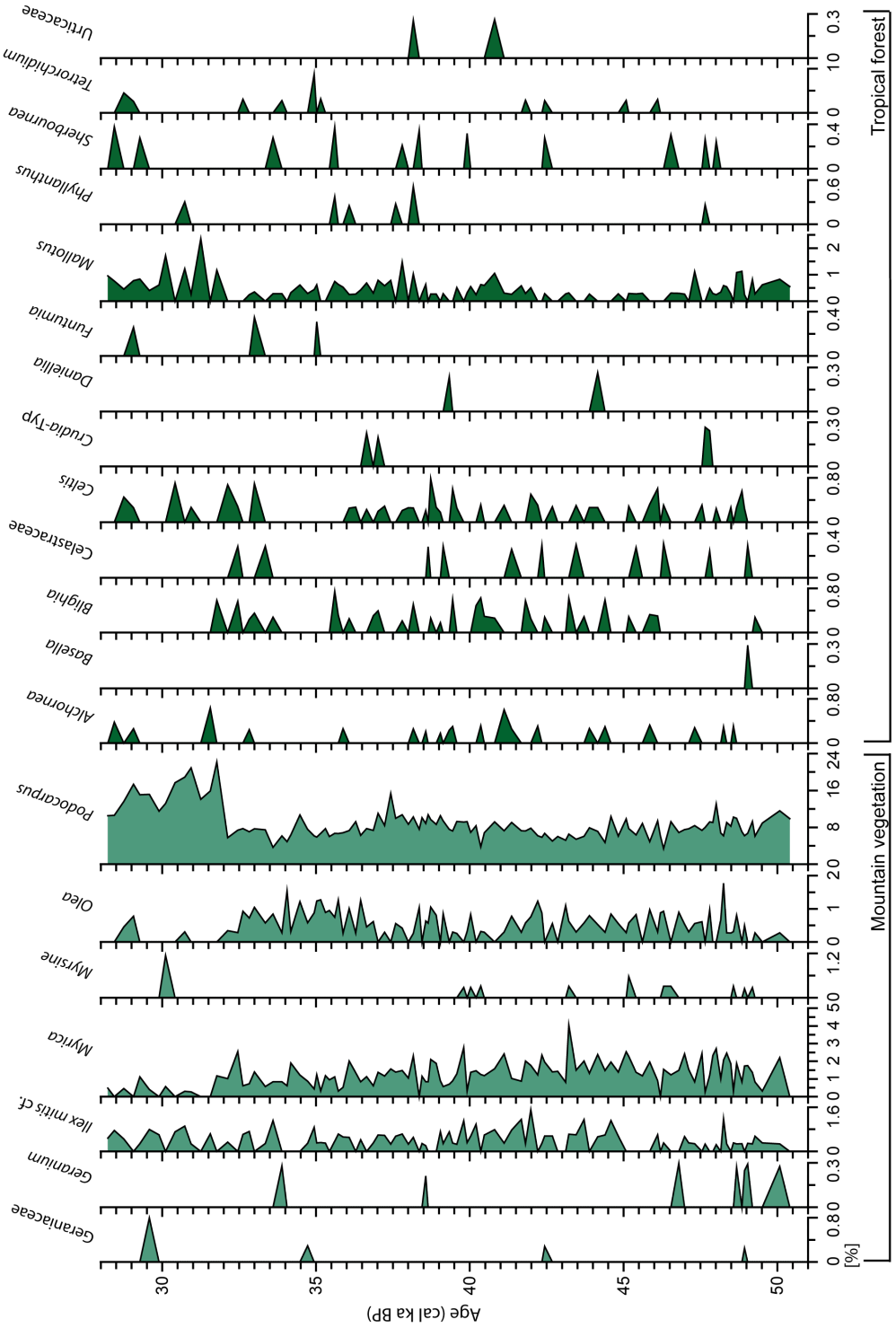
Urticaceae
Tetrorchidium
Sherbournea
Phyllanthus
Mallotus
Funtumia
Daniellia
Crudia-Typ
Celtis
Celastraceae
Bligbia
Basella
Alchornea
Podocarpus
Olea
Myrsine
Myrica
Ilex mitis cf.
Geranium
Geraniaceae
0.3
10
0.40
0.60
0
2
1
0.40
0.30
0.30
0.80
0.40
0.80
0.30
0.80
240
16
8
20
1
1.20
50
4
3
2
1
1.60
0.30
0.80
0
[%]
Tropical forest
Mountain vegetation
30
35
40
45
50
Age (cal ka BP)

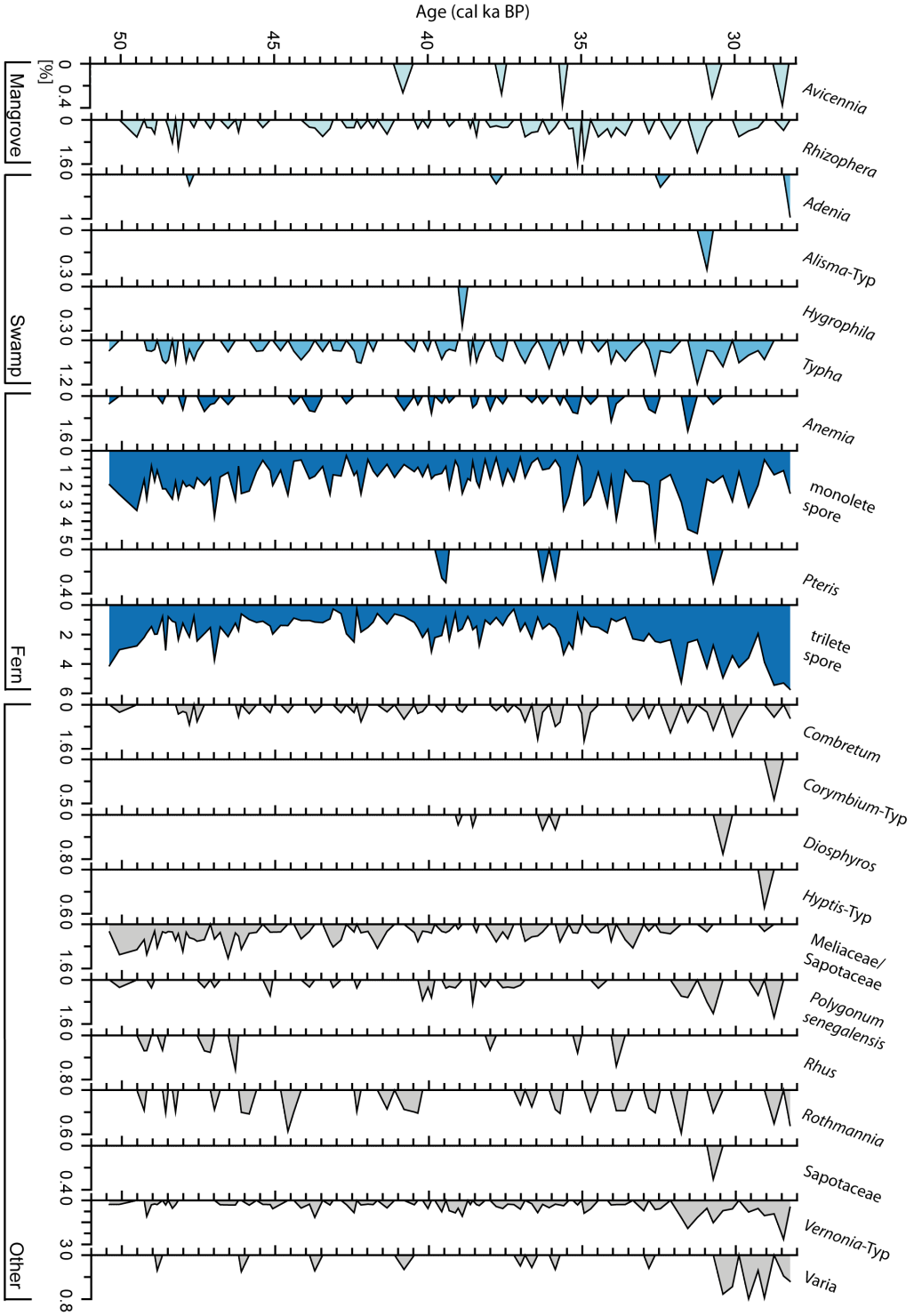
Age (cal ka BP)
50
45
40
35
30
[%]
Mangrove
Swamp
Fern
Other
Avicennia
Rhizophera
Adenia
Alisma-Typ
Hygrophila
Typha
Anemia
monolete spore
Pteris
trilete spore
Combretum
Corymbium-Typ
Diosphyros
Hyptis-Typ
Meliaceae/ Sapotaceae
Polygonum senegalensis
Rhus
Rothmannia
Sapotaceae
Vernonia-Typ
Varia